Aldo Bischi

Chemical Looping Reactor System Design

Double Loop Circulating Fluidized Bed (DLCFB)

Thesis for the degree of Philosophiae Doctor

Trondheim, May 2012

Norwegian University of Science and Technology
Faculty of Engineering Science and Technology
Department of Energy and Process Engineering

NTNU – Trondheim
Norwegian University of
Science and Technology

NTNU
Norwegian University of Science and Technology

Thesis for the degree of Philosophiae Doctor

Faculty of Engineering Science and Technology
Department of Energy and Process Engineering

ISBN 978-82-471-3591-4 (printed ver.)
ISBN 978-82-471-3592-1 (electronic ver.)
ISSN 1503-8181

Doctoral theses at NTNU, 2012:152

Printed by NTNU-trykk

Preface

The thesis is submitted in partial fulfilment of the requirements for the degree of *philosophiae doctor* (Ph.D.) at the Norwegian University of Science and Technology (NTNU).

The work was carried out at the Department of Energy and Process Engineering at the Faculty of Engineering Science and Technology.

Professor Olav Bolland has been the academic supervisor.

The Ph.D. thesis forms a part of the BIGCO2 project, performed under the strategic Norwegian research program Climit. It was founded by the partners: Statoil, GE Global Research, Statkraft, Aker Clean Carbon, Shell, TOTAL, ConocoPhillips, ALSTOM, the Research Council of Norway (178004/I30 and 176059/I30) and Gassnova (182070).

Abstract

Chemical looping combustion (CLC) is continuously gaining more importance among the carbon capture and storage (CCS) technologies. It is an unmixed combustion process which takes place in two steps. An effective way to realize CLC is to use two interconnected fluidized beds and a metallic powder circulating among them, acting as oxygen carrier. The metallic powder oxidizes at high temperature in one of the two reactors, the air reactor (AR). It reacts in a highly exothermic reaction with the oxygen of the injected fluidizing air. Afterwards the particles are sent to the other reactor where the fuel is injected, the fuel reactor (FR). There, they transport heat and oxygen necessary for the reaction with the injected fuel to take place. At high temperatures, the particle's oxygen reacts with the fuel producing CO_2 and steam, and the particles are ready to start the loop again. The overall reaction, the sum of the enthalpy changes of the oxygen carrier oxidation and reduction reactions, is the same as for the conventional combustion.

Two are the key features, which make CLC promising both for costs and capture efficiency. First, the high inherent irreversibility of the conventional combustion is avoided because the energy is utilized stepwise. Second, the CO_2 is intrinsically separated within the process; so there is in principle no need either of extra carbon capture devices or of expensive air separation units to produce oxygen for oxy-combustion.

A lot of effort is taking place worldwide on the development of new chemical looping oxygen carrier particles, reactor systems and processes. The current work is focused on the reactor system: a new design is presented, for the construction of an atmospheric 150kW_{th} prototype working with gaseous fuel and possibly with inexpensive oxygen carriers derived from industrial by-products or natural minerals. It consists of two circulating fluidized beds capable to operate in fast fluidization regime; this will increase the particles concentration in the upper section of the reactors, thus the gas solids contact. They are interconnected by means of two pneumatically controlled divided loop-seals and a bottom extraction/lift. The system is designed to be as compact as possible, to help up-scaling and enclosure into a pressurized vessel, aiming pressurization in a second phase. In addition several industrial solutions have been utilized, from highly loaded cyclones to several levels of secondary air injections.

The divided loop-seals are capable to internally re-circulate part of the entrained solids, uncoupling the solids entrainment from the solids exchange. This will provide a better control on the process increasing its flexibility and helping to fulfil downstream requirements. No mechanical valves are utilized, but gas injections. The bottom extraction compensates the lower entrainment of the FR which has less fluidizing gas availability and smaller cross section than the AR. The lift allows adjusting the reactors bottom inventories, thus the pressures in the bottom sections of the reactors. In this way the divided loop-seals are not exposed to large pressure unbalances and the whole system is hydrodynamically more robust.

The proposed design was finally validated by means of a full scale cold flow model (CFM), without chemical reactions. A thorough evaluation of the scaling state-of-the-art in fluidization engineering has been done; two are the approaches. One consists of building a small scale model which resembles the hydrodynamics of the bigger hot setup, by keeping constant a set of dimensionless numbers. The other is based on the construction of a full scale model, being careful to be in the same fluidization regime and to utilize particles with the same fluidization properties as the hot setup. In this way the surface to volume ratio is kept the same as that one of the hot rig. The idea presented in this work combines those two strategies, building a full scale CFM. In this way, it can be used for the hot rig design debugging and it is at the same time the hydrodynamic small scale model of a ten times larger industrial application.

The adopted scaling strategy and design brought to the construction of one of the world biggest and more complex fluidized bed cold flow model reactor systems. The air and fuel reactor have a height of 5 m and a diameter of respectively 0.230 and 0.144 m. The selected particles are fine and heavy being classifiable as high density Geldart A; there is almost no published literature regarding those particles utilization in circulating fluidized beds.

Extensive test campaigns have been performed to hydrodynamically validate the proposed designs. It was possible to understand and evaluate the operational window, the sensitivity to the input parameters and the key design details performance. Control strategies were qualitatively developed. The presented double loop architecture design showed good stability and flexibility at the same time, so that can also suit the requirements of other chemical processes based on two complementary reactions taking place simultaneously and continuously.

A mia nonna Maria.

Acknowledgments

First of all, I would like to thank my supervisor Prof. Olav Bolland giving me the opportunity to work with such interesting and challenging topic, to advise me along the whole Ph.D. and to believe in me.

I would like to express my gratitude to Prof. Gernot Krammer, Dr. Rahul Anantharaman, Dr. Lars Olof Nord, Mr. Jean Xavier Morin and Mr. Øyvind Langørgen. Each of these gentlemen has *de facto* co-supervised a phase of my work.

Many of the Ph.D. fellows that I got to know have been very important for me, as well as the master and bachelor students that I had the chance to supervise. We shared our challenges, we learnt from each other and supported each-other. I also would like to thank the administrative staff at the Department of Energy and Process Engineering of NTNU to provide me excellent working conditions.

The TU Wien "Chemical Process Engineering and Energy Technology" Research Division in Austria deserves my gratitude, they hosted me for some months in the more complex time of my Ph.D. and they introduced me to Chemical Engineering.

I would like to thank all the friends I made during this "travel"; people coming from all over the word in such welcoming country, Norway. I got to know so many cultures and things and I had really good time.

I thank my family and my friends in Italy, they have always been present.

The Ph.D. thesis forms a part of the BIGCO2 project, performed under the strategic Norwegian research program Climit. The author acknowledges the partners: Statoil, GE Global Research, Statkraft, Aker Clean Carbon, Shell, TOTAL, ConocoPhillips, ALSTOM, the Research Council of Norway (178004/I30 and 176059/I30) and Gassnova (182070) for their support.

Contents

Nomenclature

Roman letters

d_{50}	[μm]	mass median particle diameter
D	[m]	reactor diameter
G_s	[kg·m^{-2}·s^{-1}]	solids flux
g	[m·s^{-2}]	gravitational acceleration
h	[W·m^{-2}·K^{-1}]	heat transfer coefficient
L	[m]	reactor height
MeO_α		oxidized metal oxide
$MeO_{\alpha-1}$		reduced metal oxide
P	[Pa], [mbar]	pressure
PM1		all the particles having a d_{50} of 1μm or less
PM10		all the particles having a d_{50} of 10μm or less
ppmv		parts per million by volume
R_0	[kg·kg^{-1}]	theoretical amount of oxygen that the oxygen carrier can take up
R	[-]	coefficient of determination
T	[ºC]	temperature
toe		tonne of oil equivalent
u_0	[m·s^{-1}]	superficial gas velocity
u_{mf}	[m·s^{-1}]	particles minimum fluidization velocity
u_t	[m·s^{-1}]	particles terminal velocity
V_{cyc_entr}	[m·s^{-1}]	gas velocity at the cyclone entrance, at the inlet duct exit
wt%	[-]	weight per cent
X	[-]	degree of oxidation or conversion
Y		year

Greek letters

ΔP	[mbar]	pressure variation
ΔX	[-]	conversion difference or exploitation of the maximum oxygen capacity
λ	[-]	excess air ratio
μ	[Pa·s]	dynamic viscosity
ρ	[kg·m^{-3}]	density
φ	[-]	particles sphericity

Subscripts

g	gas
p	particles

Dimensionless numbers

Ar	[-]	Archimedes number	$d_{50}^{3} \cdot \rho_g \cdot (\rho_p - \rho_g) \cdot g \cdot \mu^{-2}$
Fr	[-]	Froude number	$u_0^{2} \cdot g^{-1} \cdot D^{-1}$
Re_p	[-]	particles Reynolds number	$\rho_g \cdot u_0 \cdot d_{50} \cdot \mu^{-1}$
	[-]	density ratio	$\rho_p \, \rho_g^{-1}$
	[-]	dimensionless flux	$G_s \cdot \rho_p^{-1} \cdot u_0^{-1}$
	[-]	geometric similarity	$L \, D^{-1}$
	[-]	superficial gas velocity/ minimum fluidization velocity ratio	$u_o \cdot u_{mf}^{-1}$

Acronyms

AD	anno domini
AR	air reactor
ARLS	air reactor loop-seal
ASTM	American Society of Testing Materials
ASU	air separation units
CAD	computer aided design
CCS	carbon capture and storage
CFB	circulating fluidized bed
CFD	computational fluid dynamics
CFM	cold flow model
CLC	chemical looping combustion
CLG	chemical looping gasification
CLOU	chemical looping with oxygen uncoupling
CLR	chemical looping reforming
CSIC	Consejo Superior de Investigaciones Científicas
DLCFB	double loop circulating fluidized bed
EPICA	European Project for Ice Coring in Antarctica
FCC	fluidized catalytic cracking
FR	fuel reactor
FRLS	fuel reactor loop-seal
GDP	gross domestic product
GT	gas turbine
HSE	health safety environment
IEA	International Energy Agency
IGCC	integrated gasification combined cycle
IPCC	Intergovernmental Panel on Climate Change
KIER	Korean Institute of Energy Research
NTNU	Norges Teknisk-Naturvitenskapelige Universitet
OC	oxygen carrier
OEL	occupational exposure limit
R&D	research and development
PDU	process development unit
PSD	particle size distribution
SEM	scanning electron microscope
TGA	thermogravimetric analysis
TSI	total solids inventory
VDI	Verein Deutscher Ingenieure

"O frati", dissi, "che per cento milia
perigli siete giunti a l'occidente,
a questa tanto picciola vigilia

d'i nostri sensi ch'è del rimanente
non vogliate negar l'esperïenza,
di retro al sol, del mondo sanza gente.

Considerate la vostra semenza:
fatti non foste a viver come bruti,
ma per seguir virtute e canoscenza".

(Dante Alighieri, Divina Commedia - Inferno, Canto XXVI, vv 112-120)

"O brothers, who amid a hundred thousand
perils," I said, "have come unto the West,
to this so inconsiderable vigil

which is remaining of your senses still
be ye unwilling to deny the knowledge,
following the sun, of the unpeopled world.

Consider ye the seed from which ye sprang;
ye were not made to live like unto brutes,
but for pursuit of virtue and of knowledge."

(Translated by Henry Wadsworth Longfellow)

1. Ph.D. Thesis organization

1.1. Project overview

The Ph.D. thesis is part of a project called BIGCLC, which was a subproject related to the BIGCO2 research and development (R&D) platform. Since 2011 the BIGCLC project was included in the BIGCCS research centre. The 150kW$_{th}$ chemical looping combustion (CLC) reactor system design, object of the Ph.D. thesis, has been developed within the BIGCO2 R&D platform. BIGCCS will provide the funding to build and commission the 150kW$_{th}$ CLC setup in 2012-2013.

The BIGCLC project consists of several working packages. The main focus is on the construction and commissioning of an innovative reactor system design and the development of new oxygen carriers (OC). In addition, effort is invested also on system simulation and process control, power cycles integration and technological, economical and environmental benchmarking. BIGCLC wanted the reactor system to make a step forward concerning the CLC state of the art, focusing on thermal load, pressurization and utilization of cheap oxygen carriers based on Norwegian ores or industrial by-products.

The design presented in the Ph.D. thesis tries to address the above-mentioned project objectives. It has been developed in a cooperation between SINTEF Energy and Research, the Norwegian University of Science and Technology (NTNU) and the consulting company CO2-H2 Eurl. A thermal load of 150kW has been chosen, because at the time the project started (2007) there were no existing setups of that size. It was decided to develop the project in three steps. First, a design suitable for a 150kW$_{th}$ atmospheric reactor system was defined. Operational flexibility and compactness have been a design priority as well as the utilization of industrial solutions. The OC particles considered in the design phase are those ones under development within the BIGCLC project. SINTEF Materials and Chemistry is in charge of this task and the work is still ongoing; for this reason just preliminary results were utilized to finalize the reactors design, in parallel with published literature from other research groups. The hydrodynamic validation of the design was done by means of the full-scale cold flow model (CFM) test campaigns. The second step consists of the construction, commissioning and testing of the hot 150kW$_{th}$ rig, possibly utilizing the OC developed within the BIGCLC project. The third step consists of re-engineering the presented design to upgrade it for pressurized conditions and test it.

Several pressurization issues have been considered during the reactor system design phase. One of those is the compactness, to be capable to enclose the reactor into a pressurized vessel. Others are the flexibility and robustness of the hydrodynamics, so that the system can better handle pressure unbalances which are bigger than those ones experienced at atmospheric conditions.

The Ph.D. thesis work represents the first of the above-mentioned three steps: the $150kW_{th}$ design development and the CFM reactor system design, construction and testing; fundamental for the $150kW_{th}$ design validation and improvement. The work has been carried out in cooperation with SINTEF Energy and Research scientists and a CO2-H2 Eurl consultant. In addition NTNU master students and laboratory technicians have been involved; the first in the execution of the CFM sensitivity tests, the latter in the reactor system maintenance, modifications, control and measurement (both with the National Instrument Corporation system design software LabVIEW and hardware installation and calibration). The polycarbonate CFM has been built by the French company CONCEPT PLAST SARL and the powder provided by the South African company DMS Powders. The NTNU Panel for Mineral Production and Health Safety and Environment, has been involved in all the aspects related to the particles handling: from the particles sieving, representative sampling and size distribution measurement to the health safety and environment (HSE) evaluations. The powder explosivity tests have been carried out by the Norwegian company GexCon.

1.2. Ph.D. thesis objectives

Consistently with the above-mentioned BIGCLC project objectives, the Ph.D. thesis aims to develop a reactor system design which can represent a step forward with respect to the state of the art for CLC of gaseous fuels. This is especially related to the reactor system operational flexibility and hydrodynamic robustness in order to better integrate it into a power system, including off-design operation and fuel conversion optimization. In addition, the development of a design leading towards chemical looping industrialization has been a thesis objective. Towards this respect the design compactness has been always kept into consideration together with a scaling strategy aiming for bigger sizes, as well as the usage of industrial solutions, whenever possible. These design characteristics have also the long term objective to serve as a basis for

other chemical looping and fluidized beds based technologies which deal with similar issues as well as for pressurized CLC.

1.3. Structure and contents summary

The Ph.D. thesis is structured as a paper collection. Chapter 2 presents the background where the thesis is inserted. First the global warming and the world energy scenario are described, to introduce the importance of carbon capture and storage as greenhouse effect mitigation tool. Afterwards the chemical looping processes are discussed, with main focus on combustion. Currently, chemical looping technologies rely mainly on fluidization engineering, as the presented design does. For this reason, an overview of the OC particles and fluidized bed reactor systems state of the art is provided. Afterwards an overview of the Ph.D. work has been provided in Chapter 3. It starts from the design and cold flow setup existing before the Ph.D. project began and tested during its first phase. The work behind the four papers is summarized together with the achieved results. In Chapter 4 the suggested design improvements, when it comes to design and particle size distribution, have been summarized and experimental results of the improved design are presented. Finally the thesis conclusions are drawn in Chapter 5, together with the recommended future work.

An overview of the four papers constituting the Ph.D. thesis is provided, Figure 1.1. Paper I defines the double loop circulating fluidized bed (DLCFB) design of the proposed 150kW$_{th}$ chemical looping combustion reactor system. A CFM without chemical reactions has been built and commissioned to debug the hot rig design. It is a full-scale model to reduce the

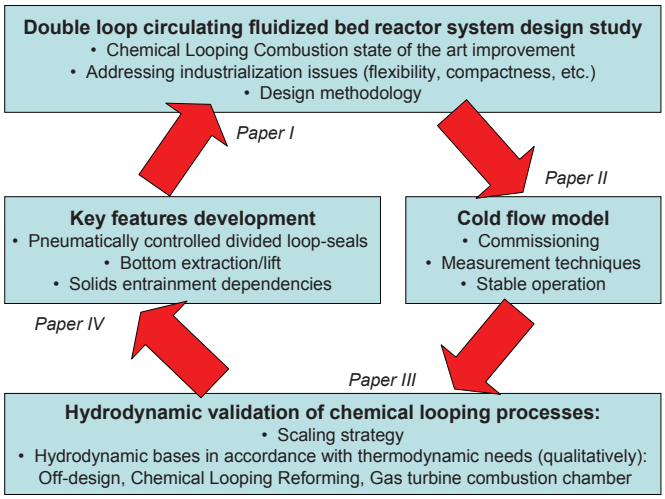

Figure 1.1: Summary of the four papers presented in the thesis with a list of the main issues addressed in each of them.

wall effects. The debugging, from the flux measurement techniques to the separated and coupled operation[1], is presented in Paper II. Paper III is focused on the adopted scaling strategy as well as on the hydrodynamic viability of large-scale chemical looping processes. Finally Paper IV presents a deep analysis of the reactor system operational window as a function of the independent inputs. It assesses the reactors key features performance and suggests improvements which need to be implemented to improve the design presented in Paper I.

The Ph.D. thesis summarizes a wide work, which major focus has been on the cold flow model construction, operation and improvement. Its main achievements, listed in Section 1.5, have been thoroughly addressed and presented. On the other hand the work has been multidisciplinary, touching many of the engineering aspects related to the experimental setup: from carbon capture and storage to the large amount of existing chemical looping processes, from the reactor system integration into power generation processes to its potential application in fluidized beds based technologies other than CLC, from semi-empirical mathematical modelling to fluidization engineering fundamentals, from project management issues to fine powder handling with its health safety and environment impact understanding.

1.4. Papers list

Paper I: **"Design study of a 150kW$_{th}$ double loop circulating fluidized bed reactor system for chemical looping combustion with focus on industrial applicability and pressurization"**, *International Journal of Greenhouse Gas Control (2011), Vol. 5, No. 3, pp. 467-474.* doi:10.1016/j.ijggc.2010.09.005.

Lab-scale feasibility of the chemical looping combustion technology has been proven. Research now is mainly focused on the development of innovative chemical looping processes, on a continuous improvement of the oxygen carriers and on the technology industrialization. A design for a 150kW$_{th}$ chemical looping combustion reactor system is proposed, trying to address design requirements that need to be fulfilled to make this technology applicable at industrial scale. In the base case it is supposed to work with gaseous fuels and inexpensive oxygen carriers derived from industrial by-products or natural minerals. It is a double loop circulating fluidized

[1] In the CFM, the air and fuel reactor can be operated separately, by re-circulating internally the solids that each of them entrains (e.g. for debugging purposes), or can be coupled exchanging mass between each other as it should be for the hot reactor system.

bed where both the air reactor and the fuel reactor are capable to work in the fast fluidization regime in order to increase the gas solids contact along the whole reactor body. They are interconnected by means of divided loop-seals, capable to re-circulate back to the reactor of origin the entrained solids, and a bottom extraction/lift, bringing solids from the fuel reactor to the air reactor. High operational flexibility is aimed, in this way it will be possible to run with different fuels and oxygen carriers as well as in different operating conditions. Compactness is a major goal in order to reduce the required solid material and possibly to enclose the reactor body into a pressurized vessel to investigate the chemical looping combustion under pressurized conditions. The design methodology summarizing all the key decisions taken during the process is presented.

Author contribution: Aldo Bischi is one of the contributors to the proposed 150kW$_{th}$ chemical looping combustion design led by SINTEF. Aldo Bischi contributed to the cold flow model construction and commissioning and he performed the majority of the cold flow model experimental tests and made the result data processing and analysis. Aldo Bischi conceived and wrote the paper with input and comments from other authors.

Paper II: **"Performance analysis of the cold flow model of a second generation chemical looping combustion reactor system"**, *Energy Procedia (2011), Vol. 4, pp. 449-456.* doi:10.1016/j.egypro.2011.01.074.

A scaled cold flow model of the proposed design has been constructed and commissioned to validate the hydrodynamics of the design solutions. First the nozzles design and the share of gas kinetic losses were verified, as well as the solids inventory control and its influence on the reactor performance. Solids flow/flux measurement techniques, a direct and an indirect one, were defined and their reliability evaluated. The air reactor and fuel reactor were first tested separately monitoring their entrainment capabilities and pressure/particles distribution, with main focus on finding the best way of operating the divided loop-seals and testing the protruding cooling panel effect on hydrodynamics. The overall reactor system, combining air and fuel reactor, was also tested. It gave satisfactory results, but the internal return legs of the divided loop-seals were sealed off to avoid back-flow of gas coming from the high pressure reactors bottom sections. Some encouraging results were also achieved reducing primary air and increasing the secondary air height, to reduce the pressure at the reactors bottom sections.

Author contribution: Aldo Bischi is one of the contributors to the cold flow model setup construction. He had a main role in the cold flow model commissioning; including auxiliary devices, health, safety and environmental evaluation and powder handling. Aldo Bischi planned the experimental tests in co-operation with other authors and he led the test execution (done by master students) on a daily basis. Aldo Bischi made all the data analysis and interpreted the results. He made the conclusions in co-operation with other authors. Aldo Bischi conceived and wrote the paper with input and comments from other authors.

Paper III: **"Hydrodynamic viability of chemical looping processes by means of cold flow model investigation"**, *Applied Energy (2012), Article in press.* doi:10.1016/J.apenergy.2011.12.051.

The cold flow model already built and commissioned, can be considered as a platform to study the hydrodynamics of chemical looping processes. A state-of-the-art evaluation within cold flow model testing and scaling criteria was done. The choice of having a full-scale (i.e. 1:1) cold model of the $150kW_{th}$ hot rig design was done, on one hand, to reduce the wall-effects which have considerably larger influence at smaller reactor diameters than on larger ones. On the other hand it can be considered the small scale hydrodynamic copy of an industrial prototype about 10 times bigger. The cold flow model was extensively tested and experimental results are presented. The aimed design condition, mirroring a chemical looping combustion process adapted to steam generation, was achieved successfully and in a stable way. The performance of the reactor system was further tested in off-design conditions to define operational guidelines for the hot operation. In addition, attempts were done to resemble other chemical looping processes (e.g. gas turbine combustion and chemical looping reforming), to get some understanding of how the actual reactor system may behave and consequently provide solid hydrodynamic basis to improve the design for those applications. In all cases, it was possible to find operational conditions capable to satisfy the cold flow model hydrodynamic requirements consistently with the actual high temperature processes.

Author contribution: Aldo Bischi planned the experimental tests in co-operation with other authors and he led the test execution (done by master students) on a daily basis. Aldo Bischi made all the data analysis. He interpreted the results and made conclusions and suggestions for

new tests in co-operation with other authors. Aldo Bischi conceived and wrote the paper with input and comments from other authors.

Paper IV: **"Double Loop Circulating Fluidized Bed reactor system for two reactions processes based on pneumatically controlled divided loop-seals and bottom extraction/lift"**, *Powder Technology* (submitted).

Many industrial processes are based on two reactions: a primary one related to the achievement of the main process objective and a secondary one which is necessary to continuously run the process. Those can be performed simultaneously and continuously by means of two interconnected fluidized beds; the design object of this study is a possible answer to the needs of those processes, especially compactness, flexibility and higher particles concentration in the upper section. The key components of the reactor system are the pneumatically controlled divided loop-seals and the bottom extraction/lift. The divided loop-seals can re-circulate back to the reactor of origin part of the entrained solids. This means that the solids flow that one reactor exchanges with the other one can be smaller than the solids flow entrained by the reactor. The lift compensates the lower entrainment capability of that one of the reactors with less fluidizing gas available and smaller cross-section. Those two features allow to uncouple the solids exchange from the solids entrainment, thus from the reactor fluidization regime. The aim of this paper is to further improve the presented design by means of an intensive test campaign finalized to better understand its operational window size and limits. It was concluded that the design can be further improved by reducing the cyclones' pressure drop due to too high gas velocity at their inlet. Another option towards this respect, is the particle size distribution reduction, this allows going down in gas velocity without reducing the solids entrainment. An increase of the loop-seal overflow height is required to increase its bottom section pressure and improve its stability. The return legs heights can be lifted up to reduce the pressure the loop-seals are exposed to. Finally some interesting dependencies of the entrained solids flux have been found (e.g. cyclone pressure drop), looking at an indirect way to monitor it on-line.

Author contribution: Aldo Bischi planned the experimental tests in co-operation with other authors and he led the test execution (done by master students) on a daily basis. Aldo Bischi made all the data analysis. He interpreted the results and made conclusions and suggestions for

design improvements in co-operation with other authors. Aldo Bischi conceived and wrote the paper with input and comments from other authors.

1.5. Scientific contribution

- Development of a chemical looping reactor system design aiming to address open issues such as conversion optimization, operational flexibility, industrialization and compactness.

- Hydrodynamic validation and performance analysis of double loop circulating fluidized bed (DLCFB) reactor system based on pneumatically controlled divided loop-seals and bottom extraction/lift.

- State-of-the-art comprehensive overview of cold flow modelling scaling strategies. Subsequent synthesis of the two most common scaling approaches strengths into one.

- Construction, commissioning and operation of one of the world biggest cold flow models finalized to the hydrodynamic study of two interconnected fluidized beds.

- Usage of high density fine particles (high density Geldart A) in circulating fluidized bed reactors.

- Finding of promising dependencies of the entrained solids flux from cyclones pressure drop and inlet gas velocities, in order to monitor the solids flux indirectly.

2. Chemical looping technologies and fluidization engineering

2.1. Global warming and energy scenario

At the beginning of the 19th century, Joseph Fourier understood the role played by the gases present in the atmosphere with respect to the thermal equilibrium of the planet [1]; nowadays this role is known as atmospheric greenhouse effect. At the end of the century, Svante Arrhenius [2] saw that an increase of carbon dioxide concentration, including the manmade one due to fossil fuel combustion, may lead to an increase of the average global temperature.

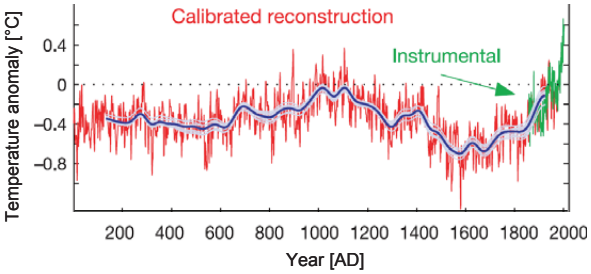

Figure 2.1: Multi proxy reconstruction (red and blues) and instrumental measurements (green) of the Northern Hemisphere mean temperature variation[2] [3].

The global average temperatures of air and ocean have unequivocally increased since mid 20th century. It is confirmed by observational climate data as shown for example in Figure 2.1, where a multi proxy calibrated reconstruction of the temperature in the Northern Hemisphere is presented (red and blues) together with measured data (green) [3]. At the same time also the concentration of anthropogenic greenhouse gases in the atmosphere has been increasing. Those gases are mainly four: carbon dioxide (CO_2), methane (CH_4), nitrous oxide (N_2O) and the halocarbons. All those gases have increased their atmospheric concentration during the industrial era, but carbon dioxide has, by far, the strongest impact, comparing all of them in terms of CO_2 equivalent[3] [4]. The analysis of air bubbles trapped in ice, allowed to evaluate the CO_2 concentration in the far past back to 600000 years ago; in Figure 2.2 the measurements of the ice cores sampled at the Antarctic stations of Vostok and EPICA (European Project for Ice Coring in Antarctica) [5]. The direct measurements of CO_2 concentrations during the last decades are shown in the last part of the graph, whose dramatic increase is represented by the quasi-vertical

[2] Temperature anomaly is calculated with respect to the 1961-1990 average.
[3] CO_2-eq describes, given a greenhouse gas, the amount of CO_2 that would have the same effect towards global warming.

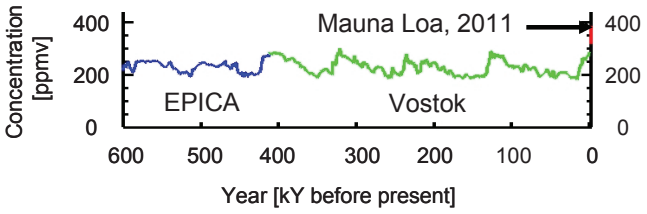

Figure 2.2: CO_2 concentrations derived from EPICA and Vostok ice cores [5]. The red bar at the side indicates the evolution of the Mauna Loa measurements[5].

red line. CO_2 concentration went from the pre industrial value of 280ppmv[4] up to an average value of about 390ppmv, measured at 2011 in the observatory of Mauna Loa, Hawaii (USA) [6].

Nowadays the scientific community widely agrees on the fact that the temperatures increases are very likely[6] a consequence of the observed increase of anthropogenic green house gases concentration in the atmosphere. In addition it acknowledges that the anthropogenic warming is likely to have a discernible influence on many physical and biological systems. This means that there will be a strong impact on the frequencies and intensities of extreme weather, climate and sea-level events and they are expected to have mostly adverse consequences on natural and human systems. For those reasons it will be of utmost importance to reduce greenhouse gas emissions in order to avoid their effects and whether not possible to mitigate it [7].

The path of the world primary energy demand, in Mtoe[7], by fuel and region, for the last years up to 2008 is shown in Figure 2.3 [8]. Those data give an idea of the fossil fuels share of the total energy needs (a). Looking at the regional perspectives, the share of the coal intensive economies of United States and China (b) is impressive. When it comes to the CO_2 emissions by economic sector, about 41% of the total comes from the power sector, 23% from the transport, 16% from the industry and 12% from residential and services. About 50% of the current man made emissions are coming from large stationary CO_2 sources like power plants, refineries or cement and iron industries [9]. In addition there are other values to keep into consideration for each region, like the population growth, gross domestic product (GDP), debt accumulation, energy intensity[8] trends.

[4] Parts per million by volume.
[5] On this time scale, the 50 years of measurements span is less than the thickness of the line, so it appears vertical.
[6] Very likely and likely assess a probability of occurrence respectively above the 90% and 66% [7].
[7] toe is tonne of oil equivalent.
[8] Energy intensity is a way of measuring the economy energy efficiency. It is calculated as units of energy per unit of gross domestic product (GDP).

Data about future scenarios are intentionally not presented, because they may differ rather much depending on the underlying assumptions. Anyhow looking at the actual energy scenario it is possible to understand that in the forthcoming years the fossil fuels will still be the predominant world source of primary energy. The International Energy Agency (IEA), in its World Energy Outlook 2010 [8] presented updated possible scenarios for the upcoming decades. The fossil fuels are well above 50% of the world primary fuel mix by 2035 for all of them, including the "best case scenario". The IEA presents such a kind of study on yearly bases and gives analogous outlooks with respect to fossil fuels. All the factors affecting the primary energy demand are carefully addressed for each different country, from the global economical situation to the technology state of the art, including deployment of technologies that are now approaching the commercialization phase e.g. carbon capture and storage, concentrating solar power and smart grids. It should be mentioned in addition that no completely new technologies, beyond those already known today, are assumed deployable before the end of the projection period.

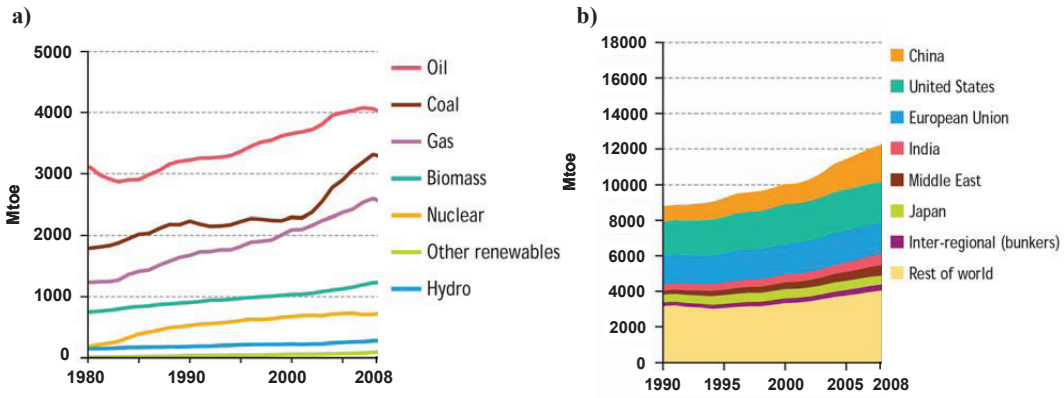

Figure 2.3: World primary energy demand by fuel a) and by region b), updated at 2008, according to the International Energy Agency (IEA) [8].

2.2. Carbon dioxide capture and storage

"Carbon dioxide capture and storage (CCS) or carbon sequestration is a family of methods for capturing and permanently isolating CO_2 that otherwise would be emitted to the atmosphere and could contribute to global climate change" [9]. CCS implementation in correspondence of the big stationary emission sources, can have a crucial role in the next decades

mitigation strategies. It can act as bridging technology, "gaining time" to allow renewable energies development up to total fulfilment of the world energy requirements. This is especially true considering the above-mentioned role of coal in the world primary energy demand: coal is responsible for no less than 40% of global CO_2 emissions, and each year 100GW of new coal-fired power capacity is built [10]. In addition the combination of CCS and biomass combustion, can contribute to negative emissions, reducing the CO_2 concentration in the atmosphere.

Once captured, the CO_2 has to be compressed up to a high pressure and relatively low temperatures. The aim is to have it as a supercritical liquid, in order to transport it and inject it into an underground long term storage site. It can be stored into depleted oil and gas reservoirs, coal formations and saline formations; the last one has by far the largest capacity potential. According to the Intergovernmental Panel on Climate Changes (IPCC) [11], it is likely that 99% or more of such stored CO_2 will be retained for 1000 years.

The aim of this work is neither to find an answer to the sustainable development nor to understand to which extent carbon capture and storage is one of the solutions to global warming. Those are among the most complex challenges humanity is facing and for sure there will not be just one solution. The intention here is to develop further one of the most promising CCS technologies. In this way an additional piece of information is provided to the scientific community and consequently to policy makers, to help taking more aware strategic decisions.

When it comes to the costs of CCS there is still a lot of uncertainty, but they are by far related to the capture, while the transport and storage are minor ones. For this reason the ongoing research activities are mainly aiming to achieve a substantial capture cost reduction and energy penalty reduction. The capture technologies are normally classified in three families: post-combustion, pre-combustion and oxy-fuel combustion.

- The post-combustion is applied to conventional power generation, it is based on processing the exhaust gases in order to chemically or physically remove the CO_2. It is attractive for the existing power plants, as long as it is the best option when it comes to retrofitting. Its main drawback is related to the energy penalty of processing large amounts of flue gases at almost ambient pressure. In fact, the CO_2 is diluted, mainly in the air N_2, being about the 4% of the processed gas with natural gas and 14% with coal combustion.

- The pre-combustion consists of a first reforming step or gasification step aiming the production of synthesis gas (syngas) ideally made of CO, H_2, H_2O and CO_2. The reforming reactions options are several e.g. auto-thermal reforming obtained with a partial combustion of the fuel or steam reforming decomposing the methane by steam and external heat. Afterwards a water gas shift reaction may convert the residual CO in H_2 and CO_2, and the gas flow can be processed to capture the CO_2 and having pure H_2 to use in the combustion process as fuel. In this case the amount of gas flow that needs to be processed is reduced, CO_2 rich and pressurized. In addition some power cycles based on solid fuels gasification, like the integrated gasification combined cycle (IGCC), are already intrinsically realizing part of the pre-combustion capture process. It is expected to be more expensive than the post-combustion techniques because of its complexity and the necessity of dedicated gas turbines. In addition, the combustion of H_2 rich fuel is more exposed to the risk of NO_x formation.
- The third carbon capture family is the oxy-fuel one. It utilizes pure oxygen instead of air in the combustion process, giving ideally just CO_2 and water vapour as exhausts. The H_2O can be easily separated by condensation and the carbon dioxide needs just to be compressed to be sent to storage. One of the drawbacks is the high temperature of such kind of combustion, thus energy losses and NO_x emission, which is handled by means of CO_2 re-circulation (up to 70%) or steam/water injection. The costs of producing such high quantities of oxygen are high. The required amount is about three times more than that one required by pre-combustion techniques. It is done either by means of expensive cryogenic air separation units (ASU) or by means of complex chemical, adsorption or membrane processes.

Each of the above-mentioned carbon dioxide capture methods is capable to reach high capture efficiencies and all their components are currently utilized in some commercial process [12]. The high costs represent the major drawback for all of them to be deployed at gigaton scale. They require high investments and especially the high energy penalties related to operation contribute to high costs. The thermal efficiency penalty for CO_2 capture is about 10% points, few points more or less depending on the technology. This implies the need of focusing in research and development to propose breakthrough technologies aiming to less energy penalty [13]. One of these promising technologies is the chemical looping combustion (CLC).

2.3. Chemical looping processes

All the above-mentioned "conventional" ways of controlling greenhouse gases emissions by capturing CO_2 are inherently related to direct combustion processes, where about 1/3 of the chemical energy of the fuel is destroyed while producing thermal energy [14]. Conventional fossil fuel combustion is highly irreversible because its thermodynamic equilibrium is reached at temperatures much higher than those ones that the materials enclosing the reaction can withstand [15]. The high difference between the energy donor and acceptor will persist even if the combustor and gas turbine (GT) will be improved, making them capable to handle higher temperatures [16]. On the top of it there is the above-mentioned energy penalty related to the capture technology. Those two are the fundamental reasons of the high energetic, thus economic, penalty of the CCS technologies.

The above-mentioned issues can be tackled following new chemical routes which innovate the combustion process in a way that utilizes stepwise the fuel chemical energy no matter the carbon capture, but in addition it separates intrinsically the combustion products streams [13]. These combustion requirements can be fulfilled by means of chemical looping processes. A chemical looping process occurs when its underlying chemical reaction takes place following a reacting scheme consisting of multiple sub-reactions. These sub-reactions make use of chemical intermediates which react and regenerate in a cyclic manner. This allows designing the chemical looping processes sub-reactions to reduce the exergy losses as well as to produce CO_2 in a different stream, easy to separate [17]. Several processes can be developed relying on this principle: from the chemical looping combustion which is the core interest of this work to the chemical looping reforming (CLR) and gasification (CLG) respectively focused on power generation and on hydrogen and syngas production.

Chemical looping conversion of carbonaceous fuels was considered first to produce syngas or pure carbon dioxide [18 and 19], then to reduce the exergy loss of a conventional combustion process [15 and 16]. The combination of these two features makes chemical looping processes of strategic importance with respect to CCS. Chemical looping combustion takes place in two steps (Figure 2.4), where a metal working as Oxygen Carrier (OC), gets oxidized and reduced in a cyclic manner, carrying the oxygen from one reactor to the other. First the OC has a strong exothermic reaction with the oxygen of the air injected in the air reactor (AR), from $MeO_{\alpha-1}$ to MeO_{α}. The air heated up and depleted of the oxygen can be utilized for example to

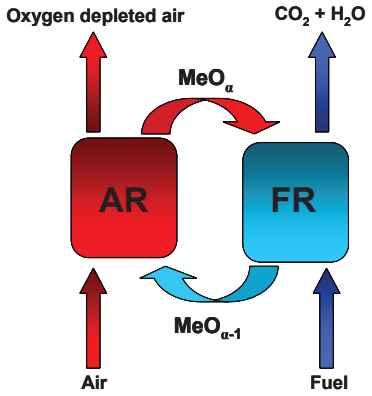

Figure 2.4: Schema of the chemical looping combustion (CLC). The oxygen carrier $MeO_\alpha/MeO_{\alpha-1}$ is oxidized exothermically in the air reactor (AR) and reduced endothermically or slightly exothermically in the fuel reactor (FR).

produce steam or to expand in a turbine if the above-mentioned reaction takes place in a pressurized environment. Afterwards the oxidized OC is sent into the fuel reactor (FR) and its oxygen reacts with the fuel, being reduced from MeO_α to $MeO_{\alpha-1}$. The reduction reaction is endothermic or slightly exothermic, depending on the OC material and fuel used, and it generates an almost pure stream of CO_2 and steam. The heat required by the endothermic reaction is carried by the OC, which can determine almost the same temperature in the two reactors when high circulation is achieved. The water vapour can be removed by condensation leaving the CO_2 available for storage, after being cooled and pressurized up to supercritical conditions.

The overall reaction obtained summing the oxidation and reduction of the OC is equivalent to the conventional combustion of the fuel and releases exactly the same amount of energy. These are the oxidation and reduction reactions for a generic OC defined as $MeO_{\alpha-1}$ reacting with a generic hydrocarbon C_xH_y:

$$MeO_{\alpha-1} + \frac{1}{2}O_2 \leftrightarrow MeO_\alpha, \tag{2.1}$$

$$C_xH_y + \left(2x + \frac{y}{2}\right)MeO_\alpha \leftrightarrow xCO_2 + \frac{y}{2}H_2O + \left(2x + \frac{y}{2}\right)MeO_{\alpha-1}. \tag{2.2}$$

The overall reaction obtained summing the above-mentioned ones is equivalent to the conventional combustion one and produces exactly the same amount of energy:

$$C_xH_y + \left(x + \frac{y}{4}\right)O_2 \leftrightarrow xCO_2 + \frac{y}{2}H_2O. \tag{2.3}$$

Auto-thermal reforming can be executed with the same system. This happen whether the amount of oxidized oxygen carrier sent to the fuel reactor is reduced down to a level where the carried oxygen is below the stoichiometric one, required having complete fuel combustion. It also

brings heat and acts as catalyst; in those cases it is important that the selected OC has good catalytic properties towards steam reforming of natural gas like the Ni-based ones [20]. In this case the reaction in the AR is the same as in the combustion case, while in the FR the partially oxidized fuel generates synthesis gas (CO and H_2):

$$C_xH_y + xMeO_\alpha \leftrightarrow xCO + \frac{y}{2}H_2 + xMeO_{\alpha-1}. \quad (2.4)$$

Syngas is also generated by the strongly endothermic steam methane reforming reaction injecting also steam in the FR:

$$C_xH_y + xH_2O \rightarrow xCO + \left(x + \frac{y}{2}\right)H_2. \quad (2.5)$$

Obviously the amount of heat generated in the AR, which needs to be extracted from the system to keep the thermal balance, reduces in correspondence of oxygen transport reduction and steam injection. In this way it can be reduced down to a level where the process is auto-thermal.

It has been proven that chemical looping combustion is one of the most promising technologies when it comes to net power efficiencies [21, 22 and 23] and capture costs [24]. The best performance is expected when integrated into a combined cycle, with the CLC reactor system tacking the place of the gas turbine combustor. In this way it can drive a GT with the depleted air and the hot exhausts can be used to generate steam for a bottoming Rankine cycle. In some configurations additional integration is proposed. A CO_2 turbine can be added to the process as well as another gas turbine after a post combustion process of the depleted air. In fact the oxygen depleted air still contains enough oxygen to combust extra fuel, but some CO_2 emission has to be tolerated in this case. Several are the first and second law studies showing the high efficiencies [21, 22 and 23] that can be reached in this way with gaseous fuel; some studies also highlight low costs in addition to the high efficiencies [24]. The main challenges are substantially the feasibility of a pressurized system and the capability of the oxygen carrier to withstand red-ox cycles at a temperature going above 900°C. The chemical looping reforming of gaseous fuels has been evaluated promising as well; a thorough evaluation of the advantages in comparison to methane steam reforming has been done by Pröll et al. [25]. In addition it is especially competitive whether pressurized, in this way the energy penalty of the H_2 pressurization after production is avoided [26 and 27].

Atmospheric chemical looping combustion of gaseous fuels is a promising option for heat generation (e.g. steam production for industrial processes) with CO_2 capture. Up to a certain size, this is an interesting option as well for combined heat and power generation and for power generation with CO_2 capture. Whether not pressurized, the chemical looping combustion of gaseous fuels for large-scale power generation has to compete with the high efficiencies of combined cycles, which compensate the efficiency losses induced by the introduction of "conventional" capture technologies. For those reasons many of the CLC research activities, at this stage of technology development, are related to solid fuels combustion, like coal [17, 28]. Those cheaper fuels are utilized for steam cycles without being capable to reach the combined cycles high temperatures and efficiencies, not even for the more efficient ultra-supercritical steam cycles. Another option to utilize solid fuels is using a gasification process which provides gaseous fuel to utilize in combined cycles, like in the IGCC process. The lower efficiencies, compared to combined cycles, and the energy penalty of the "conventional" carbon dioxide capture technologies integration, make atmospheric CLC potentially competitive for solid fuels both in combustion and gasification processes.

Focus of the current work is on the chemical looping combustion of gaseous fuels. The experimental device is designed to validate an atmospheric CLC design for steam generation. Some reforming issues are also addressed as well as some of the needs of pressurization/GT application have been considered. The long term objective is to develop a design architecture that can be hydrodynamically flexible and stable, so suitable also for other chemical looping processes. The setup object of this work is designed for combustion, as shown in Figure 2.4, by keeping stationary the reactors and circulating the OC: AR and FR are two fluidized bed reactors exchanging metallic particles acting as oxygen and heat carriers.

2.4. Chemical looping technologies

A brief overview of the approaches proposed worldwide to realize the chemical looping processes is provided in this section. The use of interconnected fluidized beds is by far the most common, it has already been tested on experimental basis and it is the chosen approach for the work presented in this thesis. In Section 2.5 and 2.6 it will be carefully addressed from particles and reactor system side, respectively.

Another option consists of alternating the gas streams and keeping stationary the reactor containing the metal oxide. It is based on packed bed technology where several reactors are operated dynamically. In this way the reactors are alternatively exposed to reducing and oxidizing conditions in a frequency that allows continuous feeding of the downstream apparatus e.g. heat exchangers or gas turbine for pressurized conditions. The main advantage is to avoid the challenge of separating particles and gas. This is especially important to avoid gas turbines blades damages. In addition it is aiming higher compactness and better utilization of the OC, optimizing its degree of oxidation. Such packed bed chemical looping reactors still present challenges for large-scale deployment. The necessity to deal with high temperature and high flow rate in a gas switching system is problematic. At the same time the bed particles replacement can be costly, so they need to be mechanically, chemically and thermally stable [29 and 30]. For the time being, the principle has been proved experimentally in a lab-scale device by Noorman et al. [31]. Also onboard hydrogen production for cars based on micro packed bed reactors has been proposed. Its goal is to tackle the hydrogen storage problem either with the possibility to regenerate the spent particles in external fuel stations fuelling the engine with water [17] or absorb on board the CO_2 generated fuelling the engine with methane [32].

A further concept which has been proposed to realize chemical looping combustion is the rotating reactor. It consists of a doughnut-shaped fixed bed rotating between the two gas streams: air and fuel. It is interesting because of compactness and higher flexibility compared to the stationary fixed beds mentioned previously. It does not require complex valving systems and the gas exits from the system radially, in a way that the increasing reactor volume can fit, expanding it, the gas volumetric flow which increase due to reactions and heating. In addition, large-scale experience comes from rotating heat exchangers used to preheat air streams e.g. Ljungström® regenerative air preheaters [33]. The particle fragmentation can be an issue here as well as in the above-mentioned case. The main challenge for the time being seems to be the gas mixing between the two separate gas streams. The concept has been widely tested on a lab-scale experimental set up by SINTEF Material and Chemistry [34] and important information has been collected to improve the design.

Other interesting chemical looping innovative ideas have been proposed. One is the usage of coal particles both as fuel and oxygen carriers from fuel to air reactor without the need of an intermediate OC. It uses the coal property of up taking oxygen atoms at its surface

(chemisorption) at moderate temperatures, about 500°C, and desorbe it at higher temperatures, about 700°C, in an oxygen-free atmosphere. It has been tested in a thermogravimetric discontinuous process [35]. Also the usage of direct combustion of liquid metal has been proposed and thoroughly studied in its thermodynamics. The purpose is to use different metals in liquid and gas phases both as OCs and turbine working fluid [36].

2.5. Oxygen carrier and particle characterization

The oxygen carrier is playing a crucial role in the chemical looping processes performance. R&D activities for improved OC are fundamental in order to achieve commercial success of CLC. The chemical looping reactor proposed in the thesis is a fluidized bed system, consequently the oxygen carrier is a powder which will circulate between the air and fuel reactor, being continuously oxidized and reduced. The particles used for such kind of interconnected fluidized bed system usually have a density and size distribution which make them belong to group B or A of the Geldart classification [37], Figure 2.5. In this work, Group A particles were selected, which means fine particles like for the well known and mature fluid catalytic cracking (FCC) processes. FCC was the first fine powder application in fluidization engineering [38]. The Geldart group and more specifically the density and particles size distribution (PSD) within the same group are chosen in order to fulfil the design requirements.

Fine A particles means higher surface available for the reactions to take place. This is beneficial also for the heat transfer coefficient, which is larger for smaller particles. At the same time the heat transfer coefficient increases with the particles suspension density, which depends on the fluidization regime; an example of both the dependencies is shown in Figure 2.6 [39]. Also the fluidization regimes hydrodynamics depend rather much on the particles size and material density. As shown in this thesis, those particles properties have to be selected consistently with the required hydrodynamic performance and design constraints e.g. finer or lighter particles bring more entrainment for the same superficial gas velocity. On the other hand, particles should not be too small, because it will lead to Geldart group C particles which means cohesive and difficult to fluidize because of interparticle forces. Too small particles will also be more difficult to handle within the process (e.g. cyclone efficiency) and from the health safety and environment (HSE) point of view.

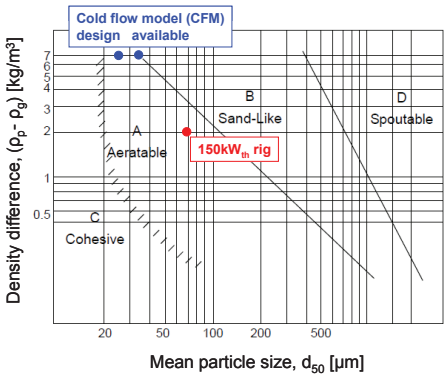

Figure 2.5: Geldart particles classification [37]. Points characterizing the particles utilized later on in the thesis are shown in the graph: the CFM design particles and available particles and the 150kW$_{th}$ hot rig particles.

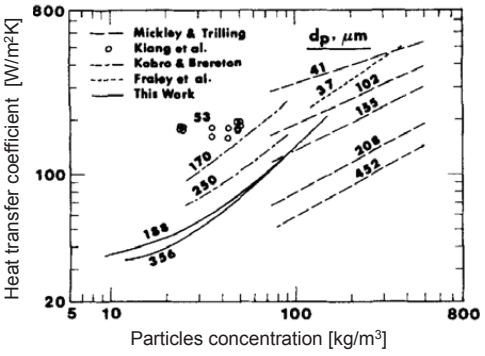

Figure 2.6: Comparison of heat transfer coefficients, h, as function of the suspension density, and particles diameter, d_p [39].

The OC production methods are several and they affect the oxygen carrier performance. For solid fuel combustion, minerals and industrial wastes have been tested as OC. Usually after a preliminary screening the most promising candidates are carefully characterized by means of thermogravimetric analysis (TGA). A second step is testing the particles, in a cyclic manner, in batch fluidized bed reactors. In both cases the particles are exposed alternatively to air and fuel, the aim is to study their reactivity, conversion and mechanical strength. Afterwards they are tested continuously in fluidized bed systems, to resemble the same kind of environment as in a CLC reactor, like in Chalmers University of Technology and Instituto de Carboquímica-CSIC of Zaragoza, where small reactor systems are used extensively to accomplish this task [40 and 41].

The oxygen carrier composition is usually based on a transition metal, such as Fe, Mn, Cu and Ni. This is setting the theoretical amount of oxygen that the oxygen carrier can take up (R_0). The addition of an inert material is required to gain mechanical strength; it is also believed to increase the porosity and reactivity of the particles. This means also that the share of active material will be less; the amount of inert is a parameter that can be varied, within certain limits, while designing the OC for a certain process. Actually, part of the active material content can change during operation either because of changes in the particles structure or because located too deep in the particle structure to be capable to participate to the reactions; Kolbitsch et al. [42],

during experiments, found about 35 wt% of active material in an OC having a theoretical value of active material equal to 40 wt%.

The material reactivity is important to fully characterize the OC performance. It provides an understanding of how much of the transport capability of the material can be actually used. An example is shown in Figure 2.7; it is a zoom of the reduction and oxidation curves, once stabilized, presented by Fossdal et al [43]. Those tests were done by 30s oxidation and 30s reduction, with 30s of flushing with nitrogen in between. This Mn ore is that one originally utilized for the design of the presented set up. The tests were done in a thermogravimetric balance, but in the interconnected fluidized bed system, the particles will not have so much time available to complete the reactions, which means that just part of the theoretical R_0 will be exploited. Such kind of experimental data help to gain an understanding of the exploitation of the oxygen capacity (ΔX) and take a qualified guess in order to design the reactor in a conservative way.

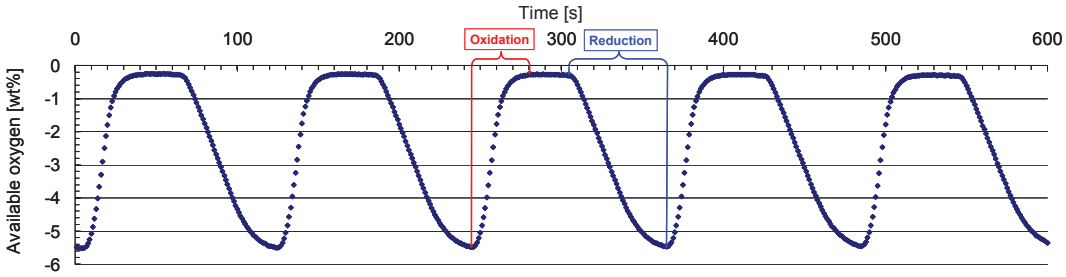

Figure 2.7: Behaviour of the measured oxygen capacity, in weight percentage, during cyclic reduction and oxidation of Mn ore at 1000ºC, those are the data utilized for the design [43].

Figure 2.7 shows also how the oxidation reaction is faster compared to the reduction one, this is a typical issue related to CLC. The reduction reaction actually continues during the flushing. The reaction rate usually depends also on the OCs conversion during the oxidation and reduction reaction, being quicker at the beginning of the reactions when the OC is fully reduced, for the oxidation reaction, or fully oxidized, for the reduction reaction. This can be noticed looking at the gradients of the reduction oxidation curves of the batch-wise tests like the presented ones. The reason is that the gas reacts first with those parts of solid particles easier to access while afterwards it is increasingly more difficult with respect to mass transfer. Studies have been done on OC samples taken from continuously operating systems, to understand more

realistically the impact of this phenomenon. Those have proven that, no matter which is the oxidation state of the particles entering the reduction reactor, they will behave as fully oxidized, in terms of reaction rate. This means a faster reaction rate which helps to achieve a better fuel conversion [44]. The amount of oxygen the oxygen carrier can take and its oxidation and reduction rate are used to conservatively estimate the required solids circulation and required residence time necessary to have full fuel conversion.

Depending on the kind of fuel utilized it is necessary to know how the OC behaves with respect to the presence of impurities, like sulphur compounds. The knowledge of mechanical properties of the particles is important in order to make life and cost estimates and to set the maximum temperature the OC can operate without sintering. The temperature will change the kinetics which usually improves for higher temperatures. As already mentioned, also the particles size influences the reactions rate, which gets higher for smaller particles.

Up to 2010 more than 700 materials have been produced and tested. Interesting and comprehensive overviews have been given by Professor Lyngfelt [45 and 46] and Professor Adánez [47] in their keynote lectures at the "1st international conference on chemical looping". Table 2.1, is summarizing the most important characteristics of the materials. Ni- based materials are the more reactive and having high oxygen transport capability, but at the same time those ones which cannot give full conversion of the fuel, maximum 99-99.5% with methane because of thermodynamic restriction. Ni-based OCs are the more expensive and also the more harmful, but there is a lot of large-scale experience because of the importance of Ni in catalysis. Cu- based materials have a high reactivity and can reach full methane conversion. They have both the reactions exothermic; also the reduction reaction is slightly exothermic, leading to a more uniform heat distribution between the reactors. It has the drawback of having lower melting temperature compared to the other materials. In addition it should be mentioned that some Mn- and Cu-

	Fe	Mn	Cu	Ni
Oxygen transport capability (R_0)	-	-	+	+
Reactivity with CH_4*	-	+	+	+
Purity CO_2	+	+	+	-
Melting point	+	+	-	+
Cost	+	+	+	-
Health and environment	+	+	+	-

*Significantly higher reactivity with CO and H_2.

Table 2.1: Summary of the most important characteristics of different oxygen carrier materials [47].

based oxygen carriers have the property to release gaseous oxygen at high temperature. This means that the released oxygen will react directly with the fuel giving better combustion, which is especially important in the case of solid fuels. Ideally the need of a carbon stripper step separating the unreacted char particles from the OC may be avoided, thus avoiding the char going from FR to AR. This phenomenon has been called the CLOU effect, chemical looping with oxygen uncoupling [48].

Some experimental studies have been performed to evaluate the OC behaviour under pressurization. García-Labiano et al. [49] and Abad et al. [50] assessed by thermogravimetric analysis that pressurization had a negative effect on the reaction rate for all the materials (Cu-, Fe- and Ni- based) tested. CO and H_2 were used as fuels. They speculate that it may be a consequence of changes in the internal structure of OC at high pressures. Siriwardane et al. [51] tested under pressure a packed bed of Ni- based material. In this case, there was a performance improvement with a significant reduction of the time required for conversion. Ortiz et al. [52] tested a Ni- based material under chemical looping reforming conditions, semicontinuously in a fluidized bed. Tests were done for different reaction temperatures and OC to fuel molar ratios, without giving negative effects when it comes to the distribution of the process gas product. Xiao et al. [53] studied coal combustion and found an improvement of the reduction reaction of their iron ore based material, both with respect to fuel conversion and OC reduction rate. This was the consequence of an improvement of the gasification rate of the coal as first step which led to the combustion reaction rate improvement accordingly. The performance peak is at about 5bar, while it is worsening going higher in pressure.

Summarizing, on one hand the pressure effects are very much depending on several case specific factors like the type of oxygen carrier, fuel and pressure range. This means that specific tests need to be carried on the selected material at the same pressure the reactor will be operated. On the other hand it is possible to conclude that it will have important consequences from a reactor system point of view. In fact, x times higher pressure brings about x times higher density of gas, in case of ideal gas assumption. This means that, keeping the same thermal load, the volume flow of gas available to fluidize the reactors will be x times smaller, while the mass of reactants in the reactors will be the same. So the challenge is to provide the same amount of solids exchange between the reactors in order to accomplish the reactions with just 1/x of the volumetric gas flow available. In fact, in many fluidized bed systems the volumetric gas available

is also utilized to control the solids exchange, as partially done in the design presented in this thesis. In this way, it will not be possible to simply keep the same design as the atmospheric case and just increase x times the mass flows of gases to have the same volumetric flow as before, thus the same gas velocities. This will most likely provide the same solids exchange as in the atmospheric case, but the solids capacity of transporting and releasing oxygen, as we have seen, will not be enough to react with the higher amount of fuel because the oxygen carrier performance does not necessary improve for high pressures. The issues highlighted in this paragraph need to be kept in mind while designing chemical looping processes for pressurized applications.

2.6. Chemical looping fluidized bed reactor systems

Fluidized beds systems have been applied for decades in a wide range of industrial processes [38], from combustion or gasification of solid fuels [54 and 55] to hydrocarbon cracking with more than 400 units in operation worldwide [56]. They operate continuously, provide a homogeneous temperature inside the reactors and tolerate a wide spectrum of PSD. In addition some of those deal with complex processes consisting of two reactions taking place simultaneously. The FCC is a good example; one reactor is cracking endothermically heavy hydrocarbons by means of catalytic metallic particles used also as heat carrier, while the other reactor regenerates the metallic particles from carbon deposition and produces the heat required by the process. The usage of fluidized beds systems is, for the time being, the best option for the industrial development of chemical looping technologies.

Above 4000h of operational experience for CLC have been achieved all over the world, utilizing different fuels, oxygen carriers and fluidized bed systems. More than 700 materials based on Ni, Co, Fe, Cu and Mn have been used in several facilities with a thermal load in the range of 0.3 and 140kW. This proved that almost 100% conversion can be reached together with 100% of CO_2 capture as summarized by Prof. Anders Lyngfelt in a wide overview [46]. Looking at those CLC setups it is possible to notice how the reactors design has evolved. The main objective of the first CLC reactors, such as the 10 kW_{th} units, developed at Chalmers University of Technology [57] and at the Instituto de Carboquímica - CSIC [58] was to demonstrate the feasibility of this technology and it was done with natural gas. After this first step, research

started to be focused towards the solution of other more specific problems. The $10kW_{th}$ prototype built and operated by IFP Energies nouvelles and Total, has among its main objectives a good control of the solids flow exchanged between the reactors. This is realized by means of bottom extraction/lifts utilized to exchange the solids among air and fuel reactors, both bubbling beds [59]. A second $10kW_{th}$ reactor has been built and operated at Chalmers University of Technology to utilize solid fuel: petroleum coke and bituminous coal. The solid fuel CLC concept was proved and the separation of unreacted coal particles from the oxygen carrier was addressed by means of a carbon stripper after the bubbling bed FR [28]. The $10kW_{th}$ reactor of Southeast University tested coal and biomass as fuel, having a spouted bed as FR [60]. The Alstom $15kW_{th}$ prototype has a high integrated design which utilizes loop-seals with double exits to be capable to re-circulate part of the solids back to the reactor of origin, reaching 99% of methane conversion with Ni based oxygen carrier [45]. The Korean institute of energy research (KIER) had an earlier $50kW_{th}$ prototype with a bubbling bed FR connected to the circulating fluidized bed (CFB) AR with a slide valve [61]. Recently KIER presented a new design with the same thermal load; here both the reactors are bubbling beds and act as well as loop-seal because the downcomers are immersed in the beds. The aim of this setup is to be pressurized up to 6 bar [62]. Other small sized setups exist like the Chalmers 300W [40] and the Instituto de Carboquímica - CSIC [41] 500W ones. Those are usually utilized to validate, with continuous reduction/oxidation operation, the performance of the OCs resulted more promising during the batch-wise tests (Section 2.5).

The $120/140kW_{th}$ reactor system of Vienna University of Technology [42, 44 and 63] is the experimental set up which reached, for the time being, the biggest thermal load and addressed the most scale-up issues. It is compact, because it utilizes a turbulent circulating fluidized bed as FR instead of a bubbling bed. Bubbling beds require big dimensions and inventory to go up in scale, in this way the gas velocities can be low and gas slip is avoided. This design, shown in Figure 2.8 a), has proven to be intrinsically stable from hydrodynamic point of view. The bottom loop-seal creates a hydraulic link between the two reactors, therefore a variation of solids entrainment from the AR is automatically compensated by the mass, thus weight, accumulating in the FR which pushes as a consequence more or less solids back to the AR. This design has proven to be capable to reach high solids exchange and to control the solids circulation, while at the same time the FR operation can be tuned to optimize the fuel conversion utilizing the FR internal re-circulation. This flexibility, including part load, is fundamental to integrate the reactor

system into a power cycle [63]. In addition this setup was also used as auto-thermal reformer, reducing the solids, thus oxygen, exchange [25]. The compactness, stability and flexibility of this configuration are a milestone for the chemical loping reactor system development and scalability. In fact, as an example, it is currently used as basis to develop a FR capable to combust solid fuels by means of some FR modifications, Figure 2.8 b). The FR is divided into several vertical sections after cross section reductions and its fluidization velocity is reduced, this implies counter-current flow inside the reactor body as well as high particles density for each of the above-mentioned vertical sections [64]. In addition also an up-scaling of the original design, for gaseous fuels, up to $10MW_{th}$ demonstration plant is ongoing. The project has been presented and a scaled model without chemical reactions is under construction to validate it [65].

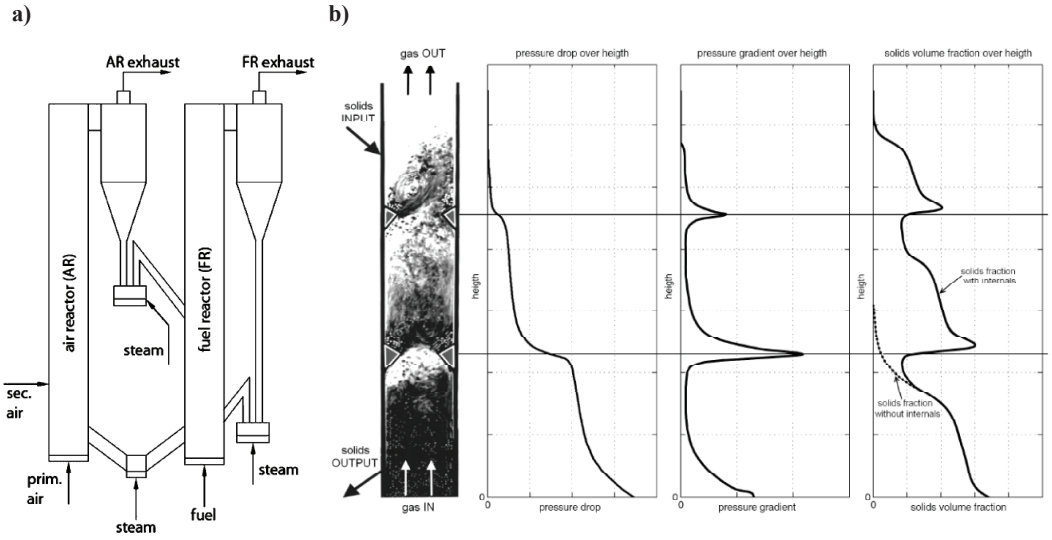

Figure 2.8: Principle setup of the dual circulating fluidized bed reactor system of Vienna University of Technology [63] a). On the right, b), a zoom is shown of the fuel reactor body after internals were added. Qualitative pressure drop, pressure gradient and solids volume fraction are illustrated [64].

As mentioned in the chemical looping processes Section 2.3, pressurization has a primary importance. It is essential to make the chemical looping combustion and reforming of gaseous fuels competitive. Up to now, no experimental fluidized beds reactor systems for pressurized chemical looping processes have been built and operated successfully. Just batch-wise tests were

done under pressurization; Section 2.5 provided a short overview of the results which have shown to be case specific, anyhow big kinetics improvement should not be expected. When it comes to the reactor system, just few authors tried to address the challenges that can be expected. In fact, pressurized circulating fluidized bed is not a mature technology; there were a lot of research activities going on early nineties which led to construction of some pilot plants in order to integrate coal combustion with gas turbines [66]. Their problematic performance together with the higher efficiency of supercritical steam boilers, reduced rather much the interest for that technology. One of the main concerns related to pressurized CFBs, was the low availability of the plant both because of the higher incidence of breakages due to complexity and longer procedure to shut down and depressurize the system in order to do maintenance [67]. Few are the studies about how the pressure increase will affect the solids flow patterns inside the reactor body. According to Richtberg et al. [68] it will actually lead to a more homogenous axial and radial solids distribution. While the gases will increase their density linearly with the pressure, the particles concentration in the reactors and their oxygen uptake will not change so much. In addition the chemical looping processes consist of two reactors whose difference in pressure may create a challenge to the overall reactor system operability. At pressurized conditions the pressure unbalance will be amplified, making bigger the challenges faced at atmospheric conditions, like those ones described in the thesis (Paper II, III and IV). All these facts do not make the atmospheric CLC designs directly utilizable under pressurized conditions, but a re-engineering is required.

The research groups previously mentioned as well as other ones are increasing their effort in chemical looping combustion, presenting new reactor systems and configurations. Many of them have focus on coal combustion [69 and 70] as well as liquid fuels [69], gasification [17] and hydrogen production [71]. Some of them combine, for gasification and H_2 production purposes, the chemical looping process based on metallic oxygen carriers either with their capability of having more than two oxidation levels or with the CO_2 capture capability of limestone typical of post-combustion carbonation/calcination loops [17, 71 and 72]. There are also other ongoing industrial projects aiming to go up in scale, reaching the MW size, like Alberta Innovates-Technology Futures [73], Bertsch Energy together with Vienna University of Technology [65 and 74], Total together with IFP Energies nouvelles [75] and Alstom [76]. The latter is now commissioning a 1 MW_{th} coal-based setup at the Darmstadt University of Technology [77] as

well as a 3 MW_{th} limestone unit. The calcium is used instead of the metallic OC because of its capability of reacting with CO_2 and O_2, thus carrying them. Ca and CaS give $CaCO_3$ and $CaSO_4$, respectively, with the exothermic reactions.

3. 150kW$_{th}$ chemical looping reactor system design and cold flow model validation

Several experimental setups worldwide have successfully proven the lab-scale feasibility of atmospheric chemical looping combustion (CLC). The aim, at this stage, is to bring the chemical looping combustion stepwise towards commercialization being capable to develop configurations suitable for industrial applications. At the same time, processes with a higher degree of complexity are under development for hydrogen production, liquid and solid fuels combustion, gasification as well as pressurized applications for combined cycles. The majority of the ongoing studies, existing setups and up-scaling plans, are based on fluidized bed systems, with special focus both on oxygen carriers and reactor system development.

The overview provided in the previous Chapter represents the chemical looping state-of-the-art where this thesis is put into a context. The aim here is to develop a reactor system design which can be at the same time hydrodynamically flexible and robust, in a way that can manage high fuel conversion and good off-design performance while fulfilling the system downstream requirements. Considering that such kind of fluidized bed processes cannot be scaled linearly [78, 79 and 80], also a step forward with respect to reactor size is aimed.

3.1. Preliminary reactor system design.

A small-scale cold flow model (CFM) was built by SINTEF Energy and Research in order to verify the hydrodynamics of a proposed CLC design with 100kW of thermal load. A drawing and a picture of the Lexan® model are shown respectively in Figure 3.1 a) and b). The air reactor (AR) was made of a wider bottom section and an upper riser with smaller cross section. The fuel reactor (FR) was a bubbling bed in order to get lower superficial gas velocities because of the slower oxygen carrier (OC) reduction kinetics. This was the same design architecture of the first successful chemical looping combustion setup, the Chalmers University of Technology 10kW$_{th}$ [57], but linearly[9] extended at a larger size. The utilized particles were based on polystyrene having a density of about 1050 kg·m^{-3} and a mass median diameter, d_{50}, of 140 μm; they belong to the Geldart group A. The CFM design was meant to be a smaller scale of the hot setup, without following any specific scaling strategy.

[9] Linear scaling refers to the same design architecture re-proposition at a bigger size. It does not mean that the 10 kW$_{th}$ prototype dimensions or design solutions have been taken and linearly increased by a scale of 10 up to 100 kW$_{th}$.

a)

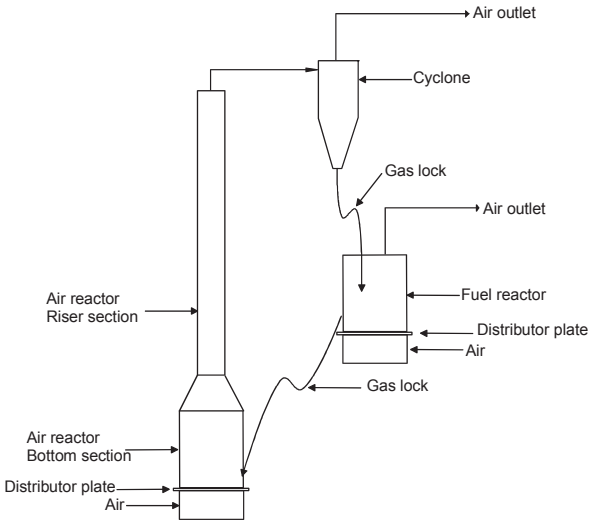

b)

Figure 3.1: Drawing a) and picture b) of the cold flow model (CFM) utilized to validate the hydrodynamics of a preliminary design of the chemical looping combustion reactor system object of the presented work.

Many of the preliminary design solutions are not suitable for industrial applications. For example the usage of perforated plates instead of nozzles may determine uneven fluidization and increase the back-sifting risk. In addition the selected seal pots and especially their return legs are not capable to circulate and control high solids flows e.g. they have a too small cross section and too long horizontal extension, which does not allow operational flexibility. The cyclone, a conventional air cleaning one, is not capable to handle high AR solids entrainment and the inlet duct is too long which implies the formation of particles dunes. In addition the FR will need a filter system or a cyclone to collect the elutriated fines.

A preliminary test campaign with this device was done facing many challenges. A thorough analysis of all those challenges was carried on, component by component, together with a deep analysis of the chemical looping and fluidization literature to understand the experienced

phenomena and the chemical looping technologies needs. It was concluded to radically modify the single components and the reactor system architecture as well as the adopted scaling strategy.

3.2. Double loop circulating fluidized bed (DLCFB) reactor system.

The proposed design architecture is based on two circulating fluidized beds interconnected by means of pneumatically controlled divided loop-seals and bottom extraction/lift, Figure 3.2. It is compact compared to the existing chemical looping setups and many design solutions are taken from industry. One of the most promising Manganese-based oxygen carriers developed by SINTEF Materials and Chemistry was utilized as design basis for the presented design. An example of its oxidation-reduction curves has already been shown in Section 2.5, Figure 2.7 [43]. The design is sized to be used with gaseous fuel and work as steam boiler; methane in the specific case. Anyhow such kind of architecture is meant to be flexible with respect to OCs and to be extrapolated to other chemical looping applications. The thermal load, 150kW, was chosen to go higher in size compare to the state of the art at the project start up. The reactor system is meant to be cooled by means of the insertion of protruding cooling panels in the AR body and eventually also in the FR. The double loop circulating fluidized bed (DLCFB) design features are described in Paper I [81]. Figure 3.2 shows that both the air reactor and the fuel reactor are circulating fluidized beds (CFB), capable to work in the fast fluidization regime in order to increase the gas solids contact along the whole reactor body. High operational flexibility is aimed at utilizing the above-mentioned divided loop-seals and bottom extraction/lift.

Both the air and fuel reactor divided loop-seals (ARLS and FRLS) are fluidized by means of three bubble caps (central, external and internal) to exert a control over the solids direction. In this way it will be possible to re-circulate back to the reactor of origin part of the solids each reactor is entraining. In addition, there is a lateral injection in the downcomer to avoid particle de-fluidization; deep Geldart A particles beds are more exposed to the risk of partial defluidization and consequent gas bypassing. The above-mentioned divided loop-seal details are shown in Figure 3.2, where an example of air reactor loop-seal operation is presented. The AR loop-seal is there circulating solids just through the external return leg without any internal re-circulation of solids; in this specific case the internal return leg is not in use[10]. In the loop-seal

[10] The term return leg “not in use”, is not referred to a specific loop-seal return leg, but to that one, if any, of each loop-seal return legs which is not utilized during a specific test. This happen whenever a loop-seal is utilized to circulate the solids 100% on one side (Figure 3.2), the return leg facing the other side is “not in use”.

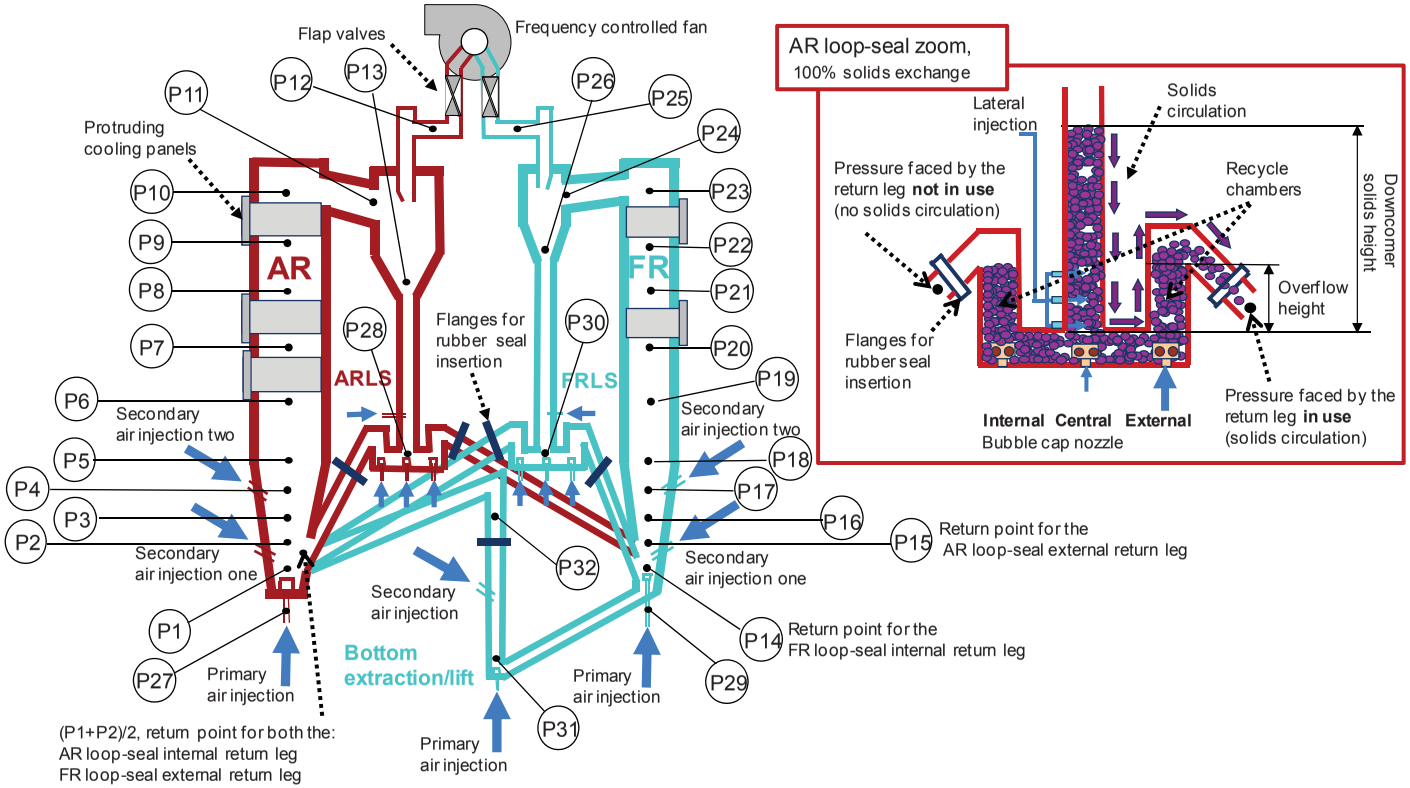

Figure 3.2: The double loop circulating fluidized bed reactor system design. The blue arrows represent the gas injections. The location is shown, of the 32 differential pressure transmitters utilized in the cold flow model, as well as the location of the protruding cooling panels and the location of the flanges where rubber seals can be inserted to block it in an airtight way. On the right, a zoom of the air reactor loop-seal is shown, it simulates solids circulation 100% on the external return leg.

zoom is also highlighted the overflow height of the recycle chamber which has shown to have a big impact on the maximum pressure achievable in the bottom section of the loop-seal (Chapter 4). The lift is utilized to shift mass from the reactor with less entrainment capability, the FR, to the other one, AR. In fact in the hot process the volumetric flow of gas available to fluidize the FR is less than that one available for the AR, so the FR was designed with a smaller cross section in order to have superficial gas velocities capable to give fast fluidization regime. The less gas available and the smaller cross section make the FR entraining less solids compare to the AR. In this way, the lift allows fulfilling the overall mass balance requirements maintaining steady-state operation and allows controlling the inventory, thus bottom pressure, inside the reactors. The latter is very important to fulfil the reactor system pressure balance and to not expose the divided loop-seals to high pressure unbalances. Further solids entrainment control is exerted by means of the availability of three gas injection points each reactor, primary, secondary one and secondary two, highlighted in Figure 3.2.

These features should allow running with different fuels and oxygen carriers as well as different operating conditions such as variation in air excess, complying with the downstream requirements. Compactness is also a major goal in order to reduce the required solids inventory and possibly to enclose the reactor body into a pressurized vessel (highlighted in Figure 3.6, b) to investigate the chemical looping combustion under pressurized conditions.

All the main actions and decisions undertaken along the design path have been summarized in Paper I. First, input parameters needed to be established according to the project requirements and resources available. Mass and heat balances, design and hydrodynamic calculations were performed. All the missing parameters were assessed iteratively in order to achieve a reactor with the above-mentioned characteristics. A key step of the design procedure has been the hydrodynamic validation; it is necessary before constructing any hot setup in order to tackle eventual shortcomings and find the best operational window. According to the chosen strategy, first a preliminary evaluation was done of the fluidization regime, both by means of comparison to similar cases in the published literature and by means of the empirical Grace classification [82]. J.R. Grace developed an empirical diagram where it is possible to have an understanding whether the selected superficial gas velocity and particles are giving the desired reactor fluidization regime. Afterwards, the proposed design hydrodynamics have been validated by means of the construction of a scaled polycarbonate model, whose scaling strategy is

described in the upcoming Section 3.3. The cold flow model construction, commissioning and deep test campaign are described in the thesis, being the core of the work.

Another option could have been the 150kW$_{th}$ design validation by means of mathematical modelling. Anyhow, the scientific community still does not feel confident of using modelling alone, to scale up a new process [55 and 79]. The existing mathematical models can be roughly divided into two categories, the empirical models and the computational fluid dynamics (CFD) models. The empirical models are more engineering oriented and they utilize experimental results by means of data fitting in order to overcome the discrepancies between theory and real reactors performance [55]. The CFD tries to keep into account all the physical correlations down to micro-scale phenomena. It is acknowledged to have a great potential, but still it is not considered reliable as the basis for construction of an experimental fluidized bed-type setup [79].

Anyhow, some attempts were done to investigate more thoroughly the reactors hydrodynamics by means of simulations. This was done in an early stage before the construction of the cold flow model in order to preliminarily verify the feasibility of the required values of solids entrainment and reactors exit concentration. It was also possible to carry out evaluations of the particles concentration along the reactors height and estimate the mass of particles present in the AR and FR. The simulations were performed just for the reactor bodies without developing a model for the whole reactor system.

Several design solutions are innovative, like the bottom extraction, the pneumatically controlled divided loop-seals, the three injection points in the reactors and the heavy loaded cyclones which adopt more than one specific solution e.g. sharp inlet duct cross section restriction, eccentric and diverging vortex finder. For this reason, it is not possible to find in published literature mathematical models or correlations describing exactly those features. The development of a mathematical model including those solutions would have cost a big effort and, at the same time, it is not sure that it would have predicted with sufficient accuracy the hot rig performance.

For the above-mentioned reasons the Levenspiel [83] “$10 approach” was followed: it means that to predict/interpret such complex phenomena it is worth to start always with the simplest model and then adding complexity on it according to the requirements. Some reactors hydrodynamic studies were done relying on the models of Kunii-Levenspiel [84 and 85], Adanez et al. [86], Davison [87] and Pallares et al. [88]. All those models are based on the solids

concentration exponential decay. The missing parameters which are necessary to describe the concentration decay were "borrowed" from literature cases; anyhow none of those was precisely fulfilling the reactor specific features. In addition the same job was done by means of the commercial software Ergun [89] which utilizes the empirical flow pattern models of Berruti [90] and Horio [91].

Figure 3.3 shows the pressure profiles obtained with the latter models, directly validated with the experimental results measured after the CFM commissioning. The presented test is a design case[11] with air and fuel reactor operated separately. The inventories and superficial gas velocities were respectively 45kg and 1.9 $m \cdot s^{-1}$ for the AR and 50kg and 2.2 $m \cdot s^{-1}$ for the FR. It is possible to see that the two empirical models can tackle the reactor behaviour from order of magnitude and trend point of view, but there are big discrepancies especially in the bottom section, which has fundamental importance in order to understand the pressure unbalance faced by the two divided loop-seals return legs. This figure is interesting to show how it may be misleading to rely just on such kind of models for complex fluidized bed reactor system design. In addition those tests were done with separated reactors, considerably reducing the possible inputs and interdependencies.

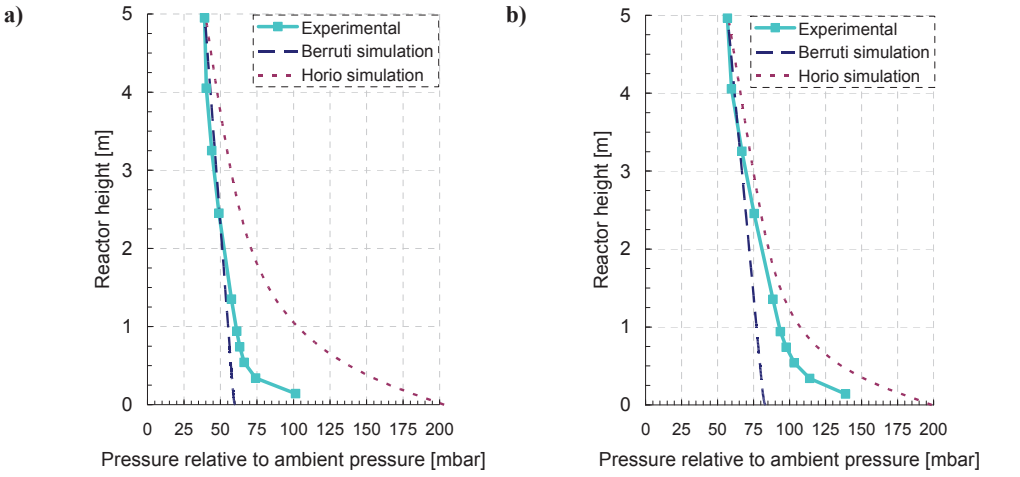

Figure 3.3: The solid lines show the reactors pressure measurements for design case separate operation. The two dotted lines represent the simulations results obtained with the Berruti [90] and Horio [91] empirical models. With a) and b) are labelled respectively the air and fuel reactor.

[11] The design test cases presented in Figure 3.3 are the same presented in Paper I for the reactors separate operation.

It was concluded necessary to validate the design hydrodynamics by means of a cold flow model. Anyhow, such kind of modelling has big importance in a second phase when the experimental setup already exists and works, to describe its behaviour and interpret the physics behind it.

3.3. Cold flow model scaling strategy and design

The hydrodynamic validation is a key step in order to finalize the proposed design. In fluidization engineering this is usually done by means of the construction of a scaled model of the actual reactor system, without chemical reactions: cold flow model. A successful cold flow modelling validation with deep understanding of hydrodynamics is necessary before moving further on and constructing a hot rig. The scaling strategy adopted to design the CFM of the presented reactor system is thoroughly addressed in Paper III; it tries to combine two existing scaling approaches.

The first scaling strategy is more academic and consists of building a small scale atmospheric copy of the hot reactor system keeping constant a set of dimensionless numbers derived by non-dimensionalizing the equations of motion for particles and fluid. The most known sets of scaling relationships are that of Glicksman, full [92] and simplified sets [93]. This strategy has several limitations, like the risk of ending up into a fluidization regime different from that one under investigation and the utilization of particles belonging to a different Geldart group (Figure 2.5), with different fluidization properties. In addition, the inter-particle forces are not considered. Often it is not even possible to achieve a full match of the dimensionless numbers, because of practical limitations.

The other approach consists of building a full-scale CFM, keeping the same particles size and density as would be the case with chemical reactions and high temperatures. This is common approach within the industrial world. In this way the difference in surface to volume ratio between the CFM and the hot setup will be reduced, thus the wall effect. A larger model leads to a smaller surface to volume ratio reducing the wall friction effects, which play a big role in the hydrodynamics of fluidized bed systems. In fact, it is proven that over a certain reactor diameter size, the rate of change of hydrodynamic parameters as function of the reactor diameter reduces

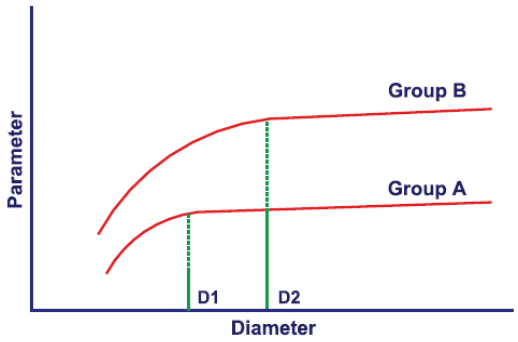

Figure 3.4. Hydrodynamic parameter variation (e.g. bubble size, solids hold-up) as function of the reactor diameter, for different particles groups [79].

its value levelling off to an almost constant value (Figure 3.4). This means that for bigger reactor sizes, hydrodynamic parameters, like the solids hold up, will change less and in an almost linear way with the reactor diameter [79].

Summarizing, the scaling strategy of the current work tried to combine the above-mentioned two approaches. On one hand the model is built at full-scale, having the same dimension as the 150kW$_{th}$ reactor system; this helps trouble shooting the actual hot rig, developing process control methodologies and understanding the sensitivity of the reactor system to several design and operational parameters. Ideally the particle size distribution (PSD) and density, ρ_p, are kept the same as the hot rig, but it was not possible in the case under investigation because the cyclone designs have been frozen for finer PSD, thus smaller superficial gas velocities. Anyhow the particles were selected belonging to the same Geldart group A (shown in Figure 2.5, the upper blue points represent the two sets of particles utilized in the CFM and the lower red point represents the hot rig particles) and also the fluidization regime of the reactors was the same according to the Grace [82] empirical classification. On the other hand the superficial gas velocity, the particle size and density were selected in order to fulfil the simplified Glicksman criteria of similarity with an industrial application/prototype plant of about 15MW thermal load. The cyclones were sized according to those values, so that a radical change in gas velocity and particles determines the need of cyclone re-design. In this way the CFM can be also used to resemble the hydrodynamics of a reactor system about 10 times bigger.

Concluding the hot 150kW$_{th}$ rig, once built, can be utilized as a process development unit (PDU) for the industrial application/prototype plant in order to address some industrial concerns. This means that in this way the cold and hot models can provide together a solid basis to scale up the proposed design. Figure 3.5 is summarizing the scaling strategy highlighting the reasons behind each connection.

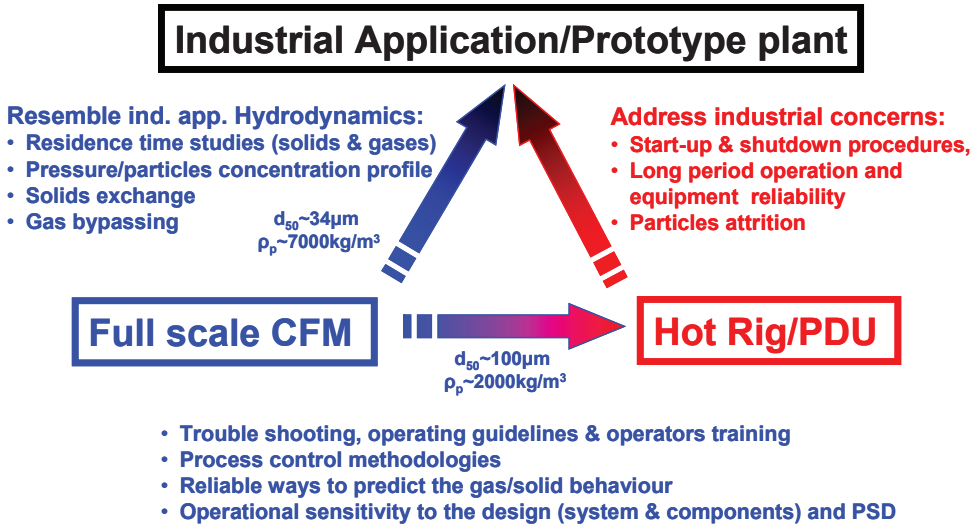

Figure 3.5: Schema summarizing the correlations between the cold flow model (CFM), the large-scale industrial application/prototype plant and the 150kW$_{th}$ hot rig/ process development unit (PDU).

The full-scale cold flow model was built according to the design presented in Paper I and according to the scaling strategy summarized in this section and carefully addressed in Paper III. The setup is shown in Figure 3.6, a) with a picture and b) with the computer aided design (CAD) drawing. Both the reactors have 5 m height and a diameter of 0.230 and 0.144 m, respectively for the air and fuel reactor. The downcomers, return legs and the bottom extraction/lift have the same size of 0.102 m. The fluidizing air is injected in 16 independent injection points highlighted in Figure 3.2 and controlled by means of Brooks® Smart Mass Flow Controllers, model 5853. Those provide the injected air flow in Normal conditions which correspond to atmospheric pressure and 0°C, for this reason also the temperature of the injected air is measured in order to derive each time the actual air flow. A filter box located on a scale in the basement below the rig is utilized to collect and quantify the particle losses on-line. This allows keeping track of the total solids inventory (TSI) which needs to be systematically refilled in order to do not affect the system performance, as shown in Paper II. It also allows making an evaluation of the cyclones performance, by means of rough collection efficiency estimations. In addition, a frequency controlled fan in the filter box is utilized together with two flap valves located downstream each

a)

b)

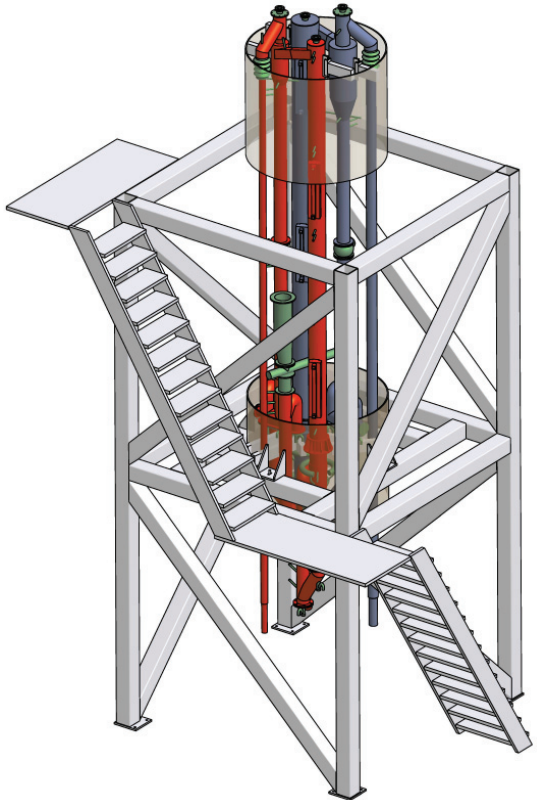

Figure 3.6: The cold flow model object (CFM) of this study is shown with a picture a) and with a computer aided design (CAD) drawing b). These figures help to understand how high and compact is the reactor system. Three are the levels: ground with the bottom section and the control station based on the National Instrument Corporation system design software LabVIEW, intermediate with the loop-seals, refilling and entrainment measurement points, upper with the cyclones. The CAD design b) highlights how the reactor system can ideally be enclosed in a cylinder with the diameter slightly above 1m.

cyclone to set the required backpressure, usually kept equal to zero. The pressure is monitored on-line by means of 32 differential pressure transmitters. Those are Fuji FCX-AII having an accuracy of ±0.065% of the calibrated span (320mbar). The conventional location of the pressure transmitters is shown in Figure 3.2. Plastic hoses connect the transmitters to the taps on the reactor system walls; they are inclined downwards and periodically flushed with air in order to avoid particles back-flow, this have shown to affect the pressure measurements in several circumstances, giving values higher than the actual ones. The air and fuel reactor transmitters are differential: the air reactor ones are referenced to the AR exit pressure P10, while this is referenced to the atmospheric pressure. The FR pressure transmitters are referenced to P23, which is referenced to the atmospheric pressure. This way of measuring the static pressure is expected to better buffer the impact of hydrodynamic perturbations propagating through the reactor bodies.

3.4. Health safety and environmental evaluation of the cold flow model, with focus on the utilized particles.

Once the reactor system has been designed, an important task before starting with the CFM test campaigns was to assess the health, safety and environmental risks (HSE). Main HSE focus has been on the air quality and dust explosion risk; both are consequences of the fine particles utilized.

The adopted scaling strategy guided towards particles with a mass median diameter, d_{50}, of about 25 μm and density of about 7000 $kg \cdot m^{-3}$. Such high density can be achieved with a metal which has also the advantage of reducing the static electricity usually generated in cold flow models. A Fe-Si alloy with about 80% Iron was chosen. It was not possible to find in open literature circulating fluidized beds utilizing such fine and heavy particles in order to gain knowledge about their behaviour and benchmark the results of the experimental campaign, but just some fluidization studies which labelled it as high density Geldart A [94]. This combination of density and PSD in first instance was not found, so the adopted particles size was bigger compared to the above-mentioned 25 μm. Atomized Ferrosilicon powder with a d_{50} of 34 μm was utilized; it is produced by the company DMS Powders [95]. PSD is shown in Figure 3.7 and about ten percent of it is below 10 μm. On one hand, during operation the powder may fraction

and get even finer. This has to be kept in mind for HSE reasons as long as fines are the easier to lose through the cyclones and will concentrate in the filter box. On the other hand this process of fines losses will imply bigger PSD inside the reactor system as shown in Paper IV. The samples to measure the PSD were taken according to the American Society for Testing and Materials (ASTM) standards B 215 [96] and measured by means of a laser diffraction particle size analyzer Beckman Coulter LS230 [97] which provides a volume based PSD. Figure 3.8 is a picture taken with the scanning electron microscope (SEM); it shows the rounded irregular shape of the particles. The particles sphericity, φ, was estimated to be about 0.75, relying on two-dimensional studies performed on the same DMS Powders particles by de Vos et al. [94].

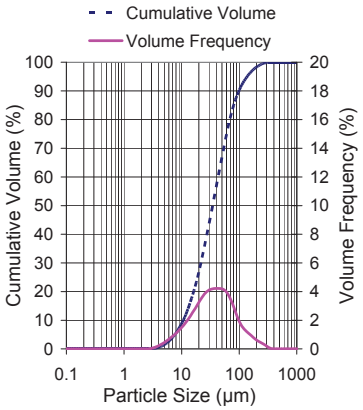

Figure 3.7: Particle Size Distribution (PSD) of the Fe-Si Powder used in the Cold Flow Model (CFM) experiments (without any sieving to obtain the design PSD).

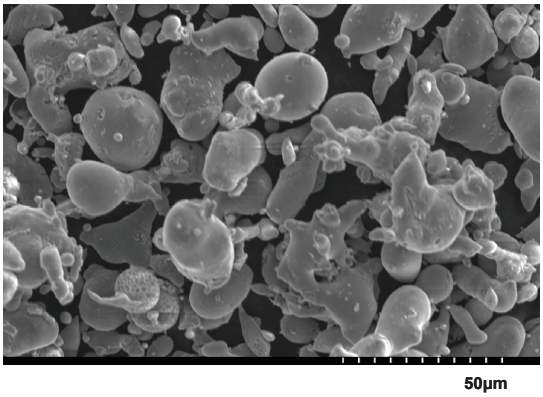

Figure 3.8: Image of the Fe-Si sample (unsieved), taken in a scanning electron microscope (SEM).

The calculated minimum fluidization velocity, u_{mf}, and terminal velocity, u_t, are respectively 0.0014 $m \cdot s^{-1}$ and 0.11 $m \cdot s^{-1}$ for the particles having a d_{50} of 25 μm. The 34 μm ones have higher values of u_{mf} and u_t respectively equal to 0.0026 $m \cdot s^{-1}$ and 0.19 $m \cdot s^{-1}$. The presented values have been calculated by means of empirical correlations [80]. This shows how finer particles are easier to fluidize. In fact the fluidization onset achievement requires smaller velocity, u_{mf}. Also the particles shape irregularity plays a role: lower sphericity implies a smaller u_{mf} because the particles are easier to fluidize and a smaller u_t because of the bigger drag.

The PSD influence on the circulating fluidized beds (CFB) solids entrainment has been confirmed by experimental studies. Mastellone et al. [98] had a clear increase of solids entrainment with finer particles. The same study evaluated also the influence of the particles density showing how high density particles determine higher solids concentration in correspondence of the reactor bottom section; this is consistent with the high bottom densities experienced for the high density Geldart A particles utilized in the present work. Basu et al. [99] in addition to the entrainment increase, showed how a finer PSD determines higher pressure in correspondence of the loop-seal bottom section; this fact will improve the divided loop-seal stability with respect to pressure unbalances.

Considering the air quality, studies were done to evaluate continuously the particle concentration in several points at the experimental setup [100]. Measurements were done together with the NTNU Panel for Mineral Production and Health, Safety and Environment by means of a light-scattering laser photometer that provides real-time aerosol mass readings: DustTrak^{TM} DRX Aerosol Monitor, model 8533 [101]. The sampling points were located where usually the operators are, during a period corresponding to a full working day. Each of the measured concentrations was utilized together with the chemical composition of the Fe-Si alloy to be compared with the substance exposure limits. The measured concentrations of particles from PM1 up to PM10[12] showed a risk classified as low. The average particles concentration was about one tenth of the Norwegian occupational exposure limit (OEL) [102], which is equal to one fourth of the value provided by the manufacturer in the safety data sheet, 10 mg·m^{-3}, which means 2.5 mg·m^{-3}. The concentration measured during the procedure of inventory refilling was higher than that one measured during standard operation, it increased for a period of about 30 minutes reaching pikes from 0.5 mg·m^{-3} of the PM1 up to 0.9 mg·m^{-3} of the PM10. For this reason it was decided to install two suction arms that can be placed just above the emission points, during particle handling. Those are connected directly with a dedicated filter box as long as the finest particles were not retained, by "conventional" vacuum cleaners utilized in first instance for this scope.

After a preliminary evaluation of the dust explosion risk it was not possible to exclude the likelihood that an accident could happen. Fine metallic particles can theoretically oxidise exothermically reacting with the oxygen present in the air. The finer the PSD is, the bigger the

[12] PM10 are all the particles measuring 10 μm or less and PM1 are all the particles measuring 1 μm or less.

surface area for unit of mass is: this means that the particles offer a wider surface to the contact with O_2 and the hazard is bigger. The free energy of formation of the Iron oxides and Silicon oxides is negative therefore the oxidation reaction is spontaneous from a thermodynamically point of view. The particles and oxidant are for sure well mixed in the reactor system; the particle concentration may be too high to be explosive. Anyhow, the different particles/oxidant combinations within the reactor are many, depending on the fluidization regime under testing. This means that the explosible concentration range is likely to be achieved. In addition, it happens in a confined environment, the reactor system, so that it may determine a smaller primary explosion. The blast wave of the primary explosion can for example entrain the particles lying on the floor around the reactor, disperse and ignite the larger quantity of dust into a dramatic secondary explosion. The static electricity generated due to the contact between particles and reactor body is partially reduced using metallic particles and reactor system metallic components connected with some copper wires to the ground. Some static electricity is still present. The finest particles stick to the walls of polycarbonate and sometimes electric sparks are generated. Those sparks provide the potential ignition source to dust explosions [103-106]. For those reasons a particle sample was sieved, to have a finer size approaching the original d_{50} requirements slightly above 20 μm. This was sent to the company GexCon AS, which performed an explosibility test trying to ignite the sample according to the Association of German Engineers (VDI) standard procedure [107]. The powder was found not explosive.

Both the air quality and the dust explosion risk have been carefully evaluated and excluded. Those issues are a direct consequence of the fineness of the PSD adopted together with the large size of the experimental setup. This implies the usage of large amounts of fine particles (hundreds of kg) with all the difficulties to handle it safely.

3.5. Cold flow model commissioning

The operational and measurement procedures definition has been the first commissioning step. In this paragraph some of the most important procedures are listed. Safe start-up and shut down procedures were defined as well as the way to systematically collect, quantify and refill the mass losses in order to keep the total solids inventory constant and do not affect the reactor system performance. It was defined how to take reliable direct measurements of entrained solids flux and how to place and flush the pressure transmitters in order to avoid dust plugging. Those

issues have been continuously updated during the whole test campaign period. In this way it has been possible to improve the procedures both to better accomplish the demanded tasks and to fit to the changes in design or operation.

Before operation, the nozzles design was verified with empty reactor computing their pressure loss. The mass inventory was quantified in two ways. One way was to measure the solids level in the reactor system when it was shut down, thus calculating the volume occupied by the particles. The density of a packed bed of particles was evaluated separately, just putting the particles into a known volume and weighting it, obtaining about 4000 $kg \cdot m^{-3}$. The other way consists of deriving the mass present inside the reactors during operation by pressure measurements [108]. It is called active mass because it is that one actively participating at the reactions in the hot case vs. the parasitic which is that one in the downcomers, loop-seals, and lift. The solids flow/flux measurement techniques reliability was object of studies as well. The conventional direct technique consists of measuring the height of the column of particles accumulated in the downcomer after a sharp loop-seal fluidization shut down. An indirect technique was also tested, it consists of closing a perforated flap valve placed in the downcomer [109]. In this way, the gas coming from below fluidizes the amount of powder which accumulates on the flap-valve, once closed. The entrained solids flux value is proportional to the gradient of the pressure drop measured across the flap valve/fluidized bed as function of the time. This is true if minimum fluidization conditions are achieved for the particles above the flap valve. Several tests were done to understand the reliability of the solids flow/flux measurements together with a simplified error assessment [110]. These operations have been described in Paper II.

The air reactor and fuel reactor were then operated separately monitoring their entrainment capabilities and pressure/particles distribution (Paper I). They were isolated from each other by means of a rubber seals in the interconnection pipes; the cold flow model pipes have five flanges where it is possible to insert the rubber seals whether required (Figure 3.2). Air and fuel reactors were tested for different inventories, exit[13] superficial gas velocities and primary/secondary air injection combinations. Also the divided loop-seal performance was studied thoroughly (Paper II), to understand the best way of operating it with respect to solids

[13] Superficial gas velocity at the reactor exit; in this way the superficial gas velocity value depends neither on the primary/secondary air combination nor on the reactor geometry which has constant diameter at the exit. All the reactor superficial gas velocities in the thesis refer to the exit velocity unless specified otherwise.

flow/flux circulation increase. During the separate operation just the internal return leg was utilized being the loop-seal fluidized with the central and internal bubble cap nozzles (loop-seal described in Section 3.2, Figure 3.2). The lateral air injection was utilized as well, in order to keep fluidized the particles in the downcomer; this is especially useful in case of high columns of Geldart A particles. The possible combinations were explored to find the highest solids circulation together with a stable fluidization regime in the loop-seal, avoiding large pressure fluctuations and a slugging fluidization regime. It was concluded that the solids circulation increases with the increase of each of the above-mentioned gas injections. This is true up to a certain volumetric gas flow injection rate in the central bubble cap nozzle; above this value the system is not sensitive any more to the gas fluidization and the solids fluctuations get bigger together with the measured pressure fluctuations. The loop-seal has always been capable to adjust the pressure in correspondence of its bottom section to the pressure of the reactor in correspondence of the point where the return leg in use merges. P28 adjusts to (P1+P2)/2 and P30 adjusts to P14 (Figure 3.2), being this the case of internal re-circulation of solids. This means that the pressure drop across the solids accumulated in the downcomer varied according to the pressure faced by the return leg in use. This is both a consequence of the amount of solids accumulated in the downcomer and of the velocity of the gas relative to the solids flowing downwards. The last one has always to be directed upwards and can be adjusted by tuning the loop-seal fluidization [99]. The solids circulation upper limit for reactors separate operation was achieved as consequence of reactors inventory and/or superficial gas velocity increases. The average downcomer particle level increased with the solids entrainment up to a point where the accumulated solids were abruptly reducing their level and then increasing it again in a cyclic manner. This affects the active inventory inside the reactor body and the pressure measured in the bottom section of the loop-seal increases its fluctuations up to the unusual values of ± 25mbar.

In addition, also the insertion of dummy panels was tested (Figure 3.2), they represent the 150kW_{th} reactor system cooling devices, necessary to fulfill the heat balance. The insertion of heat transfer surfaces is also utilized in industrial boilers to better control the furnace temperature. The boilers height usually is not increased above 40m due to economic considerations; this means that high thermal loads can be handled with the help of cooling panels insertion [111]. Here it is tested how those insertions influence the reactor hydrodynamics testing different configuration. No big change was experienced looking at the solids entrainment. Figure 3.9

shows how the particles concentration behaves in the air reactor upper section (4 m) for the different cooling panels combinations; the set of tests is that one described in Paper II and the cooling panes location is shown qualitatively in Figure 3.2. The concentration increases in correspondence of the panels insertion; this happen also for the upper panel, but with a smaller magnitude. The concentration is directly derived from the pressure measurements neglecting friction and acceleration, especially because those are located in the upper 4m above the end of the conical bottom section, where the flow is fully developed. The higher pressure drop being measured may also depend on the turbulences and friction induced on the flow by the panels rather than being the consequence of solids concentration increase. Further tests need to be done in order to measure the local concentration by means of non-isokinetic suction probes [112-114].

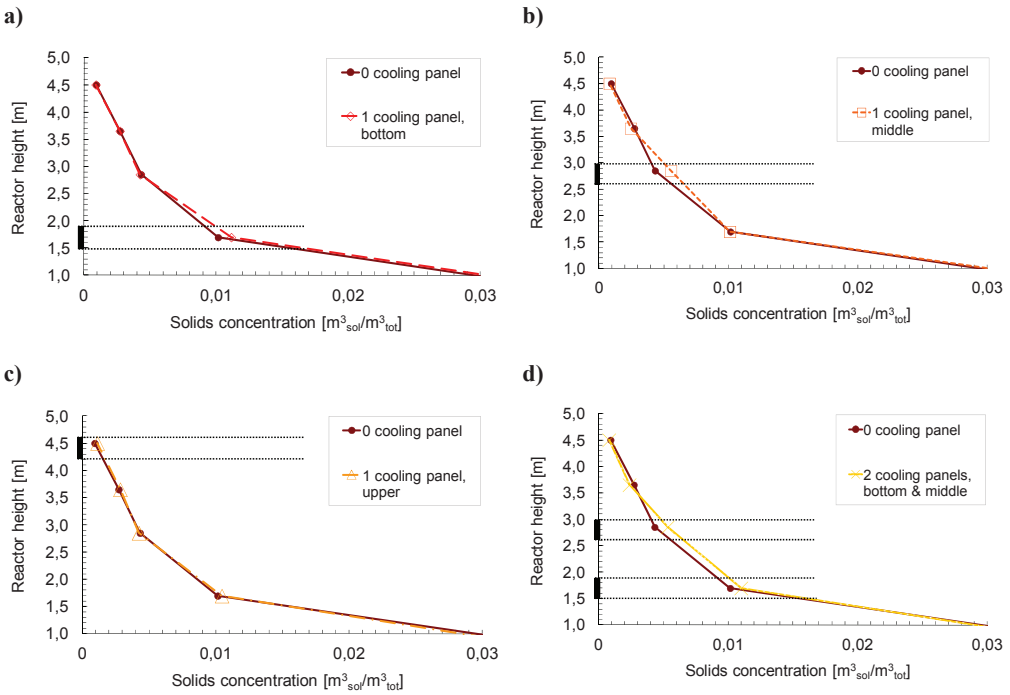

Figure 3.9: Solids concentration in the upper section (upper 4 meters) of the air reactor in correspondence of four different combinations of the dummy cooling panels insertion. Those are the cases studied and described inside Paper II [110]. Cases a), b) and c) represent tests done with one cooling panel inserted in the bottom, middle and upper position of the reactor upper section, while two cooling panels are inserted for the case d).

This will help to understand if the pressure increase is effectively determined by a solids concentration increase. It was not possible to assess it by visual observation, because of finer particles sticking to the reactor walls due to static electricity and because the phenomenon is not so big.

Afterwards the rubber seals between air and fuel reactor were removed and the overall reactor system was tested in coupled operation, with the solids being exchanged among the reactors through the external loop-seals return legs, fluidized by the external bubble cap nozzles (as in the AR loop-seal zoom of Figure 3.2). The divided loop-seals also in this case automatically adjusted their bottom pressure to the pressure of the point where their return leg in use merges, the external one for these tests. The air reactor loop-seal was adjusting its pressure to the point of the fuel reactor where its external return leg merges (P28 adjusts to P15, Figure 3.2). At the same time the fuel reactor loop-seal adjusted its bottom pressure in order to be capable to be higher than the pressure at the point where its external return leg merges with the air reactor (P30 adjusts to (P1+P2)/2, Figure 3.2).

The challenge of the system operation has been related to the high pressure unbalance that the divided loop-seal may experience between its two return legs. This is especially true for the above-mentioned cases of full solids exchange between the two reactors. It may happen that the pressure which the return leg not in use faces is higher than the pressure experienced by the return leg in use. As previously said, the pressure in correspondence of the bottom section of the loop-seal, has proven to fit to the pressure of the return leg in use, reaching values somehow higher than this in order to ensure solids circulation. This means that one of the loop-seals may be exposed, through the return leg not in use, to a pressure higher than the pressure reached at its bottom section. In this case there is a gas back-flow through the downcomer, which determines a dramatic loss of particles through the cyclone. For the actual design, this phenomenon usually happened for the fuel reactor loop-seal where P30 automatically adjusts its value above that one of (P1+P2)/2, when the fuel reactor exchanges 100% of the entrained solids with the air reactor. P14 is the pressure experienced by the FR loop-seal internal return leg, when it is not sealed off by means of the rubber seal insertion, and it can be higher than P30. This is also the consequence of the internal FR loop-seal return leg merging the very bottom section of the FR and facing P14 where the pressure is the maximum the FR can reach, instead of P15. At the same time the other loop-seal is operating safely because it faces the high pressure with the return leg in use, so the

pressure of its bottom section adjusts to it (P15, Figure 3.2) and the low pressure of the return leg not in use is not creating any problem.

With the actual design, it was possible to operate the reactor system inserting a valve in the return legs not in use. Seals were introduced, as if it was a cone valve fully closed, and smooth performance was achieved according to design needs of 2 $kg \cdot s^{-1}$ exchange. If no valves are used, it is required to carefully control the bottom pressures of the reactors and avoid a big difference between them. Ideally, according to the measured values, a difference of 30 mbar between the two return points of air and fuel reactor for each loop-seal should not be exceeded to be sure to operate safely. Those points are located in correspondence of (P1+P2)/2 and P14 for the FR loop-seal and (P1+P2)/2 and P15 for the AR loop-seal, Figure 3.2. In this way the divided loop-seal facing a high pressure with the not in use return leg, will not be harmed. The options to control the bottom pressures without reactor system design modifications are several. For example the total solids inventory can be reduced, the primary air injection can be reduced or the secondary air height can be increased[14]. Those ways of controlling the bottom pressure impose limitations to the maximum amount of solids which is possible to circulate. The bottom extraction/lift usage has proven to be the best operational way to equalize the bottom pressures.

The lift can compensate the higher solids entrainment arriving from the air reactor to the fuel reactor. In addition it can reduce the FR inventory down to a level where its bottom pressure is not determining back-flow risks. In fact the internal return leg of the fuel reactor in the actual design is the critical one because it merges the reactor body in the very bottom (Figure 3.2), thus encountering the highest pressure. This is obtained utilizing the lift as turbulent bed while it was previously utilized as bubbling bed just relying on the gravity, to transport the particles from FR to AR. Its overflow height is too high so it cannot be used as a loop-seal, in that way immobilizes a high amount of mass and determines a too high pressure in the FR bottom. All those issues are described in Paper II, Paper IV and partly in Paper III.

[14] The secondary air heights presented in Figure 3.2 are those ones utilized for the majority of the tests. Tests were also performed with the fuel reactor secondary one air injection located at a higher position in the reactor, 0.40 m vs. the 0.17 m qualitatively shown in the figure.

3.6. *Hydrodynamic validation of chemical looping processes*

A good understanding about how to reach stabile operation with the actual design has been achieved in the commissioning phase, Section 3.5. The share of total solids inventory inside each reactor body can be controlled by means of the lift fluidization. This means controlling the pressure in the reactors bottom section, thus the pressure difference between the divided loop-seals return legs. Once this knowledge was achieved, the targeted design conditions were reached; their performance was stable and repeatable in terms of solids exchange and fluidization regimes. Afterwards, the reactor system has been object of an experimental campaign to verify and to study its hydrodynamics while resembling off-design conditions and other chemical looping processes conditions. All the results of this experimental campaign have been summarized in this section and carefully presented in Paper III.

As already mentioned the reactor system at design conditions resembles the hydrodynamics of an atmospheric boiler utilized for steam production. The example shown in Figure 3.10, a) shows the general arrangement for a typical circulating fluidized bed boiler [54]. At industrial scale, the CLC reactor system is supposed to replace it, being integrated in the steam cycle in a similar manner according to the case specific circumstances. The cold flow model was operated to resemble the steam boiler hydrodynamics at off-design conditions. Attempts were done to increase the fuel reactor solids concentration, in the upper section. The idea was to increase the gas particles contact all-over the reactor body having less mass in the bottom section and more in the upper one; at the same time a big share of the entrained solids was re-circulated internally to increase the FR solids residence time. This should help to improve the fuel conversion and more in general to have more options to control the FR fluidization regime according to the oxygen carrier and the fuel. Part-load conditions were successfully tested; resembling the hydrodynamics of a hot rig with a fuel input down to about 70% and 50% compared to the design case. The load was also increased up to an input of about 115% of the design case.

The last step was to try to address the hydrodynamic viability of other kind of chemical looping processes: the gas turbine (GT) combustion and the chemical looping reforming. In the gas turbine case the chemical looping combustion hot rig would go to take the place of the combustion chamber of a gas turbine, as shown in Figure 3.10, b), being inserted into a pressurized vessel as already suggested by Xiao et al. [116] and Wolf [117]. Pressurization is

a)

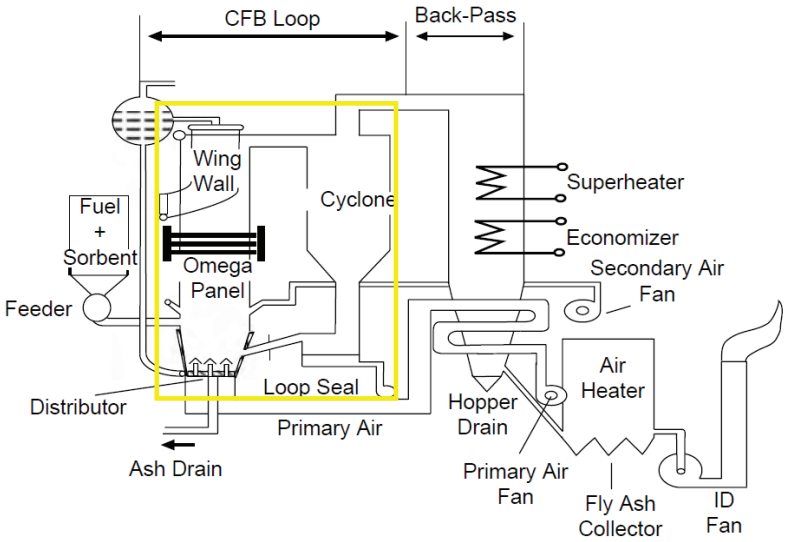

b)

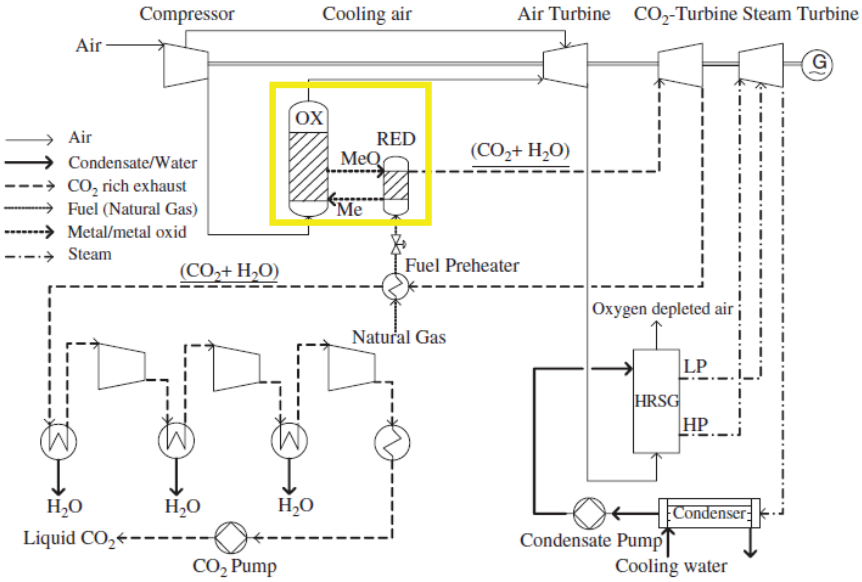

Figure 3.10: Examples of chemical looping combustion reactor system integration. Figure a), taken from Basu [54], shows the typical arrangement for a circulating fluidized bed steam boiler. Figure b) shows the usage of the CLC as a combined cycle gas turbine combustor [115].

challenging, especially for the system availability and control of two interconnected pressurized reactors. Looking at the hot process as a whole, two main changes are expected in the GT case: a higher overall excess air ratio, λ, and a high pressure. The first will determine an increase of air reactor volumetric gas flow keeping constant the FR one. This will also imply a reduction of the cooling duties in favour of the higher exhaust stream exiting from the AR. The second, as explained in Section 2.5, determines a gas density increase linearly with the pressure increase, while the density and most likely the performance of the solids OC will be the same. Keeping the same design implies that fuel injection increase (as the pressure increase) is required to keep the same volumetric flow as before. This implies the need of more OC circulation, roughly it increases linearly with the pressure increase, unless part of the required fuel to keep the same volumetric gas flow is compensated with CO_2 re-circulation or the oxygen needs are partially compensated with O_2 injection directly in the FR. For the CFM, this means an increase of AR fluidization and solids entrainment/exchange, while keeping the FR with the same superficial gas velocity or less and balancing with the bottom extraction. In this way it is possible to explore to which extent the actual, atmospheric, design can handle the pressurized requirements.

Chemical looping reforming (CLR) resembles the hydrodynamics of a hot rig used to produce a syngas by supplying less oxidized solids to the FR, less than the stoichiometric amount. In the CFM tests this was done in two ways; either reducing the AR solids entrainment or increasing the AR internal re-circulation while reducing the external exchange. Also in this process, as for the gas turbine case, it would be beneficial to pressurize the reactor system to increase the net plant efficiency. The availability and control challenges of pressurized processes are the same as in the chemical looping combustion case. As explained in the last paragraph of Section 2.5, the OC may not be capable to fulfil the FR oxygen requirements for a full combustion under pressurized conditions. In fact, the OC performance may be about the same as the OC performance for the atmospheric combustion or slightly better, while the amount of fuel injected will need to be increased in order to keep the same volumetric gas flow as in the atmospheric case. Same volumetric gas flow allows to keep the same fluidization regime in the reactor without radically changing the reactor system design. This “incomplete combustion” is beneficial for the reforming reaction, instead of being a challenge as for the pressurized combustion. It goes towards the process requirements direction; in fact the goal of CLR is a partial combustion.

3.7. Procedure to operate the cold flow model according to the hot process requirements.

The procedure followed to operate the cold flow model is presented in this section. The aim is to have the CFM working both in a stable manner and consistently with the expected hot process requirements from a qualitative point of view. It is summarized in the flow-sheet of Figure 3.11 and it was utilized for the cases presented in the previous Section 3.6.

First of all, the reactor system design has to be defined. In the above-mentioned cases no design changes are considered; anyhow in the gas turbine case a smaller fuel reactor cross section can be an option to achieve the aimed fast fluidization regime reducing the requirements of fuel injection increase and exhaust re-circulation. The oxygen carrier performance is as well defined at a design stage; this is important because it is used to determine the amount of solids exchange theoretically required for a specific application. Together with the OC performance, also the thermal load[15] of the case studied is fundamental: to determine the oxygen, thus the solids exchange, required, to determine the system cooling duties and consequently design the cooling system and to know the amount of fluidizing gas available in the fuel reactor. Finally it is required to know how the reactor is integrated within the system; in fact it is necessary to design the heat exchangers and determine the exhaust gas flow rates and temperature requirements for downstream applications.

With those inputs it is possible to determine the amount of gas which can be utilized to fluidize the FR. In addition it is possible to play with the primary/secondary fuel injection, steam injection and re-circulate part of the exhaust CO_2 to be capable to tune the solids concentration within the FR body and solids entrainment in order to find the best fluidization regime according to the process objectives. A further degree of freedom is given by the divided loop-seal which allows to internally re-circulate part or all the entrained solids. This is important both to tune the reactor fluidization regime and, together with the usage of the lift, to uncouple the solids entrainment from the solids exchange. In this way downstream requirements can be met. This can also be done utilizing the bottom lift to exchange the solids while the reactor and loop-seal operation can be focused on the desired fluidization regime or vice versa exchanging solids by the loop-seal and reducing the lift exchange to vary the fluidization regime; it will affect rather

[15] This term and other ones like steam, excess air ratio, CO_2 re-circulation etc. refer to the hot process. The variations of these parameters mentioned along in the section correspond to variations of air injection in the cold flow model operation.

much the bottom inventory in first instance. The loop-seal has to be properly fluidized avoiding circumstances like particles defluidization in the downcomer or like slugging fluidization regime which determines pressure fluctuations and gas leakages, and possibly maximizing the pressure drop across the solids column in the downcomer exerting a control over the gas velocity [99].

Based on the system input, it is possible to determine the amount of solids to circulate in order to provide the necessary oxygen to the FR. Afterwards it is possible to determine the amount of fluidizing air to utilize for the AR fluidization, this has to be capable to entrain the required amount of solids consistently with the excess air ratio appropriated for the application. The solids entrainment is the first process requirement. It is especially important to be capable to fulfil the upper limit, the AR has to be capable to entrain at least as many solids as required to be exchanged. As well as for the previous case the primary/secondary share can be used to tune the solids concentration and entrainment. The entrainment can be uncoupled from the solids exchange by means of the divided loop-seal usage. This will offer a degree of freedom more to have sharp control over the solids exchange according to the process requirements. In addition it will also allow exerting some control over the solids distribution in the reactor body for heat exchange needs as well as some control over the volumetric flow and temperature of the exhaust gasses according to downstream needs. This is especially true for the AR rather than the FR, because here the highly exothermic reaction takes place. The idea is to set the priority among these options according to the process integration requirements, which are case specific. An example to clarify the idea is whether lowering the solids exchange by entrainment reduction or by internal re-circulation; the latter means higher gas flow with its impact on the reactor system heat balance. The oxidation reaction for chemical looping processes has quick kinetics, so that the AR fluidization regime has secondary importance in comparison with the required entrainment, fundamental for the FR fuel conversion.

Finally the lift fluidization has to be utilized firstly to balance the reactors bottom pressures and avoid that a too big pressure unbalance may damage the loop-seal performance. The pressure difference allowed is not an absolute value, for the actual design it will be better to have it below 30mbar, anyhow it depends on the loop-seal design, on the height where the return legs merge with the reactors (thus the pressure they face in the reactors) and on the operational conditions e.g. pressure fluctuations have proven to be higher for higher solids circulation. In addition the lift has to fulfil the mass balance being capable to transport, together with the solids

going through the FR loop-seal to the AR the same amount of solids coming from the AR loop-seal to the FR, to reach steady state conditions. Finally if possible it can be utilized to help the achievement of the required fluidization regimes in the reactors as well.

Last step consists of the achievement of an overall equilibrium of all these parallel operations, of FR tuning to achieve the best fluidization regime, AR tuning to exchange the required amount of solids exchange with possibly the downstream requirements fulfilment and lift tuning to be capable to balance the situation.

The tested chemical looping configurations provided useful information, especially from qualitative point of view both to improve the actual design and to understand how to combine the hydrodynamic and thermodynamic reactor system needs. The reactor system has been modified to address design limitations found out during the test campaign and to widen its operational window, those modifications have been presented in the following chapter. Anyhow the defined procedure about how to operate such double loop circulating fluidized bed reactor system design is methodologically valuable also for the final design. Process simulations of the industrial application/prototype plant, including heat and mass balances, should be carried on in the future to be capable to provide also some quantitative figures of the hot process requirements. Those can be hydrodynamically validated while working in parallel with the improved rector system CFM according to the presented procedure.

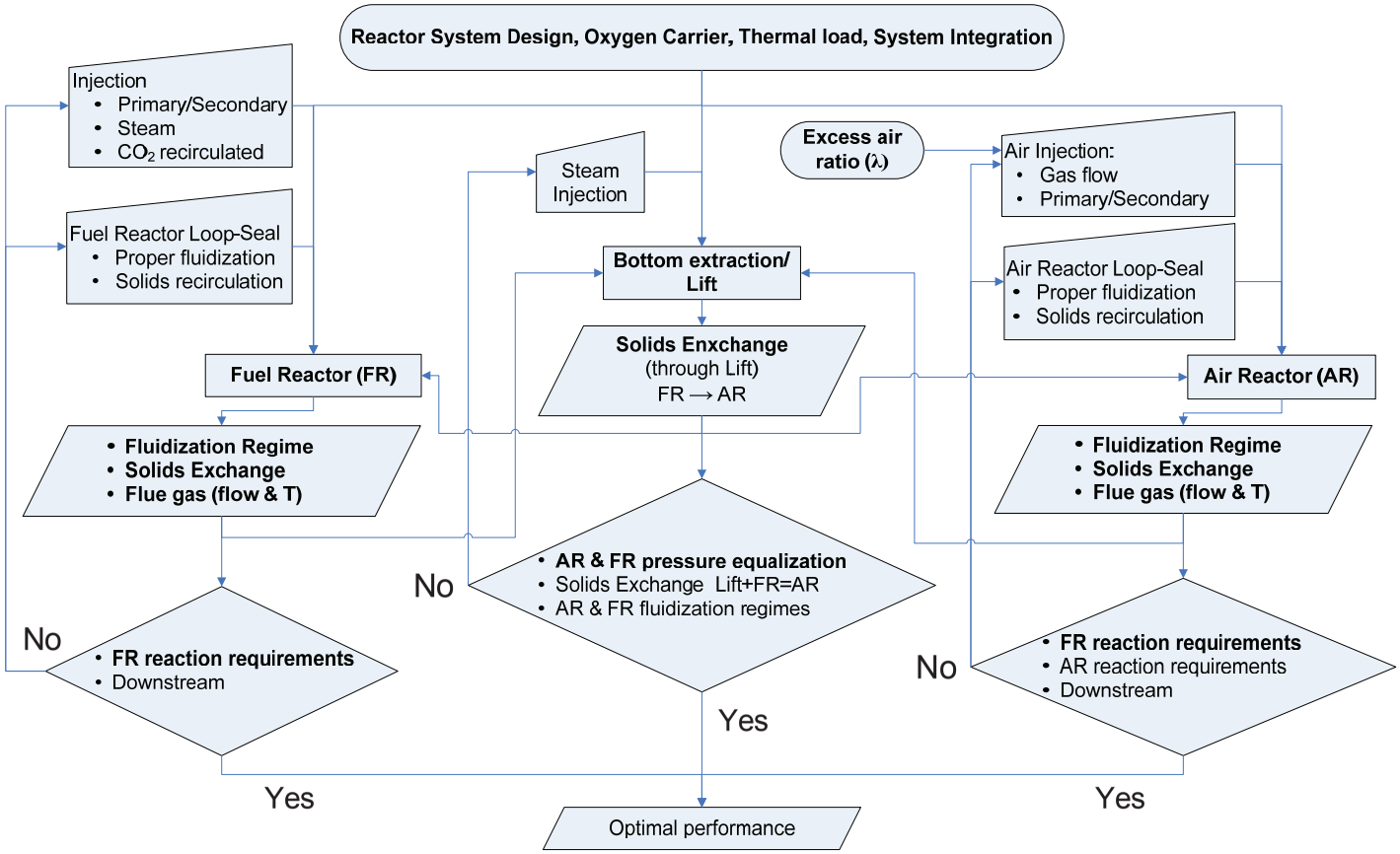

Figure 3.11: Flow sheet representing the procedure followed to operate the cold flow model in a way it could work both in a stable manner and be consistent with the hot process requirements keeping its needs into consideration from qualitative point of view.

4. Double loop circulating fluidized bed design evaluation and finalization

4.1. Design evaluation and improvement suggestions

In addition to the above-mentioned chemical looping processes of combustion and reforming, many are the industrial processes based on two reactions that can be performed continuously by means of two interconnected fluidized beds. Examples are: the fluidized catalytic cracking, biomass gasification, gasification with selective transport of CO_2, the carbonation/calcination post-combustion CO_2 capture and the sorption-enhanced reforming. All those processes have a primary reaction related to the achievement of the main process objective and a secondary one which is necessary to continuously run the process. The proposed design is sized for a $150kW_{th}$ atmospheric chemical looping combustion reactor system for steam generation (Paper I). The double loop circulating fluidized bed (DLCFB) reactor system idea can be utilized also to fulfil the requirements of such kind of processes, especially when it comes to compactness for scale-up purposes and increase of gas-solids contact in the reactor upper section [118].

A cold flow model (CFM), without chemical reactions, has been dimensioned utilizing the scaling laws described in Section 3.3, built and tested to validate the hot rig hydrodynamics before construction. The performance of the DLCFB cold flow model during the experimental campaign has been studied in order to find its operational window and limits, to understand the key input parameters and to propose design improvements which will get it intrinsically more stable. Those results, summarized in this section are presented in the Paper IV of the thesis.

Long term operational stability tests as well as repeatability tests have been successfully performed, with the system showing good robustness to external perturbations. In this way it was possible to define a design condition based both on the hot rig design requirements and on the achievement of cold flow model hydrodynamic stability. Once the design condition was set, the superficial gas velocity has been varied separately in each of the two reactors, air and fuel reactor, and in the bottom extraction/lift (Figure 3.2). This was done without taking any compensating action, to re-equilibrate the reactor system hydrodynamics. In this way, it was possible to monitor how the reactor system reacts to each of these superficial gas velocity changes and to which extent it is capable to keep on working before instability onset. The reactor system showed a bigger equilibrium margin towards the fuel reactor (FR) superficial gas velocity

sensitivity; in fact the FR has a smaller section than the air reactor (AR). On the other hand, an AR superficial gas velocity increase of few decimals of meters per second (e.g. from 2.4 to 2.8 $m \cdot s^{-1}$) determines a large increase of solids flux entrainment from the AR (e.g. from 40 to 60 $kg \cdot m^{-2} \cdot s^{-1}$). This obliges to take action in the rest of the system to continue running it and to avoid all the mass shifting from the AR to the FR. The lift limitation is related to the lower superficial gas velocity limit. As mentioned in the commissioning Section 3.5, a too small value of lift superficial gas velocity gives mass accumulation in the FR body leading to a too high pressure in the FR bottom section. This reduces the margin of the divided loop-seals pneumatic control; it can be reduced down to the point where gas back-flows from the FR through the FR loop-seal return leg which is not in use, causing large mass losses through the cyclone. The same problem was encountered increasing the total solids inventory with the same reactor system fluidization conditions. A too high inventory gives a too high pressure in the FR bottom section with gas back-flow through the divided loop-seal return leg not in use and causes cyclone efficiency collapse.

A deep understanding of the divided loop-seal was achieved by means of the above-mentioned experiments, analyzing its behaviour in each of the operating conditions tested. In this way, it was possible to identify which operating conditions are critical for the loop-seal performance, determining an exposure to a large pressure unbalance till gas back-flow onset. Dedicated tests were done to better evaluate those critical operating conditions, just operating the air reactor alone, internally re-circulating the entrained flux of solids (Figure 4.1). In this way the solids were passing through the internal return leg of the air reactor loop-seal, which merges in the AR body. Air was not injected through the external bubble cap nozzle of the air reactor loop-seal, so that the external return leg merging the fuel reactor body was not in use. The other reactor was utilized as a pressure chamber to set an increasing pressure in correspondence of P15 which is faced by the return leg not in use. In this manner it has been possible to test the divided loop-seal keeping the same conditions on one side, with the return leg in use facing the pressure (P1+P2)/2, and varying the pressure on the other side, with the return leg not in use facing pressure P15.

The results tell that, with the actual design, it was possible to reach safely in the return leg not in use an average[16] pressure of 10mbar lower than that one of the loop-seal bottom section. When this difference has been reduced to zero, the particles losses become about the triple; this is due to the pressure fluctuations in correspondence of the loop-seal bottom section which, in this specific case, reached the value of maximum ± 5 mbar, because of the lower solids circulation compared to design case conditions. Going higher in value with the pressure of the return leg not in use, the mass losses increased exponentially. Keeping the pressure in correspondence of the loop-seal bottom section (P28 in the example of Figure 4.1) at least 20mbar higher than that one of the return leg not in use (P15) seems a safe solution. In this way 5 to 10mbar are kept as safety margin, based on the usual pressure fluctuations in correspondence of the bottom section of the loop-seal from ±10 to 15 mbar.

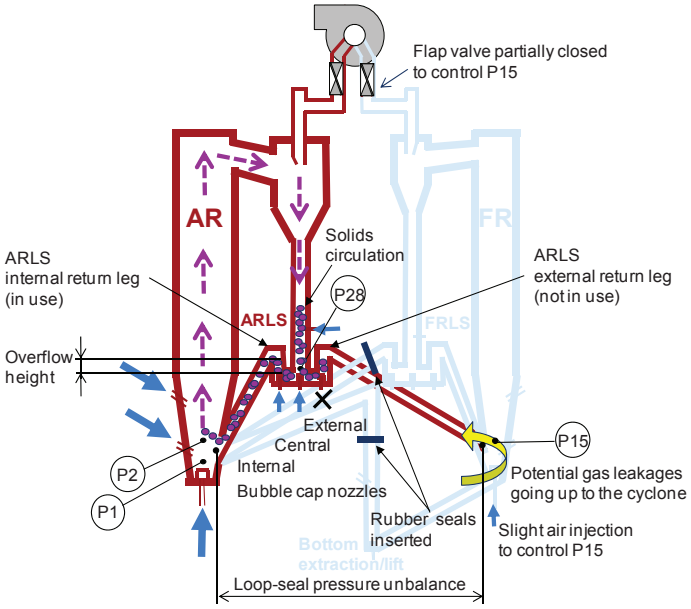

Figure 4.1: Configuration of the dedicated tests aiming to study the air reactor loop-seal critical operation due to pressure unbalance.

[16] All the pressure measurements presented are average values. The pressure values fluctuate across the average value with amplitude depending on the value itself and depending on the fluidization regime. The fluctuations of the pressure measured in correspondence of the loop-seal bottom sections are among the highest and can easily reach values between ± 10 and ± 15 mbar during stable operation. The higher values are usually reached for higher solids fluxes being processed by the loop-seals, so usually the AR loop-seal has somehow higher pressure fluctuations. Those ones in correspondence of the reactor bottom sections are among the smallest. Paper IV brings examples of pressure fluctuations (Figure 5, Figure 6 and Figure 9, a 3) and b 3).

Ideally the reactors bottom pressure can be controlled also by reactors fluidization, one way of doing it, is to increase the superficial gas velocity, which will reduce the mass in the reactor body, thus the pressure in the bottom section. Anyhow, this fact gives an increase of the cyclones pressure drop which shifts the pressure measured inside the fuel reactor body towards higher values (Figure 8 of Paper IV), somehow neutralizing the effect of the mass reduction with respect to the pressure value measured at the reactor bottom. The reactors cyclones were designed to have a certain inlet gas velocity between 20÷25 $m \cdot s^{-1}$, to be achieved with superficial gas velocities lower than those ones utilized in the test campaign: below 2 $m \cdot s^{-1}$. The available solids inventory particles size was bigger than the design one, with a d_{50} from 34 to about 50 μm. Bigger size of the available particles means that higher velocities were necessary to entrain the aimed solids flow. This information tells how important is the cyclone design, not only to have high efficiency and low erosion, but also towards the pressure balance of the overall system. Superficial gas velocities and particle size distributions (PSD) different respect to the design ones can determine a different cyclone pressure drop which affects rather much the overall system performance. For this reason the actual cold flow model should be operated with a finer PSD, as planned during the design phase. In Figure 4.2 the required PSD is shown; the d_{50} is about 25 μm and the distribution is narrower compared to the original coarser powder provided by DMS Powders [95] (Figure 3.7). The latter was sieved obtaining the volume based values presented in Figure 4.2 which were also measure a by means of a laser diffraction particle size analyzer Beckman Coulter LS230 [97]. This has been a demanding procedure because hundreds of kilograms are required. Few tests were done with the finer particles and are presented in Section 4.2.

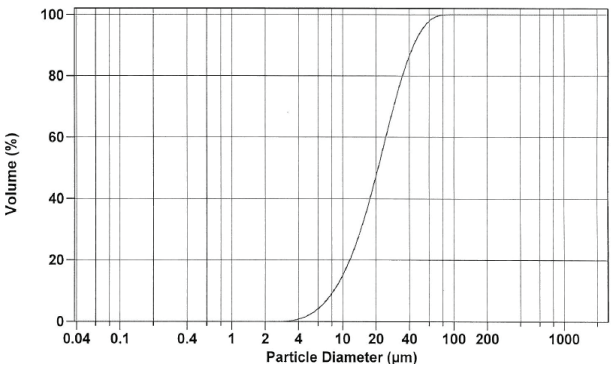

Figure 4.2. Particle size distribution (PSD), of the Fe-Si Powder batch which was sieved to obtain a smaller mass median diameter, d_{50}, of about 25 μm and narrower distribution.

The pressure measured in correspondence of the loop-seals bottom section (P_B,

Figure 4.3) has proven to easily fit to the pressure of the point where the return leg in use is merging with the reactor (P_A, Figure 4.3). If both the return legs are in use, the bottom section value (P_B) is fitting to the higher of the two pressure experienced. During the experimental campaign, the pressure measured in the bottom section of the loop-seals (P_B) has reached a value which is usually at least 50 mbar higher than that one in the return point (P_A). This pressure difference depends on the operating conditions and has reached the maximum value of about 80 mbar in the AR loop-seal during the highest solids circulation achieved. Those values of the bottom section of the loop-seals are average values, because the measured pressure can easily fluctuate up to about 10÷15 mbar across the average value, depending on the solids flux circulating through the divided loop-seal. The return leg not in use faces a value P_C depending on pressure in correspondence of the reactor point where it merges, which has proven to fluctuate maximum about ±5 mbar. Unless an automatic feedback control system is developed relying on this information, it is recommended, for the actual design, to keep the two return point pressures at maximum about 30 mbar of difference between each other, $|P_A-P_C|$. This is assessed considering the minimum pressure difference experienced, P_B-P_A, of about 50mbar, which determines the pressure in correspondence of the bottom section of the loop-seal (P_B), and considering its fluctuations which can easily reach ± 10÷15mbar. In this way, it is possible to be confident that there will be a safety margin between the lowest values reached by P_B during its fluctuations and the value of P_C.

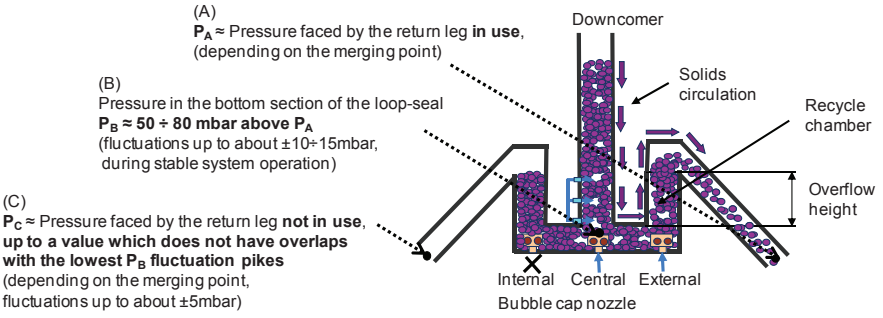

Figure 4.3. Schema of a divided loop-seal exchanging 100% of solids on one return leg (in use), with overview of the pressures experienced during stable reactor system operation and their interdependencies.

Two design modifications were proposed, in order to increase the system stability without the need to rely so much on the bottom lift capability of shifting the mass from one reactor to the other.

The first is related to the internal return leg of the FR divided loop-seal, which needs to merge the fuel reactor body at a higher level than the very bottom (Figure 4.4). 0.2 m is enough to experience big pressure reductions inside the reactor body, so in correspondence of the point where the loop-seal return leg merges. About 30 mbar is a typical value for the actual design conditions of total solids inventory (120kg) and fluidization velocities (about 2.6 $m \cdot s^{-1}$). The bottom section of the reactor system is shown in Figure 4.4. On the left side, the air and fuel reactor are represented together with the bottom extraction, after the modification implementation. In light blue, the return leg position is shown, before the modification of having it 0.2 m higher. On the right side there is a picture taken at the same bottom section before modifications. It is possible to distinguish clearly just the fuel reactor and the lift, while the air reactor is behind and difficult to see. The blue arrows represent all the potential gas flows coming from injection points and the main gas streams directions. The height increase of the point where the return leg merges, reduces the risk of gas back-flow because the pressure experienced at higher height is much lower, for the same solids inventory and fluidization regime. The previous return leg location was about doubling the reactor cross section at that height, which results in a big reduction (≈50%) of the actual superficial gas velocity, thus entrainment capabilities. In addition the primary bubble cap nozzle and the lower location of the "secondary air injection one" nozzles were just facing the return leg section. This increased the risk of having gas back-flow because the nozzles were injecting straight into the return leg opening.

Second of the proposed modifications is the increase of the air and fuel reactor loop-seal recycle chamber overflow height, for both the return legs of the two loop-seals (shown in Figure 4.5). This determines an increase of the solids columns accumulated in the return leg recycle chambers. An increase of 0.2 m was implemented; this value is almost doubling the overflow height with an expected doubling of the pressure drop between the loop-seal bottom section and the point where the return leg in use merges (P_B-P_A, Figure 4.3).

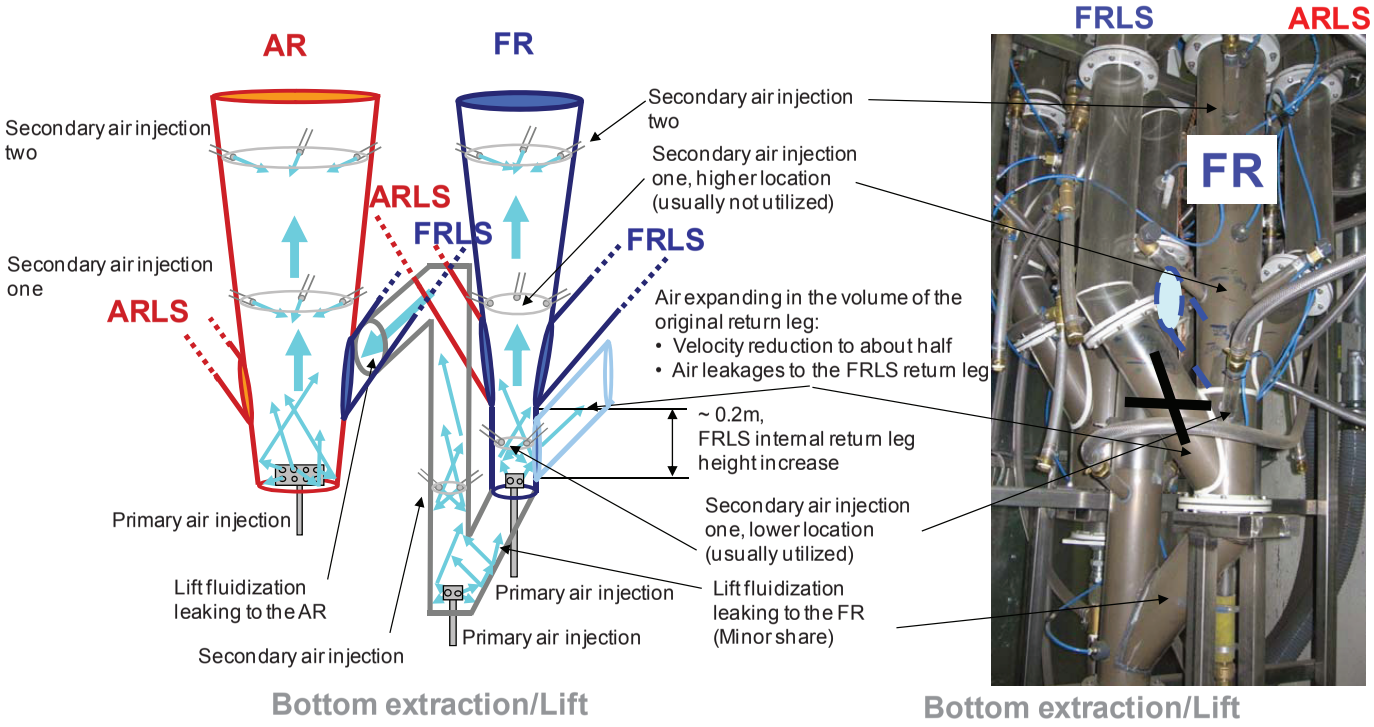

Figure 4.4: Schema (left side) and picture (right side) of the reactor system bottom section, showing the fuel reactor (FR), air reactor (AR), bottom extraction/lift, air injections and return leg locations before (light blue on the left drawing, black x on the right picture) and after the design improvement.

In Figure 4.5 the new loop-seal design is shown, on the left side with a schema while on the right side a CAD drawing shows the old one. The first one represents with purple arrows the solids circulation and with the light blue arrows the gas flow paths. The case shown is that one with full solids exchange and no internal re-circulation of solids, in fact the internal bubble cap nozzle is not fluidized. The fluidization regime in the loop-seal downcomer and in the recycle chambers have to be better understood, especially because it depends very much on the operating conditions which determine the overall pressure balance. As an example the gas direction in the downcomer is not known, and it has fundamental importance influencing the pressure drop across the downcomer particles together with the particles column height, as mentioned in Section 3.5 [99]. The gas dragged down with the solids circulating is going downwards while the gas injected from the nozzles goes partially upwards. These uncertainties related to the gas flows, thus the superficial gas velocities for each loop-seal section, have been the biggest obstacle to a deep characterization of the fluidization regimes for each loop-seal component. This is especially true because during the test campaign presented in this thesis a good understanding of the reactor system and the divided loop-seals operation had to be achieved and their design, thus hydrodynamic robustness, had to be improved. A sensitivity analysis with the usage of tracer gas

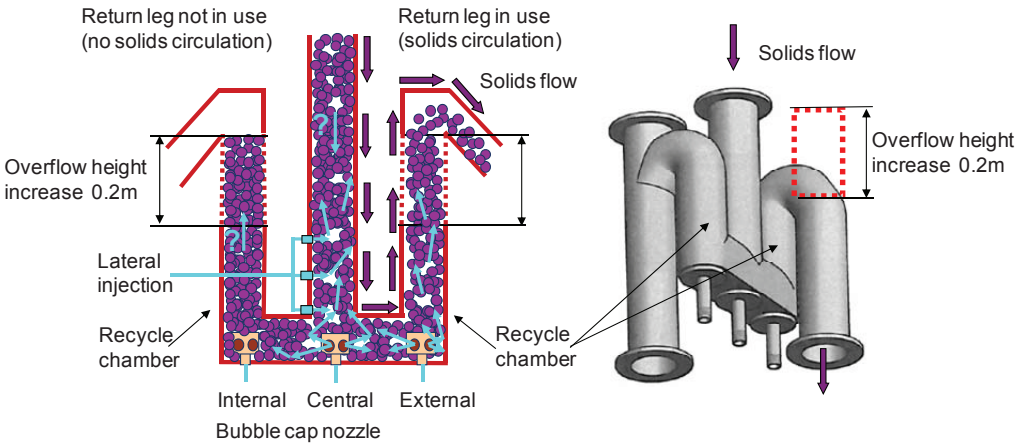

Figure 4.5: Schema (left side) showing the divided loop seal after the design improvement and CAD drawing showing it before the design improvement. The first one is also showing the solids flow and the air injections and stream directions during design case operation, without solids re-circulation in the internal return leg, which is not in use.

injections needs to be done, now that those issues have been addressed. It will provide a complete understanding of the loop-seals fluidization regimes.

The successful tests involving the whole reactor system, coupling air and fuel reactor, were collected and analyzed to find possible dependencies between the reactors solids entrainment and other parameters: both measured parameters and input parameters like the superficial gas velocity at the reactor exit, the primary/secondary air share, the total solids inventory. For each reactor, a clear dependency of the solids entrainment was found, both from the superficial gas velocity at the reactor exit and from the pressure drop measured at the reactor upper section. The key has been to look for components or regions of the reactor system which pressure drops are sensitive to small changes in solids flux and gas velocities, as suggested by Patience et al. [119]. The pressure drop in the cyclones has proved to be very much depending on both the superficial gas velocity (V_{cyc_entr}) and the solids flux (Gs), achieving a fit with a coefficient of determination, R^2, of about 0.9. The air and fuel reactors cyclones' pressure drop correspond respectively to P10-P12 and P23-P25 looking at the numbering of Figure 3.2. Those dependencies are shown in Figure 4.6 a) and b). All the utilized tests were originally performed to understand the reactor system behaviour and design limitations. This means that they were not systematically carried out to map those dependencies; in fact the operational conditions were differing rather much. Nevertheless, it was possible to find such high fit, isolating the entrained solids flux as function of the pressure drop that it generates through the cyclone. In addition, the results tell that also the superficial gas velocity entering the cyclone should be kept into account because it contributes to generate the cyclone pressure drop; both directly due to gas pressure losses and indirectly influencing the entrainment increase. In fact this is the reason why in Figure 4.6, a) the FR cyclone pressure drop is much higher than the AR one. Looking at Figure 4.6, b) it is possible to see how the FR velocities are higher than the AR ones and how much this affects the pressure drop. The intention is to develop a correlation that can be utilized to monitor on-line the entrained solids flux also for hot conditions. This indirect solids entrainment evaluation will ease the control of the overall system and especially in off-design conditions, when the amount of solids exchanged has to be varied according to the process requirements as explained in Section 3.7. Now that a good understanding of the way to operate the reactor system has been reached and the design has been improved, the promising dependencies of the cyclone pressure drop both on the solids entrainment and on the gas velocity at the exit of the inlet duct will have to be

systematically studied, as a further work, and combined together to derive an accurate G_s prediction.

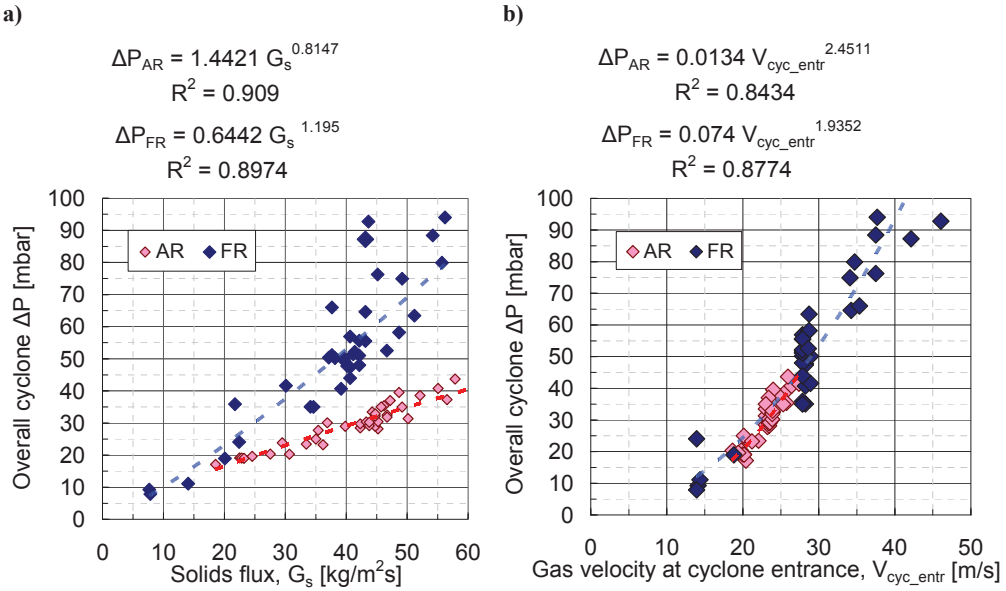

Figure 4.6: Overall cyclones pressure drop (ΔP) dependency on the entrained solids flux, G_s, a) and on the superficial gas velocity at the cyclones entrance, just after the inlet duct acceleration V_{cyc_entr} b).

4.2. Improved design performance

The design improvements proposed in the previous section have been implemented. The fuel reactor loop-seal internal return leg has been lifted of 0.2 m and now it merges in the FR body at the same height as the return leg coming from the air reactor loop-seal, according to the drawing of Figure 4.4. Both the loop-seals overflow heights were lifted of 0.2 m as in Figure 4.5. So it was possible to perform a few tests to make an evaluation of how they affect the reactor system performance. In addition a particle size distribution according to Figure 4.2 was utilized; in this way the superficial gas velocity required to exchange the same solids flow as with the coarser particles is lower. Information regarding the performance of the reactor system design case before the design modification and particles change is presented in Paper III and Paper IV.

Figure 4.7 represents the pressure profile of a test performed after all the modifications were implemented and protruding cooling panes were inserted both in the air and fuel reactor, in

the way shown in Figure 4.8. The cooling panels, three in the AR and two in the FR, were located at the heights shown in Figure 4.9 a) and b) and qualitatively in Figure 3.2. The improved design showed a higher stability allowing the achievement of a solids circulation of almost 3 $kg \cdot s^{-1}$ (almost 70 $kg \cdot m^{-2} \cdot s^{-1}$). It was done with a superficial gas velocity in the AR of just 1.5 $m \cdot s^{-1}$, including the air injected in the lift. The 3 $kg \cdot s^{-1}$ entrained from the AR were all sent to the fuel reactor, which was capable to entrain back 1.7 $kg \cdot s^{-1}$ (about 103 $kg \cdot m^{-2} \cdot s^{-1}$) with a superficial gas velocity of 1.6 $m \cdot s^{-1}$ basically doubling the maximum FR solids flow achieved with the previous design. The higher solids entrainments are the consequence of the finer particles, easier to fluidize, and the increase in total solids inventory (TSI) up to 170 kg (vs. 120 kg).

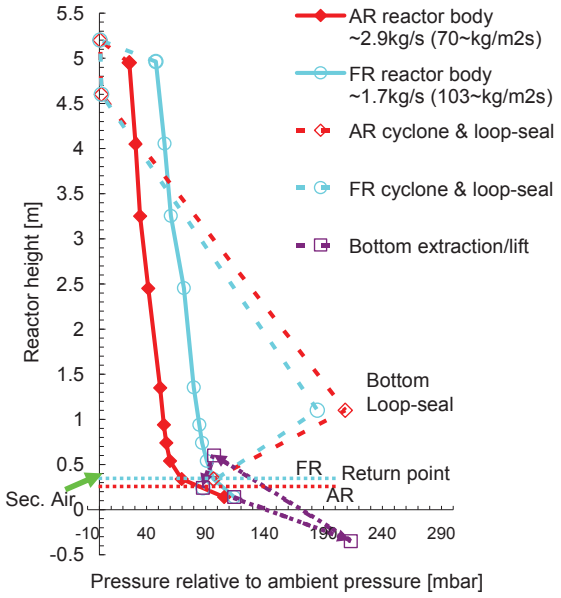

Figure 4.7: Pressure profile measured in the reactor system, after reactor improvement operated with finer particles and cooling panels inserted. Secondary air location and return points height to the air reactor (AR) and fuel reactor (FR) are highlighted.

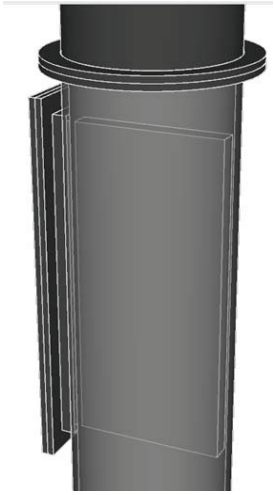

Figure 4.8: Protruding cooling panel zoom.

The higher solids inventory was in first place required to fill the higher overflow heights of the loop-seals, which allow gaining in system stability, but contribute to reduce the inventory share inside the reactors. The latter corresponds to the inventory that would actively participate in

the reactions in a hot setup. The active inventories estimated in the reactor bodies by means of pressure measurements, are lower compared to those estimated before the design change: about 28kg for the AR and 10 for the FR vs. 31 and 13kg of the design case condition before modification. They are slightly lower looking at the absolute number, but considering the TSI increase from 120 to 170kg they correspond to a large active mass reduction. The smaller active inventory (from 37% to 22% of the TSI) is mainly due to a big reduction of the mass in the reactors bottom sections, as confirmed by the concentration curves of Figure 4.9. At the same time the shift towards faster fluidization regimes determined a concentration increase in the upper section. The solids concentration in the reactors upper section is equal to about 1% of the reactor volume and sometimes even above this value till the reactor exit. Before the modification, it was dropping dramatically from the height of 2 m till the reactor exit (Figure 5 in Paper III). This is especially true for the FR, which in fact entrains a higher solids flux of about 100 $kg \cdot m^{-2} \cdot s^{-1}$ vs. 70 $kg \cdot m^{-2} \cdot s^{-1}$ of the AR.

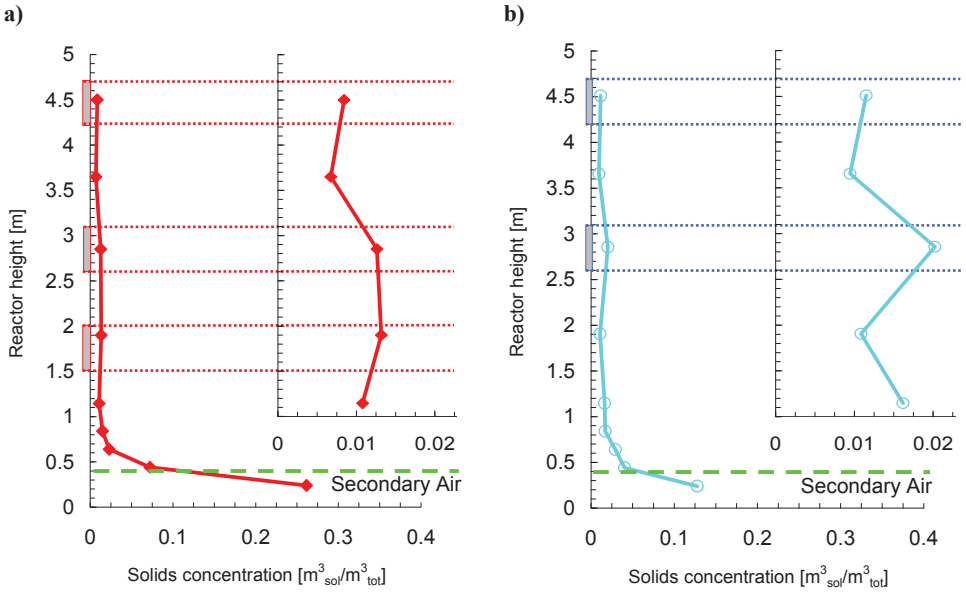

Figure 4.9: Concentration profile in the air reactor a), and fuel reactor b) bodies for the improved design test, with finer particles. The cooling panels and secondary air injections location are provided.

As a consequence of the reactors faster fluidization regimes and higher entrainment, the solids fluxes through the connecting ducts are much higher: the fluxes in the AR and FR

downcomers are about 360 and 200 $kg \cdot m^{-2} \cdot s^{-1}$, respectively about 50% and 100% increase compared to the design case before modification. The moving packed bed solids level height in the AR downcomer slightly increased up to about 0.7m and the FR one increased up to 0.6m, compared to the previous design values of about 0.6 and slightly above 0.4m, respectively for air and fuel reactor. No clogging was noticed and the loop-seal appeared smoothly fluidized with eventually small bubbles rising from the bottom nozzles. The fluidizing air injected was about the same as before the modifications, despite the higher solids circulation to deal with: it was 5, 30 and 100 $Nl \cdot min^{-1}$ for the lateral, central and external air injections respectively for both the reactors. As long as the downcomers solids level heights were measured to be about the same, the loop-seal fluidization was kept the same for those few tests. The lift gas velocity was kept at 1.5 $m \cdot s^{-1}$, as for the design case before modification. This shifted anyhow the lift fluidization regime towards faster fluidization, thus entrainment, because of the finer PSD. The higher lift entrainment is therefore another reason of the high solids circulation.

The pressure drop of both the cyclones did not vary so much, because the smaller superficial gas velocities reduced it, but the higher solids flows increased it. The solids flows almost doubled for the FR and increased of 50% for the AR. The gas velocities at cyclones inlet were about 14 and 17 $m \cdot s^{-1}$, respectively for the air and fuel reactor. The cyclones efficiencies were measured to be about 99.9%, it is slightly below the value of 99.95% reached before the modifications discussed in this section. To this respect, it has to be considered that the cyclones inlet velocities should have been somehow higher, typical values for circulating fluidized beds are above 20 $m \cdot s^{-1}$ [120]. This means that the PSD reduction, down to such fine d_{50}, did not affect so much the cyclones performance confirming the good quality of their design whose key features are mentioned in Paper I. It was not possible to find similar high density Geldart A particles to benchmark the cyclone performance. It was compared with the efficiency of high loaded cyclones operating with Geldart A fluid catalytic cracking (FCC) particles, showing to be promisingly higher [121]. A secondary cyclone to take care of this 0.1% of fine losses needs to be installed, even if it will cost in terms of extra pressure drop and extra components. Especially in hot conditions, it will help to reduce the refilling frequency, to avoid damaging the downstream equipments and it will also be important for health safety and environment (HSE) reasons. A systematic test campaign should be performed to map the cyclones efficiency according to the operating conditions and possibly each of them should be connected to a

separated filter box and scale. In this way it will be possible both to monitor the cyclones' efficiency on-line and also to analyze the PSD of the losses. In addition also the erosion problems need to be addressed; it hurt the design[17], especially in correspondence of the points where the particles stream was impacting the FR cylindrical body. It has to be understood if it is enough to reduce the superficial gas velocity at cyclone inlet, as it has been done with the finer PSD. Another option is to re-think the cyclone design, which has a tangential inlet, going to a volute inlet [122]. The latter is supposed to provide more space to the particles, which enter the cyclone already with an angle after having experienced the centrifugal force. This means that they take a circular trajectory before impacting the cyclone wall, reducing the risk of hitting it straight at their maximum velocity. The vortex finder was saved from the erosion problem by its eccentricity; in this way it was not in the particle trajectory.

The insertion of dummy cooling panels, did not affect so much the reactor performance. The panels have been tested already in the AR during the separate operation/debugging phase confirming this impression, as discussed in Paper II and in Section 3.5. The main cooling panels influence on the reactor system performance was a slight solids concentration increase in correspondence of their presence (Figure 4.9, a) and b). It happened also in other circumstances, especially for higher solids concentrations, to experience a concentration increase which was not the consequence of cooling panels insertion. Anyhow, this concentration increase is located exactly in correspondence of the panels location and is also confirmed by the above-mentioned AR tests done in the debugging phase, Figure 3.9. The panels presence is creating an obstacle to the flow resulting in a local pressure drop. Part of it is just the consequence of higher friction due to local turbulences and gas acceleration. The panels induce a cross-section area reduction which increases locally the superficial gas velocity from 1.5 $m \cdot s^{-1}$ and 1.6 $m \cdot s^{-1}$ up to 1.9 $m \cdot s^{-1}$ and 2.4 $m \cdot s^{-1}$, respectively for air and fuel reactor. What needs to be understood is, how much of the measured pressure drop is really due to the higher solids concentration. It can be done, as further work, sampling the particles concentration inside the reactor by means of non-isokinetic suction probes [112-114] or more advanced systems like optical and capacitance probes [112 and 123].

The pressure difference between the loop-seals bottom sections (P_B, Figure 4.3) and the reactors points where the return legs in use merge (P_A, Figure 4.3), had a big increase as a

[17] Design before the change in PSD, when it comes to the finer particles, too little tests have been performed in order to evaluate erosion phenomena.

consequence of the 0.2 m increase of the recycle chamber overflow height. The pressure difference P_B-P_A, (Figure 4.3) in this case is about 100mbar, slightly higher for the AR loop-seal and slightly lower for the FR one. The pressure difference experienced in the AR loop-seal was higher than the FR one before the design modifications as well; it could reach maximum values of about 80 mbar for the higher solids fluxes, while the FR was at about 50 mbar (Paper IV describes these issues for the design before the modifications were implemented). This was most likely a consequence of the higher solids flux passing through the AR downcomer and loop-seal, usually more than the double that of the FR one. The new pressure values can be noticed in Figure 4.7 and are clearly shown in Figure 4.10 a) and b), where the pressures in correspondence of the loop-seals bottom sections (P28 and P30 for air and fuel reactor respectively, Figure 3.2) are plotted together with the pressures measured in correspondence of the return points. Those are, for this operational conditions: P15, faced by the return leg in use of the AR loop-seal and by the return leg not in use for the FR loop-seal, and (P1+P2)/2, faced by the return leg in use of the FR loop-seal and by the return leg not in use of the AR loop-seal.

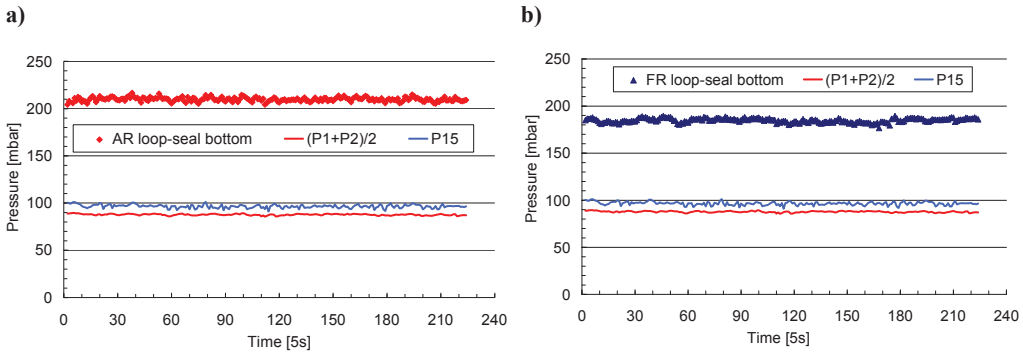

Figure 4.10: Continuous pressure measurements of the air reactor (AR), a), and fuel reactor (FR), b), loop-seals bottom pressures. Those are compared with the pressure measurements in correspondence of the points of the reactor bodies where the return legs merge: (P1+P2)/2 and P15 (Figure 3.2).

The presented case study cannot be directly compared with the results of the previous test campaign, because two crucial components have been modified and the PSD have been changed. In addition the protruding cooling panels have been inserted and several inputs have been changed like the TSI increase and superficial gas velocity reduction. Ideally would have been

interesting to implement the design modifications separately to better isolate their influence on the whole system performance. The great impact of the PSD reduction is evident because of the large increase of reactors solids entrainment, which has also the consequence of reducing the pressure at the reactors bottom section. At the same time the higher loop-seals recycle chambers overflow heights gave more stability to the system. This determined the achievement of much higher pressures in the bottom section of the loop-seals, up to above 200mbar. It made the circulation of higher amounts of solids smoother and reduced the back-flow risk, both reducing the pressure fluctuations in correspondence of the bottom section of the loop-seals, P_B (Figure 4.3), and increasing the pressure unbalance that can be achieved safely between the two loop-seal return legs, $|P_A-P_C|$ (Figure 4.3). According to those preliminary tests the pressure fluctuations went to about ± 10÷15mbar to ±5mbar (Figure 4.10) and the $|P_A-P_C|$ value can be estimated to be at least about 70÷80 mbar, from the previous 30. Those facts also indirectly helped to increase the solids circulation. In addition, such high pressure (P_B, Figure 4.3) makes easier to pneumatically control the re-circulation of entrained particles, because it is easier to win the resistance of the return point pressure were the return leg in use is merging (P_A, Figure 4.3), gaining in flexibility. The increased height of the return leg is an important improvement, but its contribution was in essence not utilized because of such high loop-seals bottom pressure and because of the reduction of the pressure at the lower section of the reactors. The increase in solids entrainment and the improvement of solids distribution control is fundamental to be capable to run the reactor system with a high variety of oxygen carriers and off-design according to the methodology presented in Section 3.7. In addition this will help the fulfillment of higher oxygen requirements, thus solids circulation e.g. partly addressing the pressurized conditions challenges.

5. Conclusions & future work

5.1. Conclusions

- The design for a 150kW$_{th}$ chemical looping combustion reactor system has been proposed and its hydrodynamics validated by means of a full scale, non-reactive, cold flow model (CFM). It consists of a double loop circulating fluidized bed (DLCFB), meant to address several issues which are still open with respect to the technology state-of-the-art. Both the air and fuel reactor are capable to operate in fast fluidization regime increasing the gas solids contact, especially to improve the reactions taking place in the fuel reactor, thus fuel conversion. Industrial solutions are used e.g. heavy loaded cyclones, bubble cap nozzles, two levels of secondary air injection and protruding cooling panels. Operation flexibility is aimed in order to have accurate control of the solids exchanged between the reactors and to better control the reactor performance according to the specific application requirements in terms of reactors fluidization regimes, solids exchange and gas streams flow and temperature. Compactness has also been a priority both for design up-scaling and future upgrading to pressurized conditions; this way it can be easily inserted into a pressurized vessel.
- The key features of the actual design can in general be utilized for fluidized bed processes based on two reactions taking place simultaneously in two different reactors which continuously exchange the bed material, thus reactants and heat, being interconnected. These have been validated from hydrodynamic point of view: an understanding of their performance as well as the best way to operate the reactor system has been reached.

  One is the pneumatically controlled divided loop-seal, which allows re-circulating back to the reactor of origin part of the entrained solids, uncoupling the solids exchange from the solids entrainment. This represents a solids exchange control parameter in addition to the "conventional" ones: superficial gas velocity, primary/secondary air injection shares and solids inventory. It increases the freedom to operate the reactors just focusing on the fluidization regime, which is ideal for the reactions and/or for the downstream needs in terms of heat load. From a fluidization engineering point of view the loop-seal design presents several unique features. Each of its two return legs is connected to a different reactor, one to the air reactor and the other to the fuel reactor. This means that each of the two return legs faces a different pressure in correspondence of the points where it merges with the reactors.

The conventional pneumatically controlled loop-seals have just one return leg or two merging at the same height of the same reactor, thus facing the same pressure. The control over the solids split and over the above-mentioned pressure unbalance, due to the different pressures experienced by the two return legs, is not exerted using mechanical valves, but utilizing gas injections in a number of points.

The other key feature is the usage of the bottom extraction/lift, which has a great potential in such kind of two-reactor configuration. It allows controlling the inventory distribution among the reactors, shifting mass from one to the other. This is a quick and effective way to control the reactors bottom pressures, which is the place where the above-mentioned loop-seals return legs merge. For this reason, it means pneumatic control over the pressure unbalance which the divided loop-seals are exposed to. This also exerts an extra control over the reactors fluidization regimes and solids entrainment.

Finally, it is necessary to fulfil the mass balance especially if one reactor has smaller cross-section and/or have less fluidizing gas availability, than the other. The method to better combine the above-mentioned two design features has been found and the reactor system has shown to be flexible and stable. They have to be operated in a way that the pressure unbalance across the loop-seals does not go above the maximum value allowed by its design: by the loop-seal recycle chamber overflow height. This task becomes more challenging when the return legs are facing higher pressures both because of reactors operation and design constraints. Reactor operation means that the aimed reactors fluidization regimes imply high pressure or means a high total solids inventory. Design constraints are related to a too high cyclone pressure drop for certain superficial gas velocities and/or a too low height of the point where the return legs merge into the reactor bodies.

- An overview of the two most common cold flow modelling scaling strategies is provided: the small scale models resembling the hot rig hydrodynamics and the full-scale models, keeping the same surface to volume ratios. The first being common in academia and the second in the industry. The innovative idea was to combine those two into a triangular correlation. The full-scale cold flow model is used to debug the 150kW_{th} hot rig design as the industry does, but at the same time the particle size distribution and superficial gas velocity are selected in a way

that the cold flow model represents the small scale hydrodynamic model of an industrial application.

- The usage of such fine particle size distribution of a so high density material represents a solution which is not easy to find in published fluidization literature, in particular for circulating fluidized beds. In the present work a high density Geldart group A powder with a d_{50} of about 34 μm and density of 7000 $kg \cdot m^{-3}$ was used. The handling of such fine particles is complex both for health, safety and environment point of view and also from a process point of view. The latter is an issue when it comes to the cyclone performance. The highly load cyclones showed a good performance, managing to have an efficiency of above 99.9%, even for the smaller particle size distribution tested of about 25 μm. The usage of such finer d_{50} of 25 μm compare to the first one of 34 μm, allowed to reach the same solids entrainment with smaller superficial gas velocity. The evaluation of its impact on such complex reactor system showed how the usage of different particle size distributions can be used as effective control factor for the overall system performance and equilibrium.
- Promising correlations linking the solids entrainment to the cyclone pressure drop and inlet gas velocity have been found. Those can be utilized as a starting point to develop a way to estimate on-line the solids entrainment. An indirect estimation, without the need for direct measurements, has fundamental importance in the overall system control, especially to control the off-design operation and the transients.

5.2. Future work

As discussed in Section 5.1, an innovative design for chemical looping processes has been presented in the Ph.D. thesis; afterwards it has been validated by means of cold flow modelling and improved after an analysis of its key components performance. Those issues which deserve a further investigation are:

- The improved design has shown promising preliminary results; though a more comprehensive test campaign is needed. The superficial gas velocities of air and fuel reactor and bottom extraction need to be varied as well as the loop-seals fluidization. This has to be done for several total solids inventories. In this way it will be possible to find the reactor system best operational conditions and more accurately the operational

window, understanding its flexibility margins with main focus on the circulation capability and pressure unbalance the loop-seal can withstand.

- The design improvements should be investigated one by one. Their separate implementation will provide important information to understand to which extent they affect the overall system performance. Further variations of those design details can be tested increasing more the return leg height and the loop-seal recycle chamber overflow height. At the same time new design changes can be implemented like other internals insertions to study different cooling configurations or devices (e.g. bayonet) as well as cyclones design modifications impact or secondary cyclones insertion downstream and their impact on the overall pressure drop.
- Promising dependencies of reactors solids entrainment with input and measured parameters have been found. The most promising is the dependency of the cyclone pressure drop both on the solids entrainment and on the cyclone inlet gas velocity. Dedicated tests should be done, with the improved design following a test matrix to define according to the acquired understanding. The objective should be to map those dependencies accurately and derive empirical mathematical correlations. This will allow on-line indirect quantification of the solids entrainment, fundamental for the reactor system control.
- A more accurate analysis of the hydrodynamic phenomena will be of utmost importance. As an example, local measurements of the particles concentration by means of non-isokinetic suction probes can be cited. Those will help to verify the assumptions done to derive the solids concentration profiles from the pressure measurements and will also help to evaluate the local impact of internals and primary/secondary air injection shares on the particles concentration. The understanding of the fluidization regime inside the divided loop-seals is another open question. The unknown downcomer gas velocity and direction has big impact on its behaviour, so that gas tracer tests for different operational conditions will help to address it. More in general also gas tracer experiments will be fundamental to understand if there are gas leakages from one reactor to the exhausts of the other one. This is a kind of test that should be performed for each of the reactor system case studies.

- A control strategy needs to be further developed, with main focus on operational transients. First the off-design cases as well as other kind of chemical looping applications, need to be simulated by means of process design software. In this way it will be possible to have an accurate evaluation of the cycle requirements to fulfil in terms of mass and heat flows, both between the reactor system and the overall process up and down-stream requirements and between the air and fuel reactor to optimize the reactions. Second step consists of verifying if the design can fulfil those requirements from hydrodynamic point of view. This can be done starting from the hydrodynamic lessons learnt and presented in this work. Among those identified as key control parameters there are: the pressure differences between the loop-seals bottom sections and the points where their return legs merge in the reactors, including the pressure fluctuations, the two reactors and lift pressure drops, thus inventories and the solids entrainment to monitor the exchanged mass. This kind of job has been done qualitatively in the thesis because it was in parallel with the ongoing design development. Now that the design has been finalized and is more robust hydrodynamically those studies need to be done also quantitatively: first at steady state and afterwards in transient conditions. The latter will help the understanding the details of how the reactor system reacts to operational changes until new equilibrium conditions achievement.

All these points represent a further evaluation of the performance of the cold flow model improved design, continuing with the work done in the Ph.D. thesis. The reactor system design has already proved to be robust, but those tests will provide a deeper knowledge especially with respect to the reactor system operation optimization and physics understanding. This will help to face unexpected situations in hot operation and eventually to further improve the design especially for operational sets located on the border of the operational window. Once these points will be addressed the hot 150kW_{th} design will be ready to be built.

In addition to the above-mentioned further cold flow model testing, the future work to do in a longer term period, once also the hot 150kW_{th} reactor system will be built, commissioned and evaluated is:

- The possibility of pressurizing the chemical looping reactor is of utmost importance both for natural gas combustion and reforming. The actual work tried to figure out some of the

challenges and address them: the possibility to increase the excess air ratio up to gas turbine cycles requirements, the compactness to enclose the reactor system into a pressurized vessel and the high flexibility and stability in operation, especially for high solids circulation. The next step should be to reengineer the actual design to tackle the pressurization open questions. One is the accurate pressure control at reactors gas stream exit; a pressure unbalance there will strongly affect the divided loop-seals operation. The pressurized conditions may easily generate a pressure unbalance which cannot be tackled simply by increasing the overflow height of the loop-seals recycle chambers. Another open issue is consequence of the fact that under pressurized conditions the gas density increases linearly with the pressure while the solids density and performance of the oxygen carrier are about the same. The reactor system design has to be modified in the direction of higher solids circulation to provide the required oxygen with the same fluidizing gas availability. The fuel reactor design can be modified to be capable to still have a circulating fluidized bed regime with less fluidizing gas availability e.g. cross-section reduction. The oxygen requirements of the fuel reactor can be reduced utilizing CO_2 re-circulation instead of part of the fuel to keep the same fluidization regime. All those ideas may be necessary at the same time, being careful to the way they affect the heat balance.

- Simulation work can be done especially regarding computational fluid dynamics (CFD) utilizing the measured results to validate the developed models.
- The cold flow model results and the hot $150kW_{th}$ results can be utilized to design and build an industrial application based on the presented double loop circulating fluidized bed. In addition once all three the set-ups, cold, $150kW_{th}$ and industrial, will be built and working the proposed triangular scaling strategy should be evaluated.
- The actual double loop circulating fluidized bed design can be adapted to the chemical looping combustion of liquid and solid fuels as well as to other chemical looping processes which require two interconnected fluidized beds. This will need to re-think some of the DLCFB components in order to fulfil the requirements of the different processes.

References

[1] Fourier J., 1824. "Remarques générales sur les températures du globe terrestre et des espaces planétaires", *Ann. Chim. Phys.*, Vol. **27**, pp. 136–167. This essay was reprinted, with slight changes, as. Fourier J., 1827. "Mémoire sur les températures du globe terrestre et des espaces planétaires", *Mém. Acad. Sci.*, Vol. **7**, pp. 569–604.

[2] Arrhenius S., 1896. "On the Influence of Carbonic Acid in the Air upon the Temperature of the Ground", *Phiolos. Mag.,* Series 5, Vol. 41, pp. 237–276.

[3] Moberg A., Sonechkin D.M., Holmgren K., Datsenko N M., Wibjörn K., 2005. "Highly variable Northern Hemisphere temperatures reconstructed from low- and high-resolution proxy data", *Nature,* Vol. 433, No. 7026, pp. 613–617.

[4] United Nations Framework Convention on Climate Change, 2011. "National greenhouse gas inventory data for the period 1990-2009". http://unfccc.int/resource/docs/2011/sbi/eng/09.pdf

[5] Intergovernmental Panel on Climate Change (IPCC), 2011. Data distribution centre. Data distribution centre. http://www.ipcc-data.org/ddc_co2.html

[6] Earth System Research Laboratory, Global Monitoring Division. "Trends in Atmospheric Carbon Dioxide". http://www.esrl.noaa.gov/gmd/ccgg/trends/mlo.html

[7] Intergovernmental Panel on Climate Change (IPCC) Fourth Assessment Report. Climate change 2007: Working Group II: Impacts, Adaptation and Vulnerability.

[8] International Energy Agency, 2010. World Energy Outlook, 2010. Rue de la Fédération 9, 75739 Paris Cedex 15, France.

[9] Bolland O., 2011. "CO_2 capture in power plants", *lecture notes.* Norwegian University of Science and Technology (NTNU), Trondheim, Norway.

[10] de Coninck H., Stephens J.C., Metz B., 2009. "Global learning on carbon capture and storage: A call for strong international cooperation on CCS demonstration", *Energ. Policy*, Vol. 37, No. 6, pp. 2161–2165.

[11] Working group III of the Intergovernmental Panel on Climate Change, [B.Metz, O. Davidson, H.C. de Coninck, M. Loos, and L.A. Mayer], 2005. "*IPCC Special Report on Carbon Dioxide Capture and Storage"*, Cambridge University Press, Editor, New York, USA.

[12] Herzog H.J, 2011. "Scaling up carbon dioxide capture and storage: From megatons to gigatons", *Energ. Econ.*, Vol. 3, No. 4, pp. 597–604.

[13] Jin H.G., Zhang X.L., Gao L., Yue L., He J.K., Cai R.X., 2008. "Fundamental study of CO_2 control technologies and policies in China", *Sci. China Ser. E*, Vol. 51, No. 7, pp. 857–870.

[14] Som S.K., Datta A., 2008. "Thermodynamic irreversibilities and exergy balance in combustion processes", *Prog. Energ. Combust.*, Vol. 34, No. 3, pp. 351–376.

[15] Richter H.J., Knoche K.F., 1983. "Reversibility of combustion processes", In: Gaggioli R.A. (Ed.), A.C.S. Symposium Series 235. Washington DC, USA, pp. 71–85.

[16] Ishida M., Zheng D., Akehata T., 1987. "Evaluation of a chemical-looping-combustion power-generation system by graphic exergy analysis", *Energy,* Vol. 12, No. 2, pp. 147–154.

[17] Fan L.S., 2010. "Chemical looping systems for fossil energy conversions", John Wiley & Sons, Inc., Hoboken, New Jersey, United States of America.

[18] Hurst S., 1939. "Production of hydrogen by the steam-iron method", *J. Am. Oil Chem. Soc.,* Vol. 16, No. 2, pp. 29–35.

[19] Lewis W.K., Gilliland E.R., 1946. "Production of pure carbon dioxide", U.S. Patent No. 2,665,971.

[20] Linderholm C., Mattisson T., Lyngfelt A., 2009. "Long-term integrity testing of spray-dried particles in a 10-kW chemical-looping combustor using natural gas as fuel", *Fuel,* Vol. 88, No. 11, pp. 2083–2096.

[21] Anheden M., 2000. "Analysis of Gas Turbine Systems for Sustainable Energy Conversion", Ph.D. thesis, KTH - Royal Institute of Technology, Stockholm, Sweden.

[22] Petrakopoulou F., Boyano A., Cabrera M., Tsatsaronis G., 2011. "Exergoeconomic and exergoenvironmental analyses of a combined cycle power plant with chemical looping technology", *Int. J. Greenh. Gas Con.*, Vol. 5, No. 3, pp. 475–482.

[23] Consonni S., Lozza G., Pelliccia G., Rossini S., Saviano F., 2004. "Chemical-Looping Combution for combined cycles with CO_2 capture*", Proceedings of ASME Turbo Expo 2004 Power for Land, Sea, and Air*. June 14-17, 2004, Vienna, Austria.

[24] ENCAP DeliverableD1.2.6, 2009. Power systems evaluation and benchmarking–public version, URL: http://www.encapco2.org/.

[25] Pröll T., Bolhàr-Nordenkampf J., Kolbitsch P., Hofbauer H., 2010. "Syngas and a separate nitrogen/argon stream via chemical looping reforming – A 140 kW pilot plant study", *Fuel,* Vol 89, No 6, pp. 1249–1256.

[26] Rydén M., Lyngfelt A., 2005. “Hydrogen and power production with integrated carbon dioxide capture by chemical-looping reforming”, *Greenhouse Gas Control Technologies 7*. E.S. Rubin, D.W. Keilh and C.F. Gilboy (Eds.). Vol. 1, pp. 125–134.

[27] Marx K., Pröll T., and Hofbauer H., 2011. “Design requirements for pressurized chemical looping reforming”, *International Conference on Circulating Fluidized Beds and Fluidization Technology - CFB-10*, May 1 - 5, 2011, Sunriver, Oregon, USA.

[28] Berguerand N., 2009. “Design and Operation of a 10kW_{th} Chemical-Looping Combustor for Solid Fuels”, *Ph.D. thesis*, Chalmers University of Technology, Sweden.

[29] Noorman S., van Sint Annaland M., Kuipers H., 2007. “Packed Bed Reactor Technology for Chemical-Looping Combustion”, *Ind. Eng. Chem. Res.,* Vol. 46, No. 12, pp. 4212–4220.

[30] Abanades J.C., Murillo R., Fernandez J.R., Grasa G., Martínez I., 2010. “New CO2 Capture Process for Hydrogen Production Combining Ca and Cu Chemical Loops”, *Environ. Sci. Technol.,* Vol. 44, No.17, pp. 6901–6904.

[31] Noorman S., Gallucci F., van Sint Annaland M., Kuipers J.A.M., 2011. “Experimental Investigation of Chemical-Looping Combustion in Packed Beds: A Parametric Study”, *Ind. Eng. Chem. Res.,* Vol. 50, No.4, pp. 1968–1980.

[32] Moghtaderi B., 2011. “Hydrogen enrichment of fuels using a novel miniaturised chemical looping steam reformer”, *Chem. Eng. Res. Des.*, article in press: DOI: 10.1016/j.cherd.2011.06.012.

[33] Ljungström F., 1938. “Heat exchange”, United States Patent Office Number: 2,313,081, March. 9, 1943.

[34] Fosse Håkonsen S., Blom R., 2011. “Chemical Looping Combustion in a Rotating Bed Reactor – Finding Optimal Process Conditions for Prototype Reactor”, *Environ. Sci. Technol.*, Vol. 45, No. 22, pp. 9619–9626.

[35] Salatino P., Senneca O., Cortese L., 2010. “CarboLoop: a novel concept of looping combustion of carbon” *Les Rencontres Scientifiques de l'IFP – 1st International Conference on Chemical Looping* - 17-19 March 2010, Lyon, France.

[36] McGlashan N.R., Childs P. R. N., Heyes A.L., 2009. “Chemical Looping Combustion Using the Direct Combustion of Liquid Metal in a Gas Turbine Based Cycle”, *J. Eng. Gas. Turb. Power.,* Vol. 133, No. 3, pp. 031701-01–13.

[37] Geldart D., 1973. “Types of gas fluidization”, *Powder Technol.,* Vol. 7, No. 5, pp. 285–292.

[38] Avidan A.A., 1997. “Fluid catalytic cracking”, in: Grace J.R., Avidan A.A., Knowlton T.M. (Eds.), “*Circulating Fluidized Beds*”, Chapman & Hall, London, 1997, pp. 466–488 (chap. 13).

[39] Wu R.L., Lim C.J., Chaouki J., Grace J.R., 1987. “Heat Transfer from a Circulating Fluidized Bed to Membrane Waterwall Surfaces”, *AIChE J.*, Vol. 33, No. 11, pp. 1888–1893.

[40] Johansson E., Mattisson T., Lyngfelt A., Thunman H., 2006. “A 300 W laboratory reactor system for chemical-looping combustion with particle circulation”, *Fuel*, Vol. 85, No. 10-11, pp. 1428–1438.

[41] Adánez J., Dueso C., de Diego L.F., García-Labiano F., Gayán P., Abad A., 2009. “Effect of Fuel Gas Composition in Chemical-Looping Combustion with Ni-Based Oxygen Carriers. 2. Fate of Light Hydrocarbons”, *Ind. Eng. Chem. Res*., Vol. 48, No. 5, pp. 2509–2518.

[42] Kolbitsch P., Pröll T., Bolhar-Nordenkampf J., Hofbauer H., 2009. “Characterization of Chemical Looping Pilot Plant Performance via Experimental Determination of Solids Conversion”, *Energ. Fuel.*, Vol. 23, No. 3. pp. 1450–1455.

[43] Fossdal A., Bakken E., Øye B.A., Schøning C., Kaus I., Mokkelbost T., Larring Y., 2011. “Study of inexpensive oxygen carriers for chemical looping combustion”, *Int. J. Greenh. Gas Con.*, Vol. 5, No. 3, pp. 483–488.

[44] Kolbitsch P., 2009. “Chemical Looping Combustion for 100% Carbon Capture – Design, Operation and Modeling of a 120kW Pilot Rig”, *Ph.D. thesis*, TU Wien, Vienna, Austria.

[45] Lyngfelt A., 2010. “Oxygen carriers for chemical looping combustion - operational experience”. In: *1st International Conference on Chemical Looping*, Lyon, France. http://www.ifp.com/actualites/evenements/congres-et-conferences/organises-par-ifp-energies-nouvelles/rs-chemical-looping.

[46] Lyngfelt A., 2011. “Oxygen Carriers for Chemical Looping Combustion – 4000h of Operational Experience”, *Oil Gas Sci. Technol.,* Vol. 66, No. 2, pp. 161–172.

[47] Adánez J., 2010. “Oxygen carrier materials for chemical-looping processes – fundamentals”. In: *1st International Conference on Chemical Looping*, Lyon, France. http://www.ifp.com/actualites/evenements/congres-et-conferences/organises-par-ifp-energies-nouvelles/rs-chemical-looping.

[48] Mattisson T., Lyngfelt A., Leion H., 2009. “Chemical-looping with oxygen uncoupling for combustion of solid fuels”, *Int. J. Greenh. Gas Con.*, Vol. 3, No. 1, pp. 11–19.

[49] García-Labiano F., Adánez J., de Diego L.F., Gayán P., Abad A., 2006 “Effect of Pressure on the Behavior of Copper-, Iron-, and Nickel-Based Oxygen Carriers for Chemical-Looping Combustion”, *Energ. Fuel*., Vol. 20, No. 1, pp. 26–33.

[50] Abad A., Adánez J., García-Labiano F., de Diego L.F., Gayán P., Celaya J., 2007. “Mapping of the range of operational conditions for Cu-, Fe-, and Ni-based oxygen carriers in chemical-looping combustion”, *Chem. Eng. Sci.*, Vol. 62, No. 1-2, pp. 533–549.

[51] Siriwardane R., Poston J., Chaudhari K., Zinn A., Simonyi T., Robinson C., 2007. “Chemical-Looping Combustion of Simulated Synthesis Gas Using Nickel Oxide Oxygen Carrier Supported on Bentonite”, *Energ. Fuel*., Vol. 21, No. 3, pp. 1582–1591.

[52] Ortiz M., de Diego L.F., Abad A., García-Labiano F., Gayán P., Adánez J., 2010. “Hydrogen production by auto-thermal chemical-looping reforming in a pressurized fluidized bed reactor using Ni-based oxygen carriers”, *Int. J. Hydrogen Energ.*, Vol. 35, No. 1, pp. 151–160.

[53] Xiao R., Song Q., Song M., Lu Z., Zhang S., Shen L., 2010. “Pressurized chemical-looping combustion of coal with an iron ore-based oxygen carrier”, *Combust. Flame,* Vol. 157, No. 6, pp. 1140–1153.

[54] Basu P., 2005. “Combustion and gasification in fluidized beds”, Taylor & Francis, Boca Raton, Florida, USA.

[55] Reh L., 2003. “Development potentials and research needs in circulating fluidized bed combustion”, *China. Part.,* Vol. 1, No. 5, pp. 185–200.

[56] Chen Y.M., 2011. “Evolution of FCC – Past Present and Future and the Challenges of Operating a High – Temperature CFB System”, *Tenth International Conference on Circulating Fluidized Beds and Fluidization Technology*. CFB-10. Sunriver, Oregon, USA. May 1-5. pp. 58–85.

[57] Lyngfelt A., Kronberger B., Adánez J., Morin J.X., Hurst P., 2005. “The grace project: development of oxygen carrier particles for chemical-looping combustion. Design and operation of a 10kW chemical-looping combustor”, In: *Greenhouse Gas Control Technologies 7*. Elsevier Science Ltd., Oxford, pp.115–123.

[58] Adánez J., Gayan P., Celaya J., deniego L.F., Garcia-Labiano F., Abad A., 2006. "Chemical looping combustión in a 10kW$_{th}$ prototype usingaCuO/Al2O3 oxygen carrier: effect of operating conditions on methane combustion", *Ind. Eng. Chem. Res*., Vol. 45, No. 17, pp. 6075–6080.

[59] Yazdanpanah M.M., Hoteit A., Forret A., Delebarre A., Gauthier T., 2011. "Oxygen Carriers for Chemical Looping Combustion – 4000h of Operational Experience", *Oil Gas Sci. Technol.,* Vol. 66, No. 2, pp 161–172.

[60] Shen L., Wu J., Xiao J., Song Q., Xiao R., 2009. "Chemical-Looping Combustion of Biomass in a 10 kW$_{th}$ Reactor with Iron Oxide as an Oxygen Carrier", *Energ. Fuel.*, Vol. 23, No.5, pp. 2498–2505.

[61] Ryu H.J., Jin G.T., Yi C.K., 2005. "Demonstration of inherent CO_2 separation and no NO_x emission in a 50kW chemical-looping combustor: Continuous reduction and oxidation experiment". In: *Greenhouse Gas Control Technologies 7*, Elsevier Science Ltd., Oxford, pp.1907–1910.

[62] Ryu H.J., Jo S.H., Park Y.C., Bae D.H., Kim S.D., 2010. "Long term operation experience in a 50 kWth chemical looping combustor using natural gas and syngas as fuels" In: *1st International Conference on Chemical Looping*, Lyon, France. http://www.ifp.com/actualites/evenements/congres-et-conferences/organises-par-ifp-energies-nouvelles/rs-chemical-looping.

[63] Kolbitsch P., Pröll T., Bolhar-Nordenkampf J., Hofbauer H., 2009. "Operating experience with chemical looping combustion in a 120kW dual circulating fluidized bed (DCFB) unit", *Energy Procedia,* Vol. 1, No. 1, pp. 1465–1472.

[64] Schmid J., Pröll T., Pfeifer C., Hofbauer H., 2011. "Improvement of Gas-Solids interaction in dual circulating fluidized bed systems", *9th EUROPEAN CONFERENCE on INDUSTRIAL FURNANCES and BOILERS Proceedings*, 26-29 April 2011, Estoril, Portugal.

[65] Marx K., Bolhar-Nordenkampf J., Proll T., Hofbauer H., 2011. "Chemical looping combustion for power generation—Concept study for a 10MW$_{th}$ demonstration plant", *Int. J. Greenh. Gas Con.,* Vol. 5, No. 5, pp. 1199–1205.

[66] Alvarez Cuenca M., Anthony E.J. (Eds.), 1995. "Pressurized Fluidized Bed Combustion". Blackie Academic & Professional, Cambdridge, UK.

[67] Werther J., One-Day Seminar on Fluidization, *Tenth International Conference on Circulating Fluidized Beds and Fluidization Technology*. CFB-10. Sunriver, Oregon, USA. May 1-5.

[68] Richtberg M., Richter R., Wirth K.E., 2005. "Characterization of the flow patterns in a pressurized circulating fluidized bed", *Powder Technol*., Vol. 155, No. 2, pp. 145–152.

[69] Lyngfelt A., 2011. "Operational Experiences with Chemical-Looping Combustion of Gaseous and Liquid Fuels", *Third IEA-GHG Network meeting on High Temperature Solids Looping Cycles*, 29-31 August, 2011, Vienna, Austria. http://www.ieaghg.org/index.php?/2009112026/high-temperature-solid-looping-cycles-network.html

[70] Thon A., Kramp M., Hartge E.U., Heinrich S., Werther J., 2011. "A Coupled Fluidized Bed System for Chemical Looping Combustion – Cold Model Investigation of the Operational Behavior", Third IEA-GHG Network meeting on High Temperature Solids Looping Cycles, 29-31 August, 2011, Vienna, Austria. http://www.ieaghg.org/index.php?/2009112026/high-temperature-solid-looping-cycles-network.html

[71] Chiesa P., Lozza G., Malandrino A., Romano M., Piccolo V., 2008. "Three-reactors chemical looping process for hydrogen production", *Int. J. Hydrogen Energ.,* Vol. 33, No. 9, pp. 2233–2245.

[72] Rizeq G., West J., Frydman A., Subia R., Zamansky V., Loreth H., Stonawski L., Wiltowski T., Hippo E., Lalvani S., 2002. "Fuel-Flexible Gasification-Combustion Technology for Production of H_2 and Sequestration-Ready CO_2", GE EER Technical DOE Report for project DE-FC26-00FT40974.

[73] Chambers A., Nikoo M., 2011. "Chemical Looping Combustion of Sour Gas", *Third IEA-GHG Network meeting on High Temperature Solids Looping Cycles*, 29-31 August, 2011, Vienna, Austria. http://www.ieaghg.org/index.php?/2009112026/high-temperature-solid-looping-cycles-network.html

[74] Bertsch O., 2011. "Overall process integration and CLC next scale design" *Third IEA-GHG Network meeting on High Temperature Solids Looping Cycles*, 29-31 August, 2011, Vienna, Austria. http://www.ieaghg.org/index.php?/2009112026/high-temperature-solid-looping-cycles-network.html

[75] Guillou F., Gauthier T., Stainton H., Rifflart S., 2011. "Chemical Looping Combustion Development and Perspectives", 16-21 October, 2011 AIChE Annual Meeting, Minneapolis, MN, USA.

[76] Marion J., Beal C., Bouquet E., Abdulally I., Andrus H.E., Edberg C., 2011. "Alstom Chemical Looping Technology Status", *2nd International Oxyfuel Combustion Conference*, 12th -16th September 2011, Yeppoo, Queensland, Australia.

[77] Ströhle J., Galloy A., Kremer J., Plötz S., Bayrak A. Wieczorek M., Epple B., 2011. "First results from a 1 MW_{th} plant for carbonate and chemical looping", *Third IEA-GHG Network meeting on High Temperature Solids Looping Cycles*, 29-31 August, 2011, Vienna, Austria. http://www.ieaghg.org/index.php?/2009112026/high-temperature-solid-looping-cycles-network.html

[78] Matsen J.M., 1997. "Design and scale-up of CFB catalytic reactors", in: Grace J.R., Avidan A.A., Knowlton T.M. (Eds.), "Circulating Fluidized Beds", Chapman & Hall, London, 1997, pp. 489–503 (chap. 14).

[79] Knowlton T.M., Karri S.B.R., Issangya A., 2005. "Scale-up of fluidized-bed hydrodynamics", *Powder Technol*., Vol. 150 No. 2, pp. 72–77.

[80] Kunii D., Levenspiel O., 1991. "Fluidization Engineering", Butterworth-Heinemann Editor, Newton, MA, USA.

[81] Bischi A., Langørgen Ø., Saanum I., Bakken J., Seljeskog M., Bysveen M., Morin J.X., Bolland O., 2011. "Design study of a 150kW_{th} double loop circulating fluidized bed reactor system for chemical looping combustion with focus on industrial applicability and pressurization", *Int. J. Greenh. Gas Con.*, Vol. 5, No. 3, pp. 467–474.

[82] Lim K.S., Zhu J.X., Grace J.R., 1995. "Hydrodynamics of gas-solid fluidization", *Int. J. Multiphase Flow*., Vol. 21, No. (Suppl. 1), pp. 141–193.

[83] Levenspiel O., 2002. "Modeling in chemical engineering", *Chem. Eng. Sci.,* Vol. 57 No. 22–23, pp. 4691-4696.

[84] Kunii D., Levenspiel O., 2000. "The K-L reactor model for circulating fluidized beds", *Chem. Eng. Sci.,* Vol. 55 No. 20, pp. 4563–4570.

[85] Levenspiel O., 2002. "G/S reactor models—packed beds, bubbling fluidized beds, turbulent fluidized beds and circulating (fast) fluidized beds", *Powder Technol*., Vol. 122, No. 1, pp. 1–9.

[86] Adánez J., Gayán P., García-Labiano F., de Diego L.F., 1994. ”Axial voidage profiles in fast fluidized beds”, *Powder Technol*., Vol. 81, No. 3, pp. 259–268.

[87] Davidson J.F., 2000. “Circulating fluidised bed hydrodynamics”, *Powder Technol*., Vol. 113, No. 3, pp. 249–260.

[88] Pallares D., Johnsson F., 2006. “Macroscopic modelling of fluid dynamics in large-scale circulating fluidized beds”, *Prog. Energ. Combust.*, Vol. 32, No. 5-6, pp. 539–569.

[89] Ergun. C.F.B., 2009. Fluidization Software. Uteam-Divergent S.A., 66 av. du Landshut-Compiègne 60200-France. URL: http://www.utc.fr/ergun.

[90] Pugsley T.S., Berruti F., 1996. “A predictive hydrodynamic model for circulating fluidized bed risers”, *Powder Technol.*, Vol. 89, No. 1, pp. 57–69.

[91] Lei H., Horio M., 1998. “A comprehensive pressure balance model of circulating fluidized beds”, *J. Chem. Eng. Jpn*., Vol. 31, No. 1, pp. 83–94.

[92] Glicksman L.R., 1984. “Scaling relationships for fluidized beds”, *Chem. Eng. Sci.,* Vol. 39, No. 9, pp. 1373–1379.

[93] Glicksman L.R., Hyre M., Woloshun K., 1993. “Simplified scaling relationships for fluidized beds”, *Powder Technol.*, Vol. 77, No 2, pp. 177–199.

[94] de Vos W., Nicol W., du Toit E., 2009. “Entrainment behaviour of high-density Geldart A powders with different shapes”, *Powder Technol*., Vol. 190, No. 3, pp. 297–303.

[95] DMS powders, Atomized FeSi, Cyclone 40. http://www.dmspowders.com/products.aspx

[96] ASTM, 2008. “Standard Practices for Sampling Metal Powders“, B 215-08. ASTM International, West Conshohocken, PA, USA.

[97] Beckman Coulter LS230. Laser diffraction particle size analyser, https://www.beckmancoulter.com/wsrportal/bibliography?docname=br-10.pdf

[98] Mastellone M.L., Arena U., 1999. “The effect of particle size and density on solids distribution along the riser of a circulating fluidized bed”, *Chem. Eng. Sci.*, Vol. 54, No. 22, pp. 5383–5391.

[99] Basu P., Cheng L., 2000. “An Analysis of Loop Seal Operations in a Circulating Fluidized Bed”, *Chem. Eng. Res. Des.,* Vol. 78, No.7, pp. 991–998.

[100] Muzi G., 2009-2010. Professor at the Institute of Occupational Medicine and Environmental Toxicology, University of Perugia, Italy. Personal communications.

[101] TSI, DustTrak™ DRX Aerosol Monitor, model 8533.

http://www.tsi.com/uploadedFiles/Product_Information/Literature/Manuals/8533-8534-DustTrak_DRX-manual.pdf

[102] Myran T., 2010. "Partikkelmålinger CLC-rigg. SINTEF, Varmeteknisk laboratorium", Air quality technical assessment done by the Panel for Mineral Production and Health Safety and Environment (Faggruppe for mineralproduksjon og HMS) of the Norwegian University of Science and Technology-NTNU.

[103] Abbasi T., Abbasi S.A., 2007. "Dust explosions-Cases, causes, consequences, and control", *J. Hazard. Mat.*, Vol. 140, No.1-2, pp. 7–44.

[104] Eckhoff R.K., 1994. "Dust explosion hazards in the ferro-alloys industry", in *52nd Electric Furnace Conference*. Nashville, TN, USA pp. 283–302.

[105] Hertzberg M., Zlochower I.A., Cashdollar K.L., 1992. "Metal dust combustion: Explosion limits, pressures, and temperatures", Symposium (International) on Combustion, 1992. Vol. 24, No. 1, pp. 1827–1835.

[106] Eckhoff R.K., "Dust explosions in the process industries", Third edition ed. 2003: Gulf Professional Publishing.

[107] VDI-GL 2263, Part 1, 1993. "Dust Fires and Dust Explosions, Test methods for the determination of the Safety Characteristic of Dust".

[108] Issangya A.S., Bai D., Bi H.T., Lim K.S., Zhu J., Grace J.R., 1999. "Suspension densities in a high-density circulating fluidized bed riser", *Chem. Eng. Sci.*, Vol. 54, No. 22, pp. 5451–5460.

[109] Nicolai R., 1995. "Experimentelle Untersuchungen zur Strömungsmechanik in einer hochexpandierten zirkulierenden Gas/Feststoff-Wirbelschicht", *Ph.D. thesis*, Eidigenössischen Technischen Hochschule (ETH), Zürich, Switzerland.

[110] Bischi A., Langørgen Ø., Morin J.X., Bakken J., Ghorbaniyan M., Bysveen M., Bolland O., 2011. "Performance analysis of the cold flow model of a second generation chemical looping combustion reactor system", *Energy Procedia,* Vol. 4, pp. 449–456.

[111] Sundaresan R., Kolar A.K., 2002. "Core heat transfer studies in a circulating fluidized bed", *Powder Technol.*, Vol. 124, No. 1-2, pp. 138-151.

[112] Werther J., 1999. "Measurement techniques in fluidized beds", *Powder Technol.*, Vol. 102, No.1, pp. 15–36.

[113] de Diego L.F., Gayán P., Adánez J., 1995. "Modelling of the flow structure in circulating fluidized beds", *Powder Technol.,* Vol. 85, No. 1, pp. 19–27.

[114] Rhodes M.J., 1990. "Modelling the flow structure of upward-flowing gas-solids suspensions", *Powder Technol.*, Vol. 60, No.1, pp. 27–38.

[115] Naqvi R., Wolf J., Bolland O., 2007. "Part-load analysis of a chemical looping combustion (CLC) combined cycle with CO2 capture", *Energy*, Vol. 32, No.4, pp. 360–370.

[116] Xiao R., Song Q., Zhang S., Zheng W., Yang Y. 2010 "Pressurized Chemical-Looping Combustion of Chinese Bituminous Coal: Cyclic Performance and Characterization of Iron Ore-Based Oxygen Carrier", *Energ. Fuel,* Vol. 24, No. 2, pp. 1449–1463.

[117] Wolf J., 2004. CO_2 Mitigation in Advanced Power Cycles - Chemical Looping Combustion and Steam-Based Gasification, *Ph.D. thesis*, KTH - Royal Institute of Technology, Stockholm, Sweden.

[118] Hofbauer H., 2011. "Introduction to Dual Fluidized Bed System for Gasification and Looping Cycles", *Third IEA-GHG Network meeting on High Temperature Solids Looping Cycles*, 29-31 August, 2011, Vienna, Austria.
http://www.ieaghg.org/index.php?/2009112026/high-temperature-solid-looping-cycles-network.html

[119] Patience G.S., Chaouki J., Grandjean B.P.A., 1990. "Solids flow metering from pressure drop measurement in circulating fluidized beds", *Powder Technol*., Vol. 61, No. 1, pp. 95–99.

[120] Muschelknautz U., Muschelknautz E., 1996. "Special design of inserts and short entrance ducts to recirculating cyclones". In: Kwauk M, Li J, editors. *Circulating Fluidized Bed Technology V*. People's Republic of China, Beijing; pp. 597–602.

[121] Fassani F.L., Goldstein Jr. L., 2000. "A study of the effect of high inlet solids loading on a cyclone separator pressure drop and collection efficiency", *Powder Technol*., Vol. 107, No. 1-2. pp. 60–65.

[122] Knowlton T.M., One-Day Seminar on Fluidization, *Tenth International Conference on Circulating Fluidized Beds and Fluidization Technology*. CFB-10. Sunriver, Oregon, USA. May 1-5.

[123] van Ommen J.R., Mudde R.F., 2008. "Measuring the Gas-Solids Distribution in Fluidized Beds–A Review", *Int. J. Chem. React. Eng.,*Vol. 6, Review 3.

Paper I

"Design study of a 150kW$_{th}$ double loop circulating fluidized bed reactor system for chemical looping combustion with focus on industrial applicability and pressurization", *International Journal of Greenhouse Gas Control (2011), Vol. 5, No. 3, pp. 467-474.* doi:10.1016/j.ijggc.2010.09.005.

International Journal of Greenhouse Gas Control 5 (2011) 467–474

Contents lists available at ScienceDirect

International Journal of Greenhouse Gas Control

journal homepage: www.elsevier.com/locate/ijggc

Design study of a 150 kW_{th} double loop circulating fluidized bed reactor system for chemical looping combustion with focus on industrial applicability and pressurization

A. Bischi [a,*], Ø. Langørgen [b], I. Saanum [b], J. Bakken [b], M. Seljeskog [b], M. Bysveen [b], J.-X. Morin [c], O. Bolland [a]

[a] Department of Energy and Process Engineering, Norwegian University of Science and Technology, NO-7491 Trondheim, Norway
[b] SINTEF Energy Research, NO-7465 Trondheim, Norway
[c] CO2-H2 Eurl, 45170 Neuville aux Bois, France

ARTICLE INFO

Article history:
Received 29 October 2009
Received in revised form
10 September 2010
Accepted 18 September 2010
Available online 2 November 2010

Keywords:
CO_2 capture
Chemical looping combustion
Double loop circulating fluidized bed
Industrial solution
Pressurization

ABSTRACT

Nowadays the lab scale feasibility of the chemical looping combustion technology has been proved. This article deals with many of the design requirements that need to be fulfilled to make this technology applicable at industrial scale. A design for a 150 kW_{th} chemical looping combustion reactor system is proposed. In the base case it is supposed to work with gaseous fuels and inexpensive oxygen carriers derived from industrial by-products or natural minerals. More specifically the fuel will be methane and a manganese ore will be the basis for the oxygen carrier. It is a double loop circulating fluidized bed where both the air reactor and the fuel reactor are capable to work in the fast fluidization regime in order to increase the gas solids contact along the reactor body. High operational flexibility is aimed, in this way it will be possible to run with different fuels and oxygen carriers as well as different operating conditions such as variation in air excess. Compactness is a major goal in order to reduce the required solid material and possibly to enclose the reactor body into a pressurized vessel to investigate the chemical looping combustion under pressurized conditions. The mass and heat balance are described, as well as the hydrodynamic investigations performed. Most design solutions presented are taken from industrial standards as one main objective is to meet commercial requirements.

1. Introduction

1.1. Chemical looping combustion

Chemical looping combustion (CLC) is one of the most promising CO_2 capture technologies when it comes to capture costs and net power generation efficiencies (ENCAP, 2009). The idea standing behind CLC was first introduced by Lewis and Gilliland (1946) in a patent to produce a gas mixture of hydrogen and carbon monoxide. Later Richter and Knoche (1983) and Ishida et al. (1987) proposed the CLC principle to reduce the exergy loss of a conventional combustion process. CLC has since then revealed to be interesting also when it comes to CO_2 capture. In fact it is an unmixed combustion process intrinsically capable of separating the CO_2 from the exhaust. Nowadays the most effective way to realize the CLC is done in two separate steps that take place in two distinct fluidized beds reactors interconnected by means of a metallic powder acting as oxygen carrier (OC). The principle that describes the aforementioned system is shown in Fig. 1. In the air reactor (AR) the oxygen of the air is strongly exothermically reacting with the OC (from $MeO_{\alpha-1}$ to MeO_{α}). The air heated up and depleted of the oxygen can be utilized either to produce steam or to expand in a turbine if the above mentioned reaction takes place in a pressurized environment. The metal oxide generated is then transported into the fuel reactor (FR). Here it reacts with the fuel being reduced from MeO_{α} to $MeO_{\alpha-1}$ in an endothermic or slightly exothermic reaction depending on the type of fuel and the type of OC material (Adánez, 2010). The reaction between fuel and oxygen produces an exhaust stream consisting principally of only CO_2 and water vapour. The water vapour can be removed by condensation leaving the CO_2 available for storage. The overall reaction obtained summing the oxidation and reduction of the OC is equivalent to the conventional combustion of the fuel and releases exactly the same amount of energy. The CLC acts as an oxy-combustion capture technique without the need for the expensive cryogenic air separation unit.

1.2. CLC reactor systems

Looking at the development of the CLC technology from its early beginning until now it is possible to notice how the design of the

* Corresponding author. Tel.: +47 73550449; fax: +47 73593580.
E-mail address: aldo.bischi@ntnu.no (A. Bischi).

1750-5836/$ – see front matter © 2010 Elsevier Ltd. All rights reserved.
doi:10.1016/j.ijggc.2010.09.005

Nomenclature

AR	air reactor
CFB	circulating fluidized bed
CFM	cold flow model
CLC	chemical looping combustion
CLG	chemical looping gasification
CLR	chemical looping reforming
CP	cooling panels
DLCFB	double loop circulating fluidized bed
FR	fuel reactor
GT	gas turbine
HSE	health, safety and environment
LHV	lower heating value
LS	loop-seal
OC	oxygen carrier
TGA	thermo gravimetric analysis
TSI	total solids inventory
Ar	Archimedes number [−]
d_{50}	mass median particle diameter [μm]
G_s	solids flux [kg m^{-2} s^{-1}]
ΔH	enthalpy change of a chemical reaction [kJ mol^{-1}]
MeO_α	oxidized metal oxide
$MeO_{\alpha-1}$	reduced metal oxide
M_{OC}	molar mass of the oxygen carrier [g mol^{-1}]
R_0	oxygen ratio [−]
Re	Reynolds number [−] $\rho_g \cdot U_0 \cdot d_{50} \cdot \mu^{-1}$
U_0	superficial gas velocity [m s^{-1}]
X	degree of oxidation [−]
ΔX	conversion difference or exploitation of the maximum oxygen capacity [−]

Bottom

actual	actual value
in	entering the reactor
out	exiting the reactor
ox	oxidized
red	reduced
p	particle
g	gas

Greek letters

λ	excess air ratio [−]
ρ	density [kg m^{-3}]
μ	dynamic viscosity [Pa s]

reactors has changed. The main objective of the first CLC reactors, such as the 10 kW_{th} ones developed at Chalmers University of Technology (Lyngfelt et al., 2005) and at the Instituto de Carboquímica (CSIC) (Adánez et al., 2006; de Diego et al., 2007) was to demonstrate the feasibility of this technology. On the other side the design of the most recent CLC reactor, the 120 kW_{th} of Vienna University of Technology (Kolbitsch et al., 2009), faced many scale-up issues like the requirement of a cooling system for the AR and the difficulty in using a bubbling bed as FR because of dimensional constraints.

Following this path SINTEF Energy Research and the Norwegian University of Science and Technology (NTNU) have worked on the design of a new 150 kW_{th} CLC reactor. It has among its main goals the use of industrial solutions making easier the step from lab-scale to industrial prototype and commercialization. In this respect fuel conversion efficiency is important and needs to be high (Lyngfelt, 2010). Thus the design choices are based on the possibility to have a homogeneous OC concentration throughout the reactor volume as well as a high OC circulation rate with the option of internal recirculation within each reactor. The arrangement should be as compact as possible to export the system into an industrial context. High compactness results in less "parasitic" OC in the connecting ducts i.e. material not actively participating in the reactions. It means a reduction in the OC costs, both the amount of material required and its handling. Furthermore it is easier to place the arrangement into a vessel for pressurized operation to integrate the CLC reactor into a gas turbine (GT) power cycle, a process expected to reach the highest efficiencies (Naqvi and Bolland, 2007).

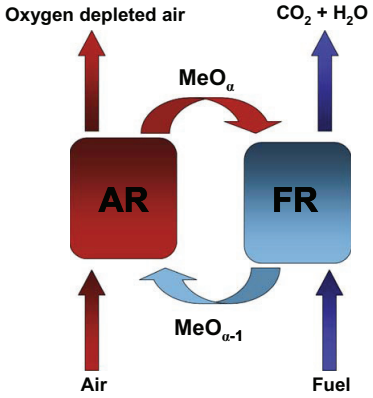

Fig. 1. The principle of chemical looping combustion. The oxygen carrier $MeO_\alpha/MeO_{\alpha-1}$ is oxidized exothermically in the air reactor (AR) and reduced endothermically or slightly exothermically in the fuel reactor (FR).

Auto-thermal reforming can be realized by means of a chemical looping process reducing the amount of oxygen, thus excess air ratio (λ), to a value smaller than stoichiometric. Such a chemical looping reforming (CLR) system will have its higher efficiency values in a pressurized process (Rydén and Lyngfelt, 2005) and the same is expected for the chemical looping gasification (CLG) as mentioned by Xiao et al. (2010). For these reasons much stress is posed on the compactness, even if the CLC reactor system design proposed in this paper is atmospheric. Overview figures of excess air and pressure for different applications of CLC/CLR/CLG processes are depicted in Fig. 2.

2. Mass and heat balance

One of the main challenges of the CLC technology is the development of the oxygen carriers (OC). In fact it must provide appropriate oxygen transport and reaction kinetics on which the reactor design is based. The ideal OC will depend on the type of

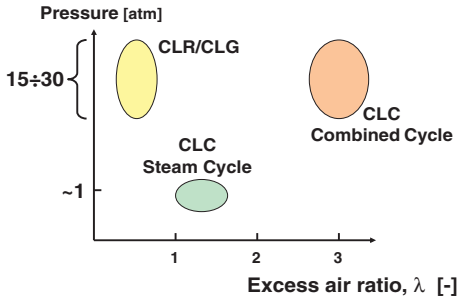

Fig. 2. Overview of operational pressure and excess air (λ) for some possible chemical looping applications: chemical looping combustion, reforming and gasification (CLC/CLR/CLG).

fuel used. Moreover the material must show good performance for a high number of reduction/oxidation cycles without substantial mechanical or chemical degradation in order to avoid fragmentation, agglomeration and loss of reactivity. In order for CLC to reach an industrial scale the OC needs to be inexpensive, available in large quantities and to meet stringent health, safety and environment (HSE) standards (Johansson et al., 2008). For these reasons Fossdal et al. (2011) at SINTEF Materials and Chemistry have performed a survey on industrial tailings and by-products as basis for producing a suitable reference OC for the CLC reactor system object of this study. From an initial screening of oxygen capacity and oxidation/reduction kinetics by means of thermo gravimetric analysis (TGA) a specific manganese ore was selected as the most promising material. The reduction and oxidation reactions for manganese oxide at the design temperature of 1000 °C will be between MnO and Mn_3O_4, while for lower temperature they will be between MnO and Mn_2O_3. Using methane as the reference fuel for the MnO/Mn_3O_4 equilibrium, the oxidation reaction within the AR and the reduction reaction in the FR are, respectively,

$$O_2 + 6MnO = 2Mn_3O_4 \quad (\Delta H = -452.3\,\text{kJ per mol } O_2) \tag{1}$$

and

$$\frac{1}{2}CH_4 + 2Mn_3O_4 = H_2O + \frac{1}{2}CO_2 + 6MnO \quad (\Delta H = 51.2\,\text{kJ per mol } O_2) \tag{2}$$

where ΔH is the enthalpy change of the reaction calculated using the chemical thermodynamic software FactSage (Bale et al., 2009). The overall reaction, as in a conventional combustion, is equal to:

$$O_2 + \frac{1}{2}CH_4 = H_2O + \frac{1}{2}CO_2 \quad (\Delta H = -401.1\,\text{kJ per mol } O_2) \tag{3}$$

According to Lyngfelt et al. (2001) the OC can be characterized by means of two properties; firstly the oxygen ratio, R_0, defined as the ratio of the mass of oxygen in the fully oxidized carrier to its total mass:

$$R_0 = \frac{M_{OC,ox} - M_{OC,red}}{M_{OC,ox}} \tag{4}$$

$M_{OC,ox}$ and $M_{OC,red}$ are respectively the molar mass of the fully oxidized and fully reduced OC. This parameter quantifies the maximum amount of oxygen that the OC theoretically can take up from the air. For the pure MnO/Mn_3O_4 reaction R_0 has a value of 0.07 [−]. From mechanical strength considerations the manganese oxide will be mixed with an inert support material such as alumina Al_2O_3. The amount of active manganese oxide is considered to be about 40–45% on a weight basis, thus reducing the oxygen ratio to about 0.03 [−].

The second parameter characterizing the OC is the degree of oxidation, or conversion X, of the OC. This is defined as the actual mass of oxygen in the OC divided by the maximum amount of oxygen in the fully oxidized state:

$$X = \frac{M_{OC,actual} - M_{OC,red}}{M_{OC,ox} - M_{OC,red}} \tag{5}$$

The degree of oxidation can be used to describe the difference between the conversion at the entrance of one reactor and at its exit, ΔX, which becomes a measure of the exploitation of the maximum oxygen capacity. From TGA cycling tests by Fossdal et al. (2011) the OC reduction process in the FR is shown to be the limiting step, being slower than the OC oxidation reaction in the AR. The exploitation of the oxygen capacity in the FR can be written as:

$$\Delta X_{FR} = X_{in,FR} - X_{out,FR} \tag{6}$$

In this case ΔX is estimated to be about 0.2 [−], based on the measured reversible oxygen capacity of the manganese ore (without any inert support) and on the residence time of the OC particles in the FR. The last one is conservatively assessed to be about 8 s which has been confirmed by cold flow model (CFM) results (see Section 3.4).

Table 1
Main design parameters of the CLC reactor system.

Design parameters	Value	Unit
Fuel thermal input	150	[kW_{th}]
Excess air ratio (λ)	1.2	[−]
Fuel LHV (methane)	50.01	[MJ kg^{-1}]
Reactors design temperature	1000	[°C]
Oxygen carrier oxygen ratio R_0	0.03	[−]
Oxygen carrier conversion ΔX_{FR}	0.2	[−]
Oxygen carrier circulation rate	2	[kg s^{-1}]
Heat release AR (Eq. (1))	169	kW
Heat release FR (Eq. (2))	−19	kW

The R_0 and the ΔX fix the needed OC mass flow between the reactors at a given fuel input. At 150 kW_{th} (3 g s^{-1} methane, based on LHV), 12 g s^{-1} of oxygen are needed to fully oxidize the fuel. Exploiting 20% of the maximum oxygen ratio R_0 of 3%, the OC mass flow needed is 2 kg s^{-1}.

A heat balance was performed to be able to dimension the heat exchangers needed to control the process. At a reactors temperature of 1000 °C and with the enthalpy changes of the oxidation and reduction reactions (Eqs. (1) and (2)), the heat release is 169.1 kW in the AR and −19.1 kW in the FR as the reduction reaction (Eq. (2)) is slightly endothermic. However, the cooling effect of the colder inlet gases compared to the reactor temperature will reduce these values of about 28 kW and 13 kW for the AR and FR, respectively. The main design parameters related to the mass and energy balance are summarized in Table 1.

It should be noted that the phase transition between MnO/Mn_3O_4 will cause a discrete density change of 14.9% that may cause stress and a brittle material. Addition of calcium in order to obtain perovskite phases will improve mechanical stability. Such calcium manganite materials were prepared and tested by Fossdal et al. (2011). Even though the theoretical oxygen ratio R_0 is reduced to 0.056 the reversible cyclic capacity and the kinetics as obtained by TGA are still almost equal to the pure manganese ore. The AR oxidation at 1000 °C will be somewhat less exothermic than the reference in Eq. (1) (ΔH = −330 kJ mol^{-1} O_2) and the FR will be slightly exothermic (ΔH = −71 kJ mol^{-1} O_2 with methane as fuel).

To gain a better understanding of the OC candidates behaviour it is important to test them, in addition to the TGA analysis, with multi cycles in batch fluidized bed reactors as well as with a continuous CLC unit (Abad et al., 2006; Gayán et al., 2010). On the other hand Vienna University of Technology (Kolbitsch, 2009) tested the performance of the OCs in the 120 kW_{th} CLC unit, finding higher reaction rates than that ones predicted from the batch tests. It means that the oxygen capacity exploitation, assumed relying on the TGA analysis can be considered conservative, thus the 2 kg s^{-1} of mass exchange between reactors. Such a mass flow will also provide the required heat at the reduction reaction, if endothermic as in the MnO/Mn_3O_4 case, and ensure a temperature in the FR with almost the same value of the AR one.

3. Results and discussions

3.1. Reactor concept

The concept for the CLC reactor system developed by SINTEF Energy Research/NTNU in Trondheim is schematically represented in Fig. 3. Both the AR and FR are circulating fluidized beds (CFB) and the system is therefore called a double loop circulating fluidized bed reactor system (DLCFB). It is adopting a configuration

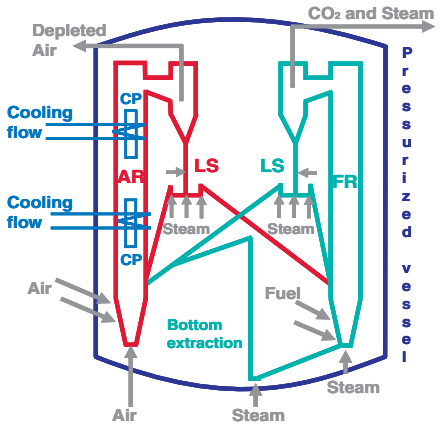

Fig. 3. Process diagram of the double loop circulating fluidized bed reactor system concept. The fluid streams for both the air reactor (AR) and fuel reactor (FR) are represented as well as the pressurized vessel, the cooling panels (CP) and divided loop-seals (LS).

with two loops architecture realized with divided loop-seals (LS) and with the FR meant to operate in fast fluidization regime. The fast fluidization regime in the FR has the objective of raising the fuel conversion with a better utilization of the upper part of the reactor increasing the gas–solids contact, despite the reduction of particle and gas residence time due to the increase of superficial gas velocity and particles entrainment. In the fast fluidization regime there is a higher particle concentration in the upper part of the reactor and a smaller bottom zone compared to a turbulent bed, indicating a more homogeneous particle distribution (Kunii and Levenspiel, 1997). The goal is to maximize the fuel conversion and the solids concentration at the reactor exit as well as to reduce the particles concentration in the bottom zone having a steep, but not a vertical concentration profile (which becomes pneumatic conveying) along the FR. This objective can be reached utilizing a fast reactor for both the FR and AR playing with the mass inventory, the secondary air injections and the loop-seals. In this way it will be possible to tune the solids concentration versus reactor height toward the desired one. Grace (1990) proved that this factor affects pretty much the conversion for fast reactions. Pröll et al. (2009a) came to the very same conclusions with their CLC set-up: they increased the conversion of methane increasing the FR fuel load. This way they increased the fluidizing velocity of the turbulent CFB towards fast fluidization regime. Anyhow these results were reached with Ni-based OC which has high reactivity; while they experienced better conversion at lower loads utilizing natural ilmenite (low reactivity OC), concluding that the optimal FR fluidization regime depends on the OC reactivity.

The two LSs in Fig. 3 will have the conventional tasks of closing the pressure loop and avoiding gas mixing between the reactors. In addition, their divided configuration will allow recirculating part of the entrained particles into the reactor of origin enabling control of the mass exchange and the particle residence time (two loops architecture). There is also a bottom extraction/lift in the FR to bring part of the solids flow to the AR through this connection. This is required to achieve the full design circulation rate and give higher degree of operational flexibility, e.g. it will allow operating the rig with the FR in turbulent regime. In the FR a minimum amount of steam will be introduced in the bottom to guarantee fluidization in case of emergency, during shut down and to tune the fluidization regime.

Table 2
Main particle and reactor dimensions.

Design parameters	Value	Unit
Particle diameter, d_{50}	70	[μm]
Particle density	2000	[kg m^{-3}]
Particle sphericity	~1	[–]
AR diameter	0.25	[m]
FR diameter	0.15	[m]
Reactor height	5	[m]

The value of λ at design conditions is between 1.1 and 1.2 as for industrial CFB boilers. On the other hand, the reactor system is intended to have the needed flexibility to operate at reduced excess air (reforming conditions), as well as higher excess air with λ up to 3 and above as this would be necessary for GT applications (Fig. 2). This will give as a consequence a higher solids entrainment which is planned to be compensated by means of the internal recirculation in the AR through the divided loop-seal.

3.2. Hydrodynamics

The main reactor dimensions must fit the requirements given by the chosen fluidization regime discussed in Section 3.1 and the mass and heat balances from Section 2. Particles size, density and sphericity are fundamental parameters with respect to fluidization regime. The particles selected for the reference case are approximately spherical with a d_{50} equal to 70 μm and a density of 2000 kg m^{-3}. A powder with such characteristics is in the group A of the Geldart (1973) classification, i.e. a typical catalyst standard, it will eventually ease the OC production.

The AR must reach a fast CFB regime entraining the required amount of 2 kg s^{-1} of OC by means of the gas flow of air. The main calculated figures for the AR are given in Table 2. They lead to the aimed CFB flow regime according to the dimensionless Grace diagram as qualitatively shown in Fig. 4 (Lim et al., 1995). The solids flux, G_s, to reach at the AR exit is equal to almost 40 kg m^{-2} s^{-1} and the particle concentration that will allow such high particles entrainment is at least around 12 kg m^{-3}. A similar approach was followed for the design of the FR; once the amount of fluidizing gas available from the 150 kW$_{th}$ of thermal load was calculated, the dimensions were set to have fast CFB regime in design conditions.

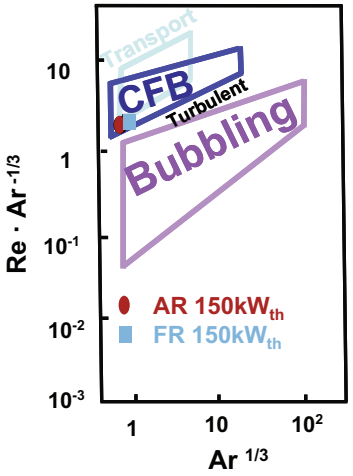

Fig. 4. Qualitative representation of the fluidization regimes of the air reactor (AR) and fuel reactor (FR) according to the classification of Grace (Lim et al., 1995).

As can be seen from Fig. 4 also the so dimensioned FR is in the aimed regime. It should give a solids flux of almost 45 kg m^{-2} s^{-1} and a concentration of at least 13 kg m^{-3} in the upper part of the reactor. In this way about half of the 2 kg s^{-1} solids flow is exchanged while the rest will be handled by means of the bottom extraction/lift. These are values calculated considering the presence of the cooling panels (CP) and without taking in account the particles backflow. In the literature it is proven that such exit particles flux values can be easily reached, in fact flux values even higher than 175 kg m^{-2} s^{-1} were reached in the work performed by Nicolai (1995). The same can be stated for the particles suspension in the upper part of the reactor: according to Basu (2005) concentration values up to 100 kg m^{-3} can be reached.

The reactors hydrodynamics were investigated more thoroughly by means of simulations in order to verify the feasibility of the required values of entrained OC and reactors exit concentrations. It was also possible to carry out evaluation of the pressure/particles concentration behaviour along the reactors bodies as well as of the total particle mass in the AR and FR. The simulations were performed with the commercial software Ergun (2009) utilizing both the Berruti's flow pattern model (Pugsley and Berruti, 1996) and the Horio one (Lei and Horio, 1998). Such kinds of models are characterized by an empirical nature. This fact in addition to the complexity and peculiarity of the reactor system made the authors opt for the CFM testing described in Section 3.4 further below.

3.3. System design

The goals of the present CLC reactor system have already been explained, as well as the concept developed for their achievement. Some of the design requirements and solutions adopted for their fulfilment are described here more thoroughly.

The gas feed system controls the fluidization and hydrodynamic behaviour once the OC particles and reactor dimensions have been chosen. The main intention is the achievement of a CFB mode having as much control as possible on the behaviour of the particles along the reactor body as described in Section 3.1. It is done by a balanced use of the primary bottom injection plus two levels of secondary ones along the bottom part of the reactor. The volume flow of fluidizing gas injected in the FR (CH_4) will triple inside the reactor body because of the reaction described in Eq. (2). A tapered section will smooth the associated velocity increase and reduce the friction losses. It will increase the gas velocity in the bottom of the reactors, both AR and FR, helping to prevent the agglomeration of particles (Grace, 1990; Legros et al., 1991). It will also give a uniform superficial gas velocity (U_0) profile across the secondary air injections (Basu, 2005) allowing a more even acceleration of the solids up to the conditions of fully developed flow. The bottom gas injection of the AR and FR is done by means of bubble cap nozzles designed according to VGB PowerTech (1994). The nozzle shape, the distance towards the reactor walls and suitable velocities of the air jets were chosen relying also on the good performance shown by the solutions experimented in the company Rheinbraun (Lambertz et al., 1993).

The reactor cooling is an important issue, especially for reactors being as compact as possible. The adopted solution is industrial with cooling panels (CP) as shown in Fig. 3. For a proper fluidization they should not be allocated too low in the reactor height to achieve a full development of the solid flux. At the same time they should not be located too close to the reactor exit disturbing the particles entrainment. Furthermore their presence will reduce the section available for the gas flow, thus increasing the gas velocity. The calculated number of panels is based on the necessary cooling duty and a heat transfer coefficient estimated to 120 W m^{-2} K^{-1}. Among the values presented by Basu (2005) this is considered realistic on the conservative side in order to match the solids suspension densities expected in the design case.

The performance of the loop-seals will be crucial for the overall system behaviour as mentioned in Section 3.1. In the present reactor design it is intended to control the OC flux, with possibility of internal recycle, without the use of mechanical valves such as a cone valve. The industrial solution according to an Ahlstrom patent (Kostamo and Puhakka, 1988) meets this requirement. Even though a mechanical valve is not a part of the proposed design it is planned for possible installation in case the external and internal circulation is not easily controlled without. The fluidization of the loop-seal is executed by means of nozzles in principle equal to the primary nozzles of the AR and FR. This solution reduces the complexity by standardizing the nozzles. To help the fluidization lateral air injections are placed in the bottom part of the downcomers, just above the loop-seals. It has proved to be effective as a means to enhance loop-seal solid circulation rate (Kim et al., 2001).

The last reactor component that deserves special care in the design phase is the heavy load cyclone. Its performance has fundamental importance to avoid particle losses. High cyclone efficiency is necessary to help satisfy particle emissions requirements and to reduce the OC refilling and the related costs. Furthermore it is essential for GT applications in which the GT working fluid must fulfil strict requirements with respect to particle concentration and particle size (Lippert and Newby, 1995; Loud and Slaterpryce, 1991). In addition the cyclones required in this case have to handle efficiently a high flux of particles in a very compact configuration. It is proven that the heavy loaded cyclones reach the best efficiency by means of a downward inclined inlet duct that intensifies the cluster formation (Hugi and Reh, 1998, 2000) and a converging section that increases the inlet gas velocity (Muschelknautz and Muschelknautz, 1996). A sharp cross section reduction may improve the performance as shown in results from the boiler of the coal power station of Goldenberg (Krohmer et al., 2006). According to Muschelknautz and Muschelknautz (1996) the gas exit tube should be placed eccentric in the cyclone in order to raise the separation efficiency. This solution was also proven in large scale, as well as the downward declination of the inlet duct, in the boiler in Zeran, Poland (Lalak et al., 2003). The vortex finder may be arranged with an increase of its cross section in the direction of the gas flow exiting the cyclone. Such a diverging vortex finder is an industrial solution used by the Electricité de France (EdF) coal power plant in Gardanne (France) (Frydrychwski-Horvatin and Vostan, 1997).

Based on the above considerations, a detailed system and component design has been carried out. In order to have a most realistic verification of the performance of all these solutions, together with the reactors hydrodynamics as already mentioned, a full scale CFM has been built and is in operation as described in the next section.

3.4. Cold flow model verification

Cold flow model (CFM) validation is a common approach for testing the reactor design before building a hot rig. This kind of validation has been used, e.g. by Chalmers (Kronberger et al., 2005) and Vienna (Pröll et al., 2009b) Universities of Technology operating CFMs that are smaller down-scaled versions of the intended hot rig. However, in the present work a full scale (1:1) CFM of the 150 kW_{th} rig design has been built as in the industrial practice in order to reduce wall effects and establish even more realistic design verification. The CFM is built in transparent polycarbonate material and all component details are equal to the hot rig design. The values of gas velocity and particles characteristics (d_{50} equal to 34 μm and material density equal to 7000 kg m^{-3}) were selected in order to end up in the same fluidization regime. The complete CFM results and related mapping of the overall stable operational window of the reactor system is out of scope of this

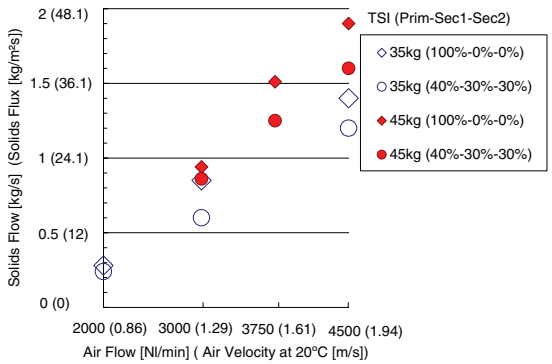

Fig. 5. Solids flow (flux) achieved in the cold flow model of the air reactor (AR) as a function of the fluidizing air flow for two different total solids inventory (TSI) and different air staging between primary, secondary 1 and secondary 2.

paper and still under investigation. Here some key results will be shown, related to the performance of the AR and FR operated separately. Fig. 5 shows how the solids flow experienced in the AR loop increases with the air flow and the total solids inventory (TSI) up to the achievement of almost 2 kg s^{-1} entrainment. At the same time it is possible also to tune the entrained flux with the air staging: increasing the secondary air share will reduce it. The same behaviour is shown by the FR in Fig. 6 up to a flow of 1.1 kg s^{-1}. The results obtained with the lower FR inventory of 35 kg are shown for sake of completeness, but these tests were performed before gaining full control on the inventory in the reactor system which then was not always the same. In addition the pressure behaviour along the AR body corresponding to the 2 kg s^{-1} flow exchange, for a TSI of 45 kg and superficial gas velocity U_0 of 1.9 m s^{-1} is shown by the continuous line in Fig. 7. The AR pressure profile confirms the fast CFB behaviour and it was used to derive the amount of mass present in the reactor, neglecting friction and acceleration forces as done by Issangya et al. (1999) and Pröll et al. (2009a). The calculated active mass in the AR was almost 28 kg which divided by the flux of 2 kg s^{-1} gives a conservative estimation of the OC residence time in the AR equal to 14 s. In addition it is also shown, in the same figure, the sensitivity of the pressure to the TSI and air staging keeping constant the superficial gas velocity. A reduction

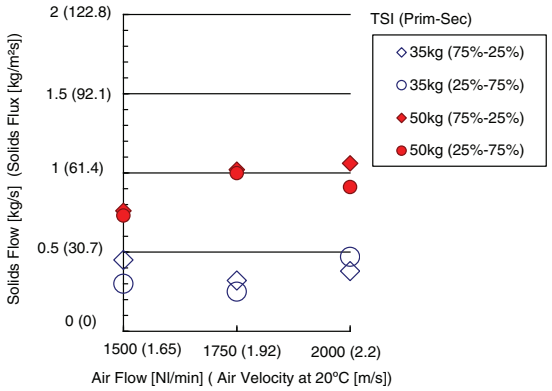

Fig. 6. Solids flow (flux) achieved in the cold flow model of the fuel reactor (FR) as a function of the fluidizing air flow for two different total solids inventory (TSI) and different air staging between primary and secondary.

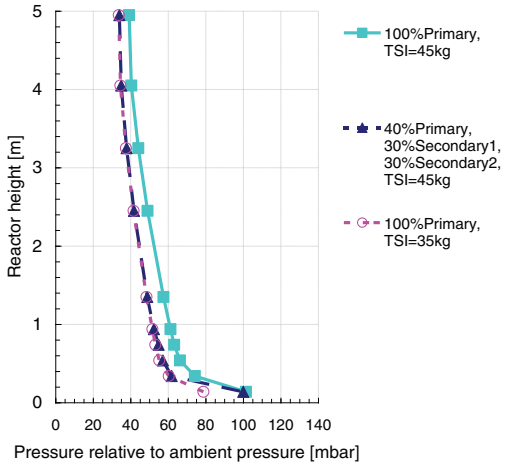

Fig. 7. Pressure profiles along the air reactor (AR) for a fixed amount of fluidizing air giving 1.9 m s^{-1} of superficial gas velocity. Three different cases are analyzed: a total solids inventory (TSI) of 45 kg and all the fluidization air introduced at the primary level, the same TSI introducing just 40% of the air at the primary level and an inventory of 35 kg with all the air at primary level.

of the primary air down to 40% keeping the TSI constant (dotted line with triangles) shifts the pressure curve down to lower values and decreases the entrained flow (Fig. 5). The dotted line with circles shows how the pressure profile is affected by a reduction of the TSI: the bottom pressure/inventory is reduced and the overall curve is shifted towards smaller values. In a similar manner Fig. 8 shows with the continuous line the pressure along the FR body for a velocity of 2.2 m s^{-1} and an inventory of 50 kg. It leads to 1.1 kg s^{-1} of solids entrainment and a calculated 16 kg inventory of active mass inside the FR. It means a particles residence time of about 8 s taking into account also the mass that should be transported through the bottom extraction/lift to achieve, at steady state, a total solids exchange of 2 kg s^{-1}. The experimental results confirm that the flu-

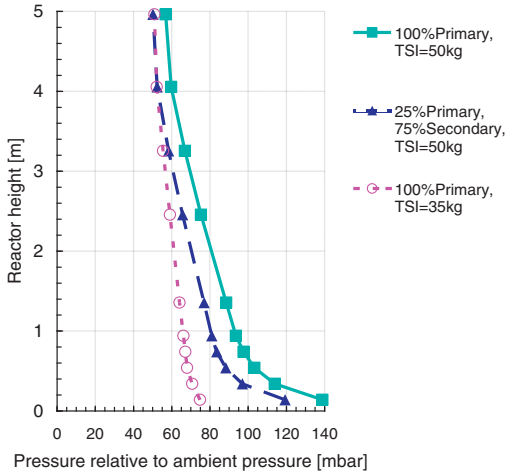

Fig. 8. Pressure profiles along the fuel reactor (FR) for a fixed amount of fluidizing air giving 2.2 m s^{-1} of superficial gas velocity. Three different cases are analyzed: a total solids inventory (TSI) of 50 kg and all the fluidization air introduced at the primary level, the same TSI introducing just 25% of the air at the primary level and an inventory of 35 kg with all the air at primary level.

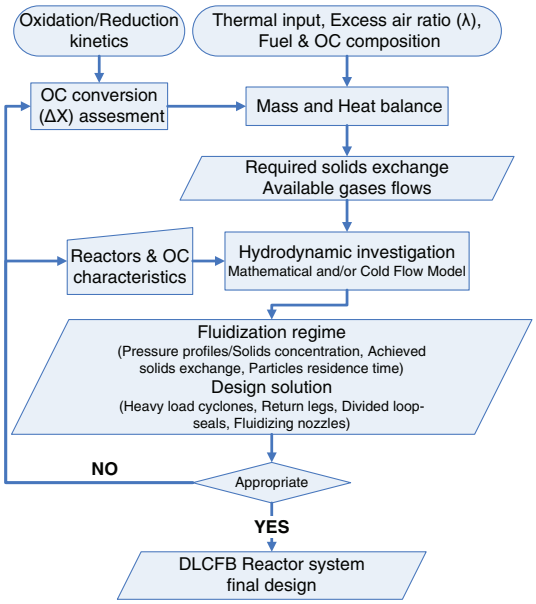

Fig. 9. Flow-sheet of the design methodology used/developed to achieve the actual design of the double loop circulating fluidized bed (DLCFB) chemical looping combustion atmospheric pilot rig of SINTEF Energy Research/NTNU in Trondheim.

idization regime, the solids entrainment and the pressure/particles concentration behaviour are affected, and thus can be regulated, by the pre-set particles inventory and by the fluidizing gas staging as well as by other factors, e.g. the fluidization of the loop-seals and the reactors backpressure. Further extensive CFM studies need to be done in order to find the best way to couple the reactors together and operate according to the different operational modes, and to generate results in order to derive correlations that can be used to fit the semi-empirical mathematical models to the actual set-up.

4. Conclusions

The design of a chemical looping combustion reactor system of 150 kW_{th} fuel input is presented. It consists of two interconnected circulating fluidized bed operating in fast fluidization mode, in design case, and interconnected by means of a "two loops architecture" (DLCFB). Together with the multiple injections fluidization system it will increase the operational flexibility. In this way the reactor system is expected to be operated in the way that will bring higher fuel conversion efficiency according to the selected fuel and oxides. The overall system is compact in order to reduce the amount of solid material and to have the possibility to be introduced into a pressurized vessel. In addition the design is making use of many industrial solutions which will lead the chemical looping technologies further towards possible commercialization.

Among the achievements of this paper there is also the development of a design methodology which is shown in Fig. 9. It starts establishing some parameters according to the project requirements and resources available. Mass and heat balances, design and hydrodynamic calculations are performed. The hydrodynamics together with the proposed design solutions are currently being tested in a cold flow model mirroring the actual reactor system. In this way it will be possible to tackle eventual shortcomings and find the best operational window. All the missing parameters are assessed iteratively in order to achieve a reactor with the above-mentioned characteristics. Concluding, this design methodology summarizes all the main actions and decisions undertaken along the design path and presents them in a modular way.

Acknowledgments

This publication forms a part of the BIGCO2 project, performed under the strategic Norwegian research program Climit. The authors acknowledge the partners: Statoil, GE Global Research, Statkraft, Aker Clean Carbon, Shell, TOTAL, ConocoPhillips, ALSTOM, the Research Council of Norway (178004/I30 and 176059/I30) and Gassnova (182070) for their support. In addition the valuable help of Mr. S. Tjøstheim during the cold flow model experimental campaign is acknowledged.

References

Abad, A., Mattisson, T., Lyngfelt, A., Rydén, M., 2006. Chemical-looping combustion in a 300 W continuously operating reactor system using a manganese-based oxygen carrier. Fuel 85 (9), 1174–1185.

Adánez, J., Gayan, P., Celaya, J., de Diego, L.F., Garcia-Labiano, F., Abad, A., 2006. Chemical looping combustion in a 10 kW_{th} prototype using a CuO/Al_2O_3 oxygen carrier: effect of operating conditions on methane combustion. Ind. Eng. Chem. Res. 45 (17), 6075–6080.

Adánez, J., 2010. Oxygen carrier materials for chemical-looping processes – fundamentals. In: 1st International Conference on Chemical Looping, Lyon, France, http://www.ifp.com/actualites/evenements/congres-et-conferences/organises-par-ifp-energies-nouvelles/rs-chemical-looping.

Bale, C.W., Bélisle, E., Chartrand, P., Decterov, S.A., Eriksson, G., Hack, K., Jung, I.H., Kang, Y.B., Melançon, J., Pelton, A.D., Robelin, C., Petersen, S., 2009. FactSage thermochemical software and databases-recent developments. CALPHAD: Comput. Coupl. Phase Diagrams Thermochem. 33 (2), 295–311.

Basu, P., 2005. Combustion and Gasification in Fluidized Beds. Taylor & Francis, Boca Raton, FL, United States of America.

de Diego, L.F., Garcia-Labiano, F., Gayan, P., Celaya, J., Palacios, J.M., Adánez, J., 2007. Operation of a 10 kW_{th} chemical-looping combustor during 200 h with a $CuO–Al_2O_3$ oxygen carrier. Fuel 86 (7–8), 1036–1045.

ENCAP Deliverable D1.2.6, 2009. Power systems evaluation and benchmarking – public version, URL: http://www.encapco2.org/.

Ergun. C.F.B., 2009. Fluidization Software. UTeam-Divergent S.A., 66 av. Du Landshut-Compiègne 60200-France. URL: http://www.utc.fr/ergun.

Fossdal, A., Bakken, E., Øye, B.A., Schønning, C., Kaus, I., Mokkelbost, T., Larring, Y., 2011. Study of inexpensive oxygen carriers for chemical looping combustion. Int. J. Greenhouse Gas Control. 5 (3), 483–488.

Frydrychwski-Horvatin, J., Vostan, P., 1997. Auslegungsgrundlagen und erste Betriebserfahrungen mit dem weltgrößten ZWS-Kraftwerk in Gardanne, Südfrankreich. In: VDI-Gesellschaft Energietechnik. VDI-Berichte, Berlin, Germany, pp. 5–19.

Gayán, P., Forero, C.R., de Diego, L.F., Abad, A., García-Labiano, F., Adánez, J., 2010. Effect of gas composition in Chemical-Looping Combustion with copper-based oxygen carriers: fate of light hydrocarbons. Int. J. Greenhouse Gas Control. 4 (1), 13–22.

Geldart, D., 1973. Types of gas fluidization. Powder Technol. 7 (5), 285–292.

Grace, J.R., 1990. High-velocity fluidized bed reactors. Chem. Eng. Sci. 45 (8), 1953–1966.

Hugi, E., Reh, L., 1998. Design of cyclones with high solids entrance loads. Chem. Eng. Technol. 21 (9), 716–719.

Hugi, E., Reh, L., 2000. Focus on solids strand formation improves separation performance of highly loaded circulating fluidized bed recycle cyclones. Chem. Eng. Process. 39 (3), 263–273.

Ishida, M., Zheng, D., Akehata, T., 1987. Evaluation of a chemical-looping-combustion power-generation system by graphic exergy analysis. Energy 12 (2), 147–154.

Issangya, A.S., Bai, D., Bi, H.T., Lim, K.S., Zhu, J., Grace, J.R., 1999. Suspension densities in a high-density circulating fluidized bed riser. Chem. Eng. Sci. 54 (22), 5451–5460.

Johansson, M., Mattisson, T., Lyngfelt, A., Abad, A., 2008. Using continuous and pulse experiments to compare two promising nickel-based oxygen carriers for use in chemical-looping technologies. Fuel 87 (6), 988–1001.

Kim, S.W., Namkung, W., Kim, S.D., 2001. Solid recycle characteristics of loop-seals in a circulating fluidized bed. Chem. Eng. Technol. 24 (8), 843–849.

Kolbitsch, P., Pröll, T., Bolhar-Nordenkampf, J., Hofbauer, H., 2009. Design of a chemical looping combustor using a dual circulating fluidized bed (DCFB) reactor system. Chem. Eng. Technol. 32 (3), 398–403.

Kolbitsch, P., 2009. Chemical Looping Combustion for 100% Carbon Capture – Design, Operation and Modeling of a 120 kW Pilot Rig. Ph.D. thesis, TU Wien, Vienna, Austria.

Kostamo, M., Puhakka M., 1988. Apparatus and Methods for Operating a Fluidized Bed Reactor. Ahlstrom Corporation. International Application Number: PCT/FI88/00056.

Krohmer, B., Röper, B., Seeber, J., Stamatelopoulos, G.N., 2006. Operating experience with measures for improvement of cyclone removal efficiency. VGB PowerTech 12, 77–81.

Kronberger, B., Lyngfelt, A., Löffler, G., Hofbauer, H., 2005. Design and fluid dynamic analysis of a bench-scale combustion system with CO_2 separation – Chemical-looping combustion. Ind. Eng. Chem. Res. 44 (3), 546–556.

Kunii, D., Levenspiel, O., 1997. Circulating fluidized-bed reactors. Chem. Eng. Sci. 52 (15), 2471–2482.

Lalak, I., Seeber, J., Kluger, F., Krupka, S., 2003. Operational experience with high efficiency cyclones: comparison between boiler A and B in the Zeran power plant, Warsaw/Poland. VGB PowerTech 9, 90–94.

Lambertz, J., Kipshagen, F.J., Mayer, B., 1993. Optimierung zirkulierender wirbelschichten mit rheinischer Braunkohle im Bereich des Gasverteilerbodens. In: VDI-Bericht 1081. Düsseldorf, Germany, pp. 157–179.

Legros, R., Lim, C.J., Brereton, C.M.H., Grace, J.R., 1991. Circulating fluidized bed combustion of pitches derived from heavy oil upgrading. Fuel 70 (12), 1465–1471.

Lei, H., Horio, M., 1998. A comprehensive pressure balance model of circulating fluidized beds. J. Chem. Eng. Jpn. 31 (1), 83–94.

Lewis, W.K., Gilliland, E.R., 1946. Production of industrial gas mixture of hydrogen and carbon monoxide. Standard Oil Development Company. United States Patent Office, Application No. 688351.

Lim, K.S., Zhu, J.X., Grace, J.R., 1995. Hydrodynamics of gas–solid fluidization. Int. J. Multiphase Flow 21 (Suppl. 1), 141–193.

Lippert, T.E., Newby, R.A., 1995. High-temperature particulate control. In: Alvarez Cuenca, M., Anthony, E.J. (Eds.), Pressurized Fluidized Bed Combustion. Blackie Academic & Professional, pp. 211–256.

Loud, R.L., Slaterpryce, A.A., 1991. Gas Turbine Inlet Treatment, GER-3419A, GE Reference Library. http://www.gepower.com/prod_serv/products/tech_docs/en/gas_turbines.htm.

Lyngfelt, A., Leckner, B., Mattisson, T., 2001. A fluidized-bed combustion process with inherent CO_2 separation; application of chemical-looping combustion. Chem. Eng. Sci. 56 (10), 3101–3113.

Lyngfelt, A., Kronberger, B., Adánez, J., Morin, J.X., Hurst, P., 2005. The grace project: development of oxygen carrier particles for chemical-looping combustion. Design and operation of a 10 kW chemical-looping combustor. In: Greenhouse Gas Control Technologies 7. Elsevier Science Ltd., Oxford, pp. 115–123.

Lyngfelt, A., 2010. Oxygen-carriers for chemical-looping combustion-operational experience. In: 1st International Conference on Chemical Looping, Lyon, France, http://www.ifp.com/actualites/evenements/congres-et-conferences/organises-par-ifp-energies-nouvelles/rs-chemical-looping.

Muschelknautz, U., Muschelknautz, E., 1996. Special design of inserts and short entrance ducts to recirculating cyclones. In: Kwauk, M., Li, J. (Eds.), Circulating Fluidized Bed Technology V. People's Republic of China, Beijing, pp. 597–602.

Naqvi, R., Bolland, O., 2007. Multi-stage chemical looping combustion (CLC) for combined cycles with CO_2 capture. Int. Greenhouse Gas Control. 1 (1), 19–30.

Nicolai, R., 1995. Experimentelle Untersuchungen zur Strömungsmechanik in einer hochexpandierten zirkulierenden Gas/Feststoff-Wirbelschicht. Ph.D. thesis, Eidgenössischen Technischen Hochschule (ETH), Zürich, Switzerland.

Pugsley, T.S., Berruti, F., 1996. A predictive hydrodynamic model for circulating fluidized bed risers. Powder Technol. 89 (1), 57–69.

Pröll, T., Kolbitsch, P., Bolhàr-Nordenkampf, J., Hofbauer, H., 2009a. A novel dual circulating fluidized bed system for chemical looping processes. AIChE J. 55 (12), 3255–3266.

Pröll, T., Ruspanovits, K., Kolbitsch, P., Bolhàr-Nordenkampf, J., Hofbauer, H., 2009b. Cold flow model study on a dual circulating fluidized bed system for chemical looping processes. Chem. Eng. Technol. 32 (3), 418–424.

Richter, H.J., Knoche, K.F., 1983. Reversibility of combustion processes. In: Gaggioli, R.A. (Ed.), A. C. S. Symposium Series 235. Washington, DC, USA, pp. 71–85.

Rydén, M., Lyngfelt, A., 2005. Hydrogen and power production with integrated carbon dioxide capture by chemical-looping reforming. In: Greenhouse Gas Control Technologies 7. Elsevier Science Ltd., Oxford, pp. 125–134.

VGB PowerTech, 1994. Gas distributor plates in fluidized bed systems. In: VGB PowerTech Service GmbH. Essen, Germany.

Xiao, R., Song, Q., Song, M., Lu, Z., Zhang, S., Shen, L., 2010. Pressurized chemical-looping combustion of coal with an iron ore-based oxygen carrier. Combust. Flame 157 (6), 1140–1153.

Paper II

"Performance analysis of the cold flow model of a second generation chemical looping combustion reactor system", *Energy Procedia (2011), Vol. 4, pp. 449-456.* doi:10.1016/j.egypro.2011.01.074.

Available online at www.sciencedirect.com
ScienceDirect
Energy Procedia 4 (2011) 449–456
Energy Procedia
www.elsevier.com/locate/procedia

GHGT-10

Performance analysis of the cold flow model of a second generation chemical looping combustion reactor system

Aldo Bischi[a,1], Øyvind Langørgen[b], Jean-Xavier Morin[c], Jørn Bakken[b], Masoud Ghorbaniyan[a], Marie Bysveen[b], Olav Bolland[a]

[a]*Department of Energy and Process Engineering, NTNU, Kolbjørn Hejes vei 1A, Trondheim NO-7491, Norway*
[b]*SINTEF Energy Research, Sem Saelends vei 11, Trondheim NO-7465, Norway*
[c]*CO2-H2 Eurl, 41 rue du Cas Rouge Marchandon, Neuville aux Bois 45170, France*

Abstract

A 150kW$_{th}$ second generation chemical looping combustion reactor system has been designed. It is a double loop circulating fluidized bed meant to achieve high solids circulation and be flexible in operation. Attention was also focused on the usage of industrial solutions and compactness, to go towards commercialization and pressurization as a further step. Both its hydrodynamic behaviour and design solutions were investigated by means of a full scale cold flow model. First the design of the nozzles and the share of kinetic losses were verified, together with the solids flow/flux measurements reliability. The air reactor and fuel reactor were then tested separately monitoring their entrainment capabilities and pressure/particles distribution, with main focus on finding the best way of operating the loop-seals and cooling panel configuration. The overall reactor system (combining air and fuel reactor) was tested achieving results close to the design values. Finally, some solutions to further improve its performance are proposed.

Keywords: Chemical Looping Combustion, Double Loop Circulating Fluidized Bed, Cold Flow Model, Industrial solution, Pressurization

1. Introduction

Within the CO_2 capture technologies the Chemical Looping Combustion (CLC) is one of the most promising both for costs and net efficiencies [1]. It is an unmixed combustion process with inherent CO_2 separation, commonly realized by means of two interconnected fluidized bed reactors. It takes place in two steps where a metal powder, working as a solid Oxygen Carrier (OC), gets cyclically oxidized and reduced carrying the oxygen from one reactor to the other. First the OC has a strong exothermic reaction with the oxygen of the fluidizing air in the Air Reactor (AR). Afterwards the oxidized OC is sent into the Fuel Reactor (FR) and its oxygen reacts with the fuel, endothermically or slightly exothermically, depending on the OC material and fuel used, generating an almost pure stream of CO_2 and steam.

SINTEF Energy Research and the Norwegian University of Science and Technology (NTNU) have designed a 150kW$_{th}$ atmospheric CLC reactor system. The chosen design solutions are aiming at high operational flexibility and fuel conversion as well as compactness for the prospective of pressurizing the reactor as a further step. It consists of

[1] Corresponding author. Tel.: +47 73550449; fax: +47 73593580.
E-mail address: aldo.bischi@ntnu.no

doi:10.1016/j.egypro.2011.01.074

two Circulating Fluidized Beds (CFB) interconnected by means of a bottom extraction/lift and divided Loop-Seals (LS) in a two loops architecture: Double Loop CFB (DLCFB) shown in Figure 1. The AR is meant to operate in fast fluidization regime while the FR both in turbulent and fast fluidization. The abovementioned loop-seals are designed as double loop-seals. The purpose is both to avoid the gas mixing between the two reactors and to lead the flow of solids entrained by one reactor into the other one or re-circulate it back to the reactor of origin. They are fluidized by means of three bubble cap nozzles: one below the downcomer (central), one just below the internal return leg (to lead the mass back to the reactor of origin) and one below the external return leg (to lead the entrained mass to the other reactor). In addition there will be lateral steam injections in the downcomers, just above the loop-seals (Figure 1). Because of the smaller amount of fluidizing gas available in the FR, compared to the AR, the bottom extraction will compensate the fact that the FR is not capable to entrain the same amount of solids as the AR. The system is cooled by means of lateral protruding Cooling Panels (CP) inserted into the AR body. The DLCFB design and the way it faces industrial and scale up issues, as the latest (second) generation of CLC reactors does, has already been described in a detailed way by Bischi et al. [2]. In order to achieve the aforementioned objectives, the hydrodynamics as well as many of the design solutions of such CLC reactor system, need to be qualitatively tested in a Cold Flow Model (CFM) without chemical reactions [3].

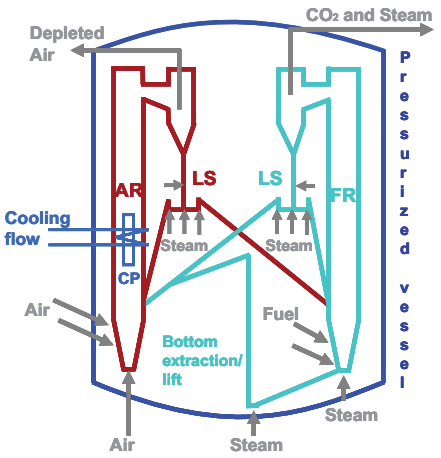

Figure 1. Process diagram of the Double Loop Circulating Fluidized Bed (DLCFB) reactor system concept [2].

2. Experimental set up and procedure

A polycarbonate CFM has been built and commissioned. It is a full scale (1:1) exact copy of the 150kW$_{th}$ hot rig design. In this way it was possible to reduce the wall effects to get more reliable design verification [4]. The two reactors are 5 meters high; the AR has a diameter of 0.23 m while the FR 0.144 m. In addition the powder characteristics as well as the operating conditions were chosen in order to end up in the same fluidization regime as the hot rig, i.e. fast CFB regime according to the empirical classification of Grace [5]. The selected material representing the oxygen carrier is a Ferro-Silicon alloy with a density of almost 7000 kg m^{-3} and a d_{50} of 34 micrometers and rounded irregular shape. These particles end up in the group A of the Geldart diagram and because of their high density are very close to the boundary with the group B [6]. An important share (above 20%) of the particle size distribution used in the tests has a diameter smaller than the foreseen critical one where the Van der Waals cohesion forces start to play a decisive role into fluidization properties [7, 8]. Anyhow, as long as the main interest for such fine particles is in the catalyst applications (thus lighter) it is quite rare to find information about high density Geldart A particles in open literature. The fluidizing gas is air and the nominal flows are selected to give a velocity of 2.2 m s^{-1} in the reactor bodies. Details of the scaling strategy can be found in Bischi et al. [9].

The rig is equipped with differential pressure transmitters distributed along the reactor bodies, cyclones and bottom of the loop-seals. At the reactor exit there is one common filter box with a frequency controlled fan so it is possible to obtain the desired backpressure, which will be the same for both the AR and the FR unless the valves at the cyclones exit are used to differentiate them. The filter box is also used to collect the powder losses and in this way monitor the cyclones efficiency and the inventory in the system. The solids entrainment is measured in two ways: a visual and an indirect way. The first one is relying on a visual measurement of the mass accumulation in the downcomer once the loop-seal fluidization is shut down. The indirect measurement is based on a perforated flap

valve located in the downcomer. This way the gas coming from below fluidizes the amount of powder accumulating on the flap valve, when closed. If the minimum fluidization condition is reached, the entrained solids flux, thus flow, can be derived from the gradient of the pressure drop (ΔP) across the flap valve due to the mass accumulated [10]:

$$G_s = \frac{d\Delta P}{dt} \cdot \frac{1}{g} \cdot \frac{A_{downcomer}}{A_{riser}} \quad . \tag{1}$$

All the pressure measurements used to evaluate the reactors performance are an average value of ten minutes steady state operation. In addition the pressure in the more sensitive points (e.g. bottom loop-seal) was constantly monitored and experiments with too high pressure fluctuations (above 40 mbar) were labelled as unstable. The solids flows/fluxes were measured at least two times and an average value was presented. In case of a standard deviation of the measurements bigger than the 10% of the average a third measurement was taken.

3. Results and discussion

The CFM was first tested without particles to check the fluidizing nozzles design and the share of kinetic pressure losses. The pressure losses across the nozzles were measured as a function of the gas flow injected through the nozzles. In this way it was possible to evaluate if the ΔP of each nozzle is in the proper range: above 20% [11] of the respective overall reactor body pressure drop in the operational design point. These values were compared with the overall reactor ΔP measured during actual operation, with solids, showing a satisfactory match both for AR and FR. The recorded pressure values along the empty reactor bodies were small due to the low design velocities (up to 2.4 m s^{-1}). The maximum values of pressure difference between the bottom of the reactors and their top was found to be in the order of magnitude of 1 mbar. This means that the kinetic pressure losses have little influence on the pressure measured along the reactor bodies during operation. Anyhow it needs to be kept in mind that the lower pressure transmitter is placed at a height of 14 cm from the reactor bottom; the bottom pressure is expected to be higher.

Another preliminary test campaign was finalized to check the reliability of the indirect solids flow/flux calculation realized by means of the pressure gradient measurements (Eq.1). The so determined solids flux was compared with the visual measurements of mass accumulation. It was of great interest for the project, in order to be capable to make use of this technique also in the 150kW_{th} hot rig, where it will not be so straightforward to have a visual measurement. The two measurement techniques matched when an auxiliary air injection below the perforated flap valve was tuned on purpose in order to achieve minimum fluidization conditions of the accumulated mass of particles. In addition, the agreement was mainly for the lower part of the solids flux range tested. In fact the momentum of the free falling solids was proven to affect strongly the fluidization of the accumulated powder in the downcomer [12]. A wide range of solids fluxes are going to be tested and they can't be foreseen in detail because of their dependency on many independent parameters. It means that we can't know in advance what the exact amount of auxiliary air will be. From these findings, and supported by literature [13], it was possible to deduct that this approach is very much depending on the operator ability of reaching the right fluidization conditions above the perforated flap valve. Thus it can't be used by itself for the hot rig and another solution applicable to high temperature conditions needs to be found.

It was noticed that it is difficult to obtain exactly the same solids flow/flux when the same experiments are not performed continuously; while they are very much consistent when executed continuously without changing settings and stopping the system. This fact shows that the "roughness" of the experimental technique used to measure the solids flow can not be the main reason for the variations in the results. The way the solids inventory distributes in the system in order to achieve steady state conditions do also play a role. A third issue affecting the solid flow is the Total Solids Inventory (TSI) control. It is closely related to the cyclones efficiency, evaluated to be very high and often above 99.9%. This is a good performance for such fine powder as can be seen in Fluid Catalytic Cracking (FCC) literature which is dealing with this kind of particle size distribution, but much lighter material [14]. Nevertheless it is worth to mention that for example in the case of a solid flow of 1 kg s^{-1} a cyclone efficiency of "just" 99.9% will mean 3.6 kg of losses in one hour. Such loss of mass will substantially affect the TSI and consequently the reactor performance. This information is of fundamental importance for the interpretation of the experimental results. The same set of tests was repeated twice for the AR with a TSI of 65kg and different refilling time of the lost mass. The results show that the 20 minutes refilling gave in average about 4% higher solids flow

than the 60 minutes one (for a set of data of 20 points of which 8 are shown in Figure 2). Also, the consistent behaviour of the larger downcomer height confirms the indication that the solids flow difference is caused by an actual change in the reactor overall mass and mass distribution.

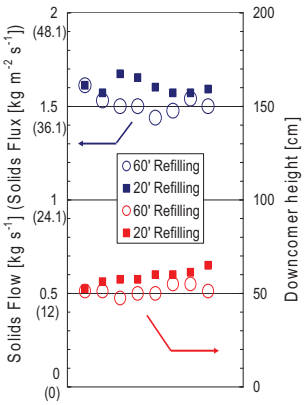

Figure 2. Set of tests performed twice with the same conditions, but with 60' and 20' refilling.

Next, the AR was run alone re-circulating internally through the divided loop-seal all the entrained solids. It was tested from part load, turbulent fluidization regime, up to an air flow corresponding to the fast CFB design flow regime. The solids flow/flux and the pressure profile along the reactor body were measured and the cyclone efficiency estimated. The TSI within the reactor system was varied as well as the combinations of primary and secondary air. The measured flow of solids was found to be clearly dependent on the TSI and the air flow, increasing with them up to 2 kg s^{-1} (flux of 48 kg m^{-2} s^{-1}). At the same time also the pressure behaviour showed its dependency from the TSI and air staging, shifting towards higher values for higher amount of solids and higher primary air share. In addition higher values of pressure gradient, thus mass, in the lower part of the reactor body are recorded, as expected [15], for turbulent regime, while the particle concentration in the upper part of the reactor increases when increasing the fluidization velocities. The same set of experiments was performed for the FR showing the same behaviour when it comes to solids entrainment and pressure behaviour. It was possible to entrain in a stable way a flow of particles up to almost half of the AR one, which is in accordance with the design. In average the bottom pressures of the two reactors running separately were shown to be on the same order of magnitude, slightly higher for the FR, picking the right operational conditions. This is an important parameter for the coupled operation control because this is the pressure where the return legs of the divided loop-seals merge into the reactor bodies. More details about the performance of the reactors operated separately can be found in Bischi et al. [2 and 9].

The way the loop-seal is operated affects quite a lot the performance of a CFB, and especially the solids entrainment [16 and 17]. For this reason the effect of the loop-seal fluidization was thoroughly investigated, varying the amount of fluidizing air injected in the central and internal nozzles for several lateral injections (that ones located in the downcomer just above the loop-seal). The aim was to understand the best way to operate the loop-seal for the actual reactor design. It means achieving high solids circulation with a stable fluidization regime in the downcomer (between minimum fluidization and minimum bubbling). For economical reasons this has to be done using a small amount of fluidizing gas because it will be steam in the hot rig. Figure 3 shows one detailed test matrix executed for a constant TSI of 55 kg in the AR operated separately (internal recirculation) and with a fluidizing air flow of 5000 Nl min^{-1}, equivalent to a superficial gas velocity of 2.2 m s^{-1}, and with an air split of 70% primary air, 15% secondary air 1 and 15% secondary air 2. The AR loop-seal will be the more heavily loaded according to the design. Each group of four points in the graph corresponds to a different value of the central nozzle fluidization (5 to 120 Nl min^{-1}) and for each of the groups the four points go from the value of 80 Nl min^{-1} up to 190 Nl min^{-1} of internal nozzle fluidization. Each different symbol (diamond, circle, and asterisk) refers to a different value of lateral air injection from 2.5 Nl min^{-1} up to 10 Nl min^{-1}. The blue points show (scale on the left) the measured solids flow/flux, while the red points show the measured height of solids in the downcomer. This is an important parameter to monitor in order to know how much of the mass is in the loop-seal downcomer rather than in the reactor body. It is possible to notice that the entrained flow of solids is appreciably increasing with the internal nozzle fluidization for the lower central fluidizations while above 40 Nl min^{-1} of central fluidization it stabilizes loosing its dependencies on the internal and central nozzles. For central nozzle fluidizations above 40 Nl min^{-1} it is not possible to distinguish clear trends, not even dependency from the lateral air injection amount. The downcomer height is consistently reduced with the increase of solids flow because, for a fixed TSI and reactor fluidization, a smoother loop-seal fluidization provides better solids circulation, thus more mass inside the reactor body, thus higher ΔP

across the reactor and higher entrainment. On the other hand the higher pressure fluctuations experienced in the bottom of the loop-seal in correspondence with higher fluidizing air, e.g. central nozzle above 40 Nl min^{-1}, means that the reactor is exposed to higher risks of gas leakages and cyclone perturbations. A similar set of experiments was performed for the AR keeping the same air flows in the reactor and loop-seal, but increasing the TSI up to 65 kg. The increase of mass reduced the dependencies highlighted previously as well as increased the solids flow together with the amount of mass in the downcomer. The increase of the downcomer solids height is necessary in order to close the pressure loop; because more mass in the system gives a higher value of pressure in the reactor bottom exactly where the return leg is merging, thus higher pressure in the loop-seal is required to balance it. The loop-seal results are not following clear trends as in the cited literature [16 and 17] most likely because both the high density Geldart A particles and the fluidizing nozzles of the present set-up represent solutions differing from the majority of the published laboratory loop-seal studies. Therefore modifications of the loop-seal fluidizing system are under investigation in order to gain better control on the solids circulation, especially to tackle circumstances where the two solids streams exiting from the loop-seal are facing different pressures, as in the coupled operation.

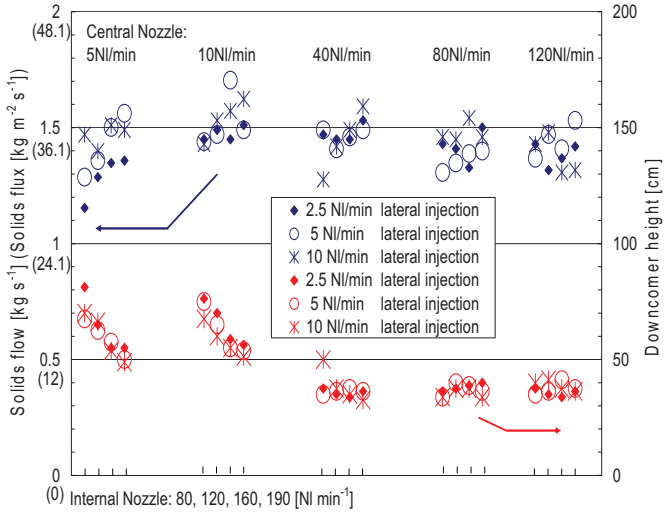

Figure 3. Set of experiments finalized to understand the air reactor dependency on the loop-seal operation (internal, central and lateral air injection) for a total solids inventory of 55 kg and air flow of 5000 Nl min^{-1}.

In this experimental campaign also the cooling panels influence on the AR performance was evaluated. Figure 4 shows the results of a test campaign conduced with a TSI of 65 kg, a total air flow going from 4000 to 5000 Nl min^{-1} and constant loop-seal fluidization. Tests were done with no cooling panels, with the lower (bott.), the middle (mid.) and the upper (up) panel separately and with the lower and middle together. The solids flow/flux was not significantly affected by panel insertion, location and number. The same applies for the measured average pressure values in the reactor body, while the pressure oscillations measured in the loop-seal bottom were in general higher for the two-panel configuration, e.g. above 20 mbar vs. 10 mbar. The test done with 100% of flow in the primary air (100%-0%-0%) showed a higher solids flow entrainment compared to the use of secondary air for the same amount of fluidizing air (50%-25%-25%). The use of only primary air was limited to 4000 Nl min^{-1} because further increase of flow generated pressure pulsations that made the system vibrating too much to operate it safely (test done just in

the two panels case). It may be related to the inventory which needs to be reduced for such operational mode; further tests to proof it need to be carried out.

All the abovementioned tests were executed running the AR and FR separately. In this way it was possible to have an accurate mapping of their operational window and choose the best way to couple them together as a DLCFB reactor system. A test campaign with the two reactors coupled was performed but the results were not as expected. A high difference of pressure between the lower sections of the reactors was experienced: the FR bottom pressure ended up being much higher. It means that each divided loop-seal was exposed to a pressure unbalance having one return leg facing a pressure much higher than the other one. This fact sums up to the abovementioned loop-seal solids flux control challenges. The combination of these two circumstances created a disturbance because of gas flowing through the internal leg of the FR loop-seal, which is not in use during coupled operation with 100% solids exchange. It also generated a high pressure in the AR loop-seal external return leg, thus a high accumulation of particles in the AR downcomer capable to push the powder flow from the AR to the FR and very likely causing unwanted gas leakages from the FR to the AR. In addition it affected the cyclones efficiency causing mass losses and resulted in a loss of control of the system performance. An attempt to operate the system was done sealing the internal return legs of the loop-seals, without exposing them to the mentioned pressure unbalance. In this way the DLCFB reactor system reached automatically a stable configuration, showing good margins of operability. Afterwards the FR fluidizing system was modified, shifting the secondary air injections to a higher position. In this way the FR bottom pressure was reduced making the overall system more easily operable and the sealing of the internal return legs of the loops-seals could be removed. An example of the obtained pressure profiles are shown in Figure 5 and are between turbulent and fast CFB fluidization regimes. In the test shown in Figure 5 the TSI in the system was approximately 120kg while the mass inventories in the AR and FR were 19 kg and 15 kg, respectively. The mass in the reactor bodies was estimated by means of the measured pressure profiles, neglecting frictional and acceleration losses [18]. A solids flow of 1.65kg s^{-1} (corresponding to a flux of 40 kg m^{-2} s^{-1}) was entrained by the AR with a superficial gas velocity of 2.1 m s^{-1} while the FR entrained 0.85 kg s^{-1} (corresponding to a flux of 51 kg m^{-2} s^{-1}) with a superficial gas velocity of 2.2 m s^{-1}. The remaining 0.8 kg s^{-1} of particles flow necessary to achieve steady state were sent to the AR by means of the bottom lift/extraction operated with turbulent fluidization at 1 m s^{-1} of superficial gas velocity and a solids flux corresponding to 100 kg m^{-2} s^{-1}. More experiments to partially equilibrate

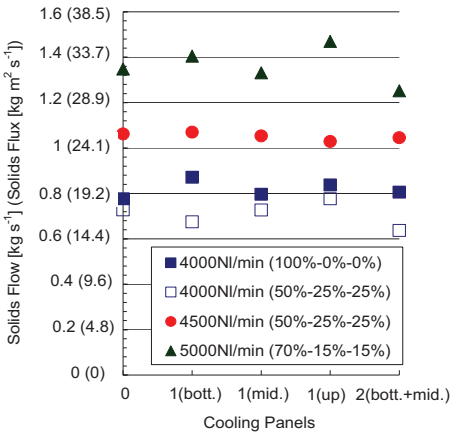

Figure 4. Solids flow/flux measurements with cooling panels insertions in different configurations.

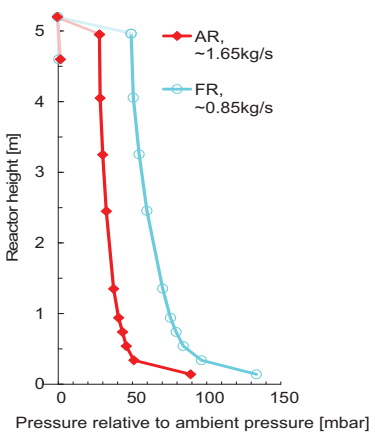

Figure 5. Pressure profiles measurement, coupled operation of Air Reactor (AR) and Fuel Reactor (FR).

the pressures between the lower sections of the reactors are on going. One of them is a reduction of the TSI which will decrease the pressures in the lower sections of the reactors. Another one is the utilization of the backpressure valves located at the cyclones exit in order to increase the AR backpressure, thus the pressure at the AR bottom. This solution will not be so straightforward because of all the interconnections between the AR and FR bodies, thus the pressure changes in one of them will affect to some extent also the other. Among the possible modifications of the loop-seals the introduction of a cone valve in each of their internal leg has proven to be an effective solution in order to face pressure difference between reactors. In fact the operation with a sealing can be considered equivalent to a cone valve fully closed. On the other hand, operating the DLCFB reactor system in a way which doesn't rely too much on active control (e.g. backpressure valves or cone valves) is more in line with the original design basis of the reactor system. Therefore the height where the loop-seals return legs, both the internal and external, are merging with the reactors can be lifted to a value where the pressure in the reactor bodies is decreased enough to make the system more easily operable with a wider stable operational window. This may cause residence time reduction and increase the risk of leakages of gas carried by the entrained solids from one reactor to the other [19], but will for sure increase the intrinsic stability of the system.

Conclusions and outlook

The full scale cold flow model of a second generation chemical looping combustion reactor system was commissioned and its performance with high density Geldart A particles was tested at a wide range of operating conditions.

The fluidizing system design was verified as well as the fraction of the kinetic losses on the overall reactor pressure drop. The suitability of an indirect measurement technique of the solids flow/flux entrainment was evaluated and compared to a more conventional direct one based on visual measurement of mass accumulation. A simplified error assessment of the direct solids flow/flux measurement was done, and the influence of the total solids inventory control and distribution on the measured values was highlighted. The cyclone efficiency was also estimated together with its influence on the abovementioned solids inventory control.

A comprehensive understanding of the stable operational window of the air and fuel reactor systems tested separately was obtained. The solids flow/flux entrainment and the pressure profiles along the air reactor and the fuel reactor were analyzed as well as their sensitivity to the parameters: superficial gas velocity, secondary air injection, solids inventory and loop-seal fluidization. Especially the way the loop-seal affects the reactors performance was systematically analyzed in order to find the best combination of air flow to the central, internal and lateral air injections. The loop-seals showed the capability of circulating the required solid flow, even if a clear trend was not found on how they ideally should be operated in order to attain a sharp and exact control. Therefore the fluidizing system of the loop-seals needs to be improved.

Furthermore, the overall double loop circulating fluidized bed reactor system performance was verified. A pressure difference was experienced between the lower sections of the two reactors, thus between the two loop-seals return legs. This made the operation of the overall system difficult. Better control was obtained sealing the internal legs of the divided loop-seals, as if a cone valve, 100% closed, was inserted. Finally, by modifying the FR secondary fluidization positions and changing the fluidizing air distribution it was possible to reduce the pressure unbalance and establish a stable solids exchange between the reactors. To that respect the system showed to be flexible and automatically adjusted the amount of solids in the downcomers to fulfil the overall pressure balance requirements.

Acknowledgments

This publication forms a part of the BIGCO2 project, performed under the strategic Norwegian research program Climit. The authors acknowledge the partners: Statoil, GE Global Research, Statkraft, Aker Clean Carbon, Shell, TOTAL, ConocoPhillips, ALSTOM, the Research Council of Norway (178004/I30 and 176059/I30) and Gassnova (182070) for their support.

References

[1] ENCAP Deliverable D1.2.6, 2009. Power systems evaluation and benchmarking – Public version, URL: www.encapco2.org.

[2] Bischi, A., Langørgen, Ø, Saanum, I., Bakken, J., Seljeskog, M., Bysveen, M., Morin, J.-X., Bolland, O., 2010. Design study of a 150kW_{th} Double Loop Circulating Fluidized Bed reactor system for Chemical Looping Combustion with focus on industrial applicability and pressurization. Int. J. Greenhouse Gas Control., doi:10.1016/j.ijggc.2010.09.005.

[3] Pröll, T., Ruspanovits, K., Kolbitsch, P., Bolhàr-Nordenkampf, J., Hofbauer, H., 2009. Cold flow model study on a dual circulating fluidized bed system for chemical looping processes. Chem. Eng. Technol. 32 (3), 418-424.

[4] Knowlton, T.M., Karri, S.B.R., Issangya, A., 2005. Scale-up of fluidized-bed hydrodynamics. Powder Technol. 150 (2), 72-77.

[5] Lim, K.S., Zhu, J.X., Grace, J.R., 1995. Hydrodynamics of gas-solid fluidization. Int. J. Multiphase Flow. 21 (Suppl. 1), 141-193.

[6] Geldart, D., 1973. Types of gas fluidization. Powder Technol. 7 (5), 285-292.

[7] Baeyens, J., Geldart, D., Wu, S.Y., 1992. Elutriation of fines from gas fluidized beds of Geldart A-type powders – effect of adding superfines. Powder Technol. 71 (1), 71-80.

[8] de Vos, W., Nicol, W., du Toit, E., 2009. Entrainment behaviour of high-density Geldart A powders with different shapes. Powder Technol. 190 (3), 297-303.

[9] Bischi, A., Langørgen, Ø., Morin, J.-X., Bakken, J., Bysveen, M., Bolland, O., 2010. Design and performance of a full scale cold flow model of an innovative chemical looping combustion reactor system. In: 1st International Conference on Chemical Looping, Lyon, France, http://www.ifp.com/actualites/evenements/congres-et-conferences/organises-par-ifp-energies nouvelles/rs-chemical-looping.

[10] Nicolai, R., 1995. Experimentelle Untersuchungen zur Strömungsmechanik in einer hochexpandierten zirkulierenden Gas/Feststoff-Wirbelschicht. Ph.D. thesis, Eidigenössischen Technischen Hochschule (ETH), Zürich, Switzerland.

[11] VGB PowerTech, 1994. Gas Distributor Plates in Fluidized Bed Systems. In: VGB PowerTech Service GmbH. Essen, Germany.

[12] Shi, D., 1996. Fluiddynamik und Wärmeübergang in einer zirkulierenden Wirbeschicht. Ph.D. thesis, Eidigenössischen Technischen Hochschule (ETH), Zürich, Switzerland.

[13] Goedicke, F., 1992. Strömungsmechanik und Wärmeübergang in zirkulierenden Wirbeschichten. Ph.D. thesis. Eidigenössischen Technischen Hochschule (ETH), Zürich, Switzerland.

[14] Fassani, F.L., Goldstain, L.J., 2000. A study of the effect of high inlet solids loading on a cyclone separator pressure drop and collection efficiency. Powder Technol. 107 (1-2), 60-65.

[15] Kunii, D., Levenspiel, O., 1997. Circulating fluidized-bed reactors. Chem. Eng. Sci. 52 (15), 2471-2482.

[16] Basu, P., Butler, J., 2009. Studies on the operation of loop-seal in circulating fluidized bed boilers. Applied Energy. 86 (9), 1723-1731.

[17] Kim, S.W., Namkung, W., Kim, S.D., 2001. Solid recycle characteristics of loop-seals in a circulating fluidized bed. Chem. Eng. Technol. 24 (8), 843-849.

[18] Issangya, A.S., Bai, D., Bi, H.T., Lim, K.S., Zhu, J., Grace, J.R., 1999. Suspension densities in a high-density circulating fluidized bed riser. Chem. Eng Science. 54 (22), 5451-5460.

[19] Geldart, D., Broodryk, N., Kerdoncuff, A., 1993. Studies on the flow of solids down cyclone diplegs. Powder Technol. 76 (2), 175-183.

Paper III

"Hydrodynamic viability of chemical looping processes by means of cold flow model investigation", *Applied Energy (2012), Article in press.* doi:10.1016/J.apenergy.2011.12.051.

Is not included due to copyright

Paper IV

"Double Loop Circulating Fluidized Bed reactor system for two reactions processes based on pneumatically controlled divided loop-seals and bottom extraction/lift", *Powder Technology* (submitted).

Is not included due to copyright